Intercellular Adhesion Molecule-1 in T cell differentiation and as a target for peptide therapy of type 1 diabetes

By

Abby L. Dotson

Submitted to the graduate degree program in Molecular Biosciences and the Graduate Faculty of the University of Kansas in partial fulfillment of the requirements for the degree of Doctor of Philosophy.

_____
Chairperson Stephen H. Benedict, Ph.D.

_____
David Davido, Ph.D.

_____
Ron Ragan, Ph.D.

_____
Dean A. Stetler, Ph.D.

_____
Thomas Yankee, Pharm.D., Ph.D.

Date Defended: April 10, 2012

The Dissertation Committee for Abby L. Dotson

certifies that this is the approved version of the following dissertation:

Intercellular Adhesion Molecule-1 in T cell differentiation and as a target for peptide therapy of type 1 diabetes

_____

Chairperson Stephen H. Benedict, Ph.D.

Date approved: April 10, 2012

Abstract

CD4+ T cells are essential for proper function of the immune system. Many facets of an immune response are dependent on help from CD4+ T cells to become activated and exhibit effector function. Memory CD4+ T cells are a differentiated subset of T helper cells that give rise to long-lasted protective immunity. Differentiation to a memory phenotype from a naïve T cell that has never encountered antigen requires two signals. Costimulatory molecules send a second signal into naïve T cells that follows stimulation of the T cell receptor and greatly affects how naïve T cells activate and differentiate. The present work centers on the ability of the costimulatory molecule Intercellular Adhesion Molecile-1 (ICAM-1) to induce activation and differentiation of CD4+ naïve T cells to effector and memory phenotypes.

We observed that costimulation through ICAM-1 generates a central memory-like population that is capable of migration to the lymph nodes and to a lesser extent the intestine. ICAM-1 costimulation is also capable of inducing memory differentiation after a short duration of signal but long-term costimulation is needed to generate a sizable population. In addition, costimulation of CD4+ naïve T cells from older individuals through ICAM-1 is able to produce memory cells more so than other costimulatory molecules. This suggesting that ICAM-1 could be utilized to help restore immune function during senescence.

ICAM-1 and its ligand leukocyte function-associated antigen-1 (LFA-1) also provide targets for blocking self-reactive T cells in autoimmune diseases. Peptides against ICAM-1 and LFA-1 were used in the type I diabetes NOD mouse model. We observed a significant delay in symptoms with therapeutically treated mice compared to

saline control mice and stopped T cell infiltration of the pancreatic islets. Additionally, T cells from treated mice were no longer able to respond to β-cell antigen indicating a shut down of the autoreactive immune response.

This dissertation is dedicated to my parents, John and Shirley. Thank you for being pretty darn awesome.

Acknowledgements

The work presented in this dissertation would not have been possible with the support of many people. First, I would like to thank my mentor, Dr. Stephen Benedict. Steve taught me to think like a scientist and prepared me for the next step in my career all the while showing me that research is not exclusive of fun and that they often work best together. Steve had to put up with a lot of my snarky comments, stupid shenanigans and incredibly clever wit. For that, he deserves a trophy or maybe sainthood. I would also like to thank Dr. Marcia Chan and Dr. Thomas Yankee. They were like second mentors to me and their advice was invaluable. I was fortunate enough to learn from their years of experience such as Marci's amazing ability to find seemingly nonexistent lymph nodes in a mouse or Tom's infinite wisdom of flow cytometry. Needless to say, they are pretty impressive people. I must also acknowledge my fellow graduate students, and often collaborators, Kelli Williams, Courtney Gdowski and Amy Newton. You ladies are why nerdy, smart chicks are so cool.

I am grateful to my committee, Dr. Stephen Benedict, Dr. David Davido, Dr. Ron Regan, Dr. Dean Stetler and Dr. Tom Yankee for all the time, advice and support you have given me. I would like to thank Nancy Schwarting and William McGuiness who provided technical assistance for the diabetes study and made a very intense experiment a lot of fun. I would like give a special thanks to John Connolly, Dennis Kemberling and Linda Wiley who were always so helpful when I had questions about general department stuff (which was often). A large amount of this work would not be possible without our generous blood donors. In my graduate career, I used over 12,400mL of human blood for experiments, which means that I needed many donors. Thank you all for being so

generous to sacrifice your time and comfort to further my research. Also, I would like to acknowledge two of the finest phlebotomists I know, Laura Kimble and Pat Moody. They were also essential to the human T cell experiments and are pretty handy with a butterfly needle.

Finally, I would like to thank my family. To my parents who had to live with me during my teenage years, I would not wish such a fate on anyone but you were pretty fantastic. Thank you for all of the love and support. And to my sisters, thank you for being strong, badass women for me to look up to.

Table of Contents

Chapter 2: ICAM-1:LFA-1 blocking peptides eliminate the T cell response in the NOD mouse model for type I diabetes.

Chapter 3: Early development of a memory T cell phenotype with costimulation through ICAM-1 that is not influenced by additional costimulation

Chapter 4: Homing potential of differentiated cells generated with ICAM-1 costimulation

Chapter 5: Costimulation of CD4+ naïve T cells through ICAM-1 generates a memory phenotype in older individuals

Chapter 6: Stimulation methods to generate murine memory T cells using ICAM-1

List of Figures and Tables

Chapter 1

Chapter 2

Chapter 3

Chapter 6

Chapter 1

Introduction and general background information

The Adaptive Immune Response

The immune system has two main branches: the adaptive immune response and the innate immune response. The innate response is not antigen specific but provides an immediate response to pathogens. The adaptive side takes longer to respond to specific antigen and yields immunological memory for a more efficient secondary response. The adaptive immune system can be broken down further into the humoral and cell-mediated immune response. Antibody production by plasma cells (derived from B cells) is the effector outcome of the humoral response. Antibodies can bind to bacteria and viruses to neutralize them, tag elements for opsonization, aggluntinate to form insoluble complexes for clearance and initiate components of complement pathways. The cell-mediated immune response is driven by CD8+ cytotoxic T lymphocytes (T_C cells) that target and kill infected cells using perforin and granzyme pathways. Macrophages are activated in the cell-mediated pathway and function to phagocytize pathogens and foreign elements. CD4+ helper T cells (T_H cells) play a role in both sides of the adaptive immune system. Th1 cells secrete interleukin-2 (IL-2), interferon-gamma (IFN-γ) and interleukin-12 (IL-12) that help to activate the cell-mediated branch of the adaptive immune system and inhibit the humoral response. Th2 cells do the opposite and promote the activation of humoral immunity and B cell activity while inhibiting Th1 function by secreting interleukins-4, -5, -10 and -13 (IL-4, IL-5, IL-10 and IL-13) **(Fig. 1.1)**. Both sides of the immune system can be controlled by regulatory T cells (Treg) that secrete IL-10 and TGF-β to suppress other immune cells or use granzyme B and perforin to suppress via cell-to-cell contact (1, 2). Regulatory T cells are important for downregulation of the

Figure 1.1

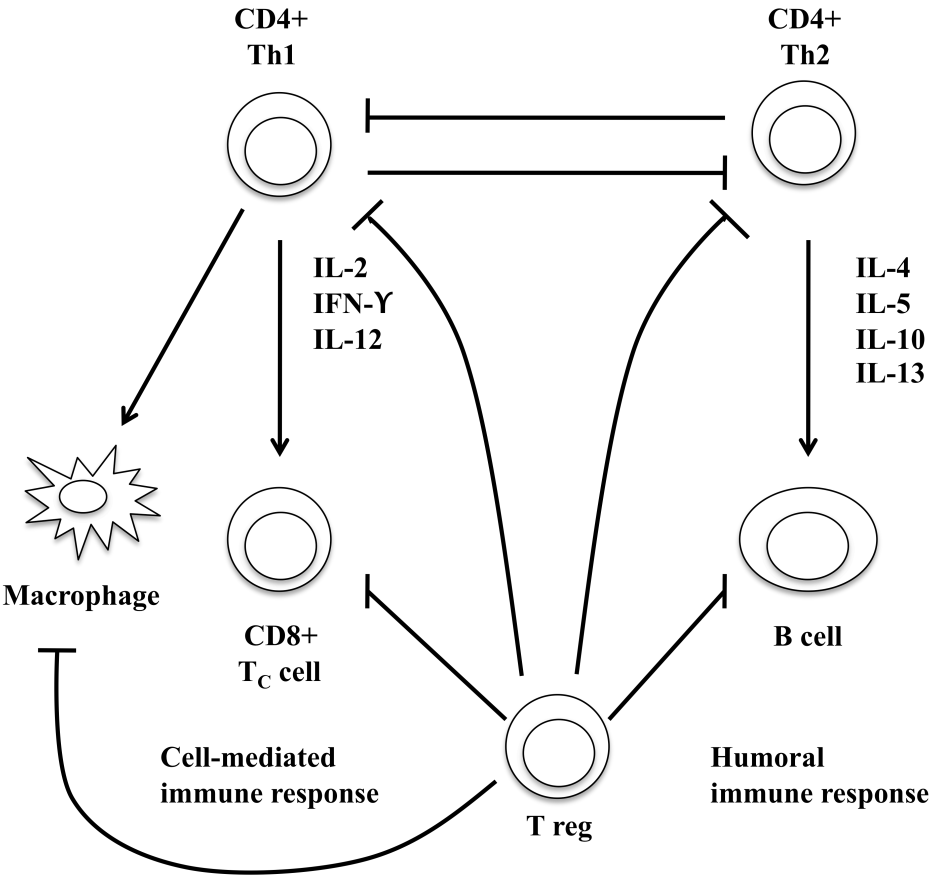
CD4+
Th1
CD4+
Th2
IL-2
IFN-Ɣ
IL-12
IL-4
IL-5
IL-10
IL-13
Macrophage
CD8+
T_C cell
B cell
Cell-mediated
immune response
Humoral
immune response
T reg

Figure 1.1. Model of the adaptive immune response. CD4+ T cells regulate both the cell-mediated (CD8+ T cell and macrophages) and hurmoral (B cell) branches of the immune response by secretion of soluble mediators. Regulatory T cells suppress the immune response.

immune system after an immune response and suppression of possible self-reactive immune cells.

T cell signaling, activation and differentiation

Naïve T cells are a subset of the T cell compartment that have recently emerged from the thymus following development to a functional cell but have not yet encountered antigen. They circulate through the periphery and secondary lymphoid organs looking for their specific antigen, which is presented by an antigen presenting cell (APC). Upon antigen recognition and binding, naïve T cells become activated to clonally expand and differentiate into an effector phenotype **(Fig. 1.2)**. Effector cells are capable of secreting cytokines and other soluble molecules that (i) signal to activate or (ii) suppress other immune cells, (iii) direct cells where to go in the body and (iv) participate in elimination of foreign elements. Effector cells have a short life span and following antigen clearance the majority of effector cells undergo activation-induced cell death (AICD). A small number of cells survive after the immune response has been resolved and become memory T cells **(Fig. 1.2)**. Memory T cells are long-lived in the body and able to activate quickly upon secondary challenge with the same antigen.

Signal 1: TCR/CD3

Naïve T cells require two signals to become fully activated. The first signal is antigen specific and received through the T cell receptor (TCR) when it binds to its

Figure 1.2

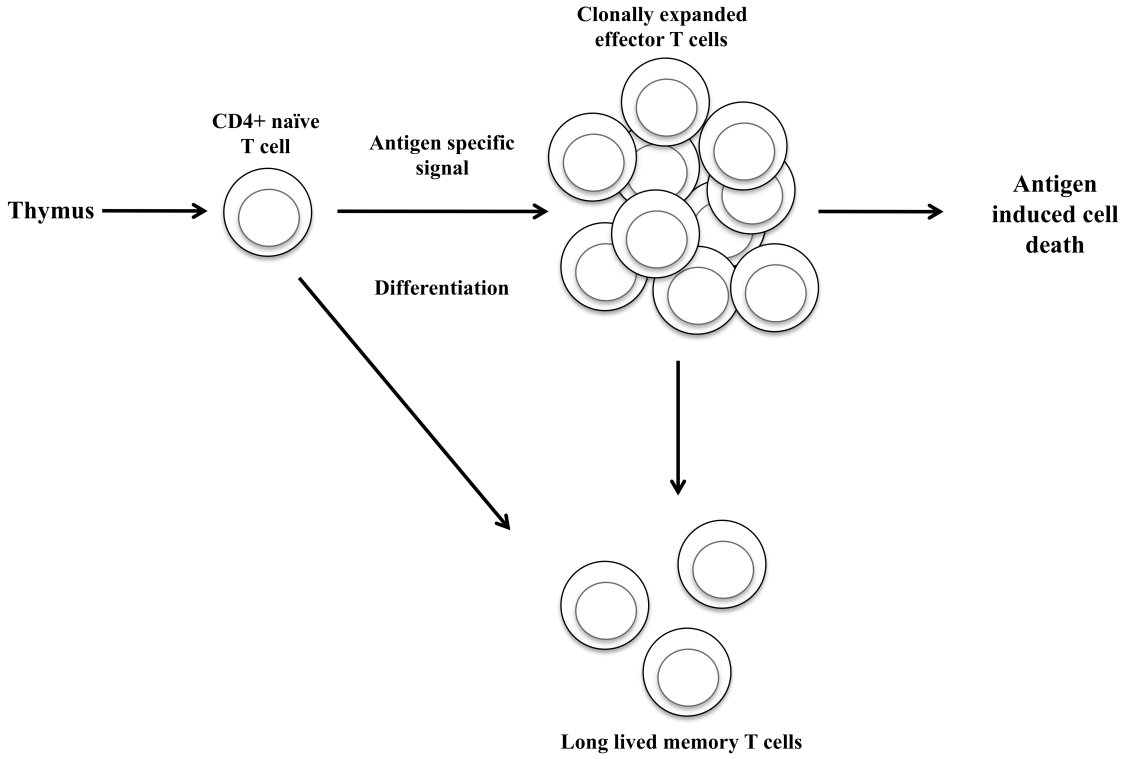
Clonally expanded
effector T cells
CD4+ naïve
T cell
Antigen specific
signal
Thymus
Antigen
induced cell
death
Differentiation
Long lived memory T cells

Figure 1.2. Model of naïve T cell activation. Upon receiving an antigen signal, naïve T cells can activate, proliferate and differentiate into effector cells. The effector population will die by apoptosis after the immune response has taken place. Memory T cells arise from either an effector population or directly following priming of the naïve cell (to be discussed in chapter 2).

cognate peptide antigen in the context of the major histocompatibility complex (MHC). The MHC is referred to as human leukocyte antigen (HLA) in humans and is expressed in two forms that designate the class and stimulating potential of the molecule. MHC class I presents antigenic peptides of 8-10 amino acids to CD8+ T cells. Class I is formed by one alpha subunit containing three domains and a β2-microglobulin molecule. MHC class II is comprised of two protein subunits (alpha and beta) and presents a larger peptide, about 13-25 amino acids, to CD4+ T cells. The T cell receptor for CD4+ and CD8+ T cells is a heterodimer that contains alpha and beta subunits and is associated with the CD3 complex. The CD3 complex is formed by delta, gamma and two epsilon polypeptides and two zeta chains (assembled as γ/ε, δ/ε and ζ/ζ dimers) and is essential for signal transduction. The CD3 chains contain immunoreceptor tyrosine-based activation motifs (ITAMs) that, upon TCR:antigen binding, become phosphorylated on tyrosine residues. This allows for activation of Src family kinases (Lck and Fyn) and Zap70, phosphorylation of transmembrane adaptor proteins and leads to activation of various transcription factor pathways (3, 4).

If the T cell only receives one signal through the TCR/CD3 complex, the cell will fail to activate and become anergic or die by apoptosis. T cells must receive a second signal through a costimulatory molecule. The costimulatory signal may be received through CD28, lymphocyte function-associated antigen-1 (LFA-1), intercellular adhesion molecule-1 (ICAM-1) as well as any of several other T cell surface proteins **(Fig. 1.3)**.

Figure 1.3

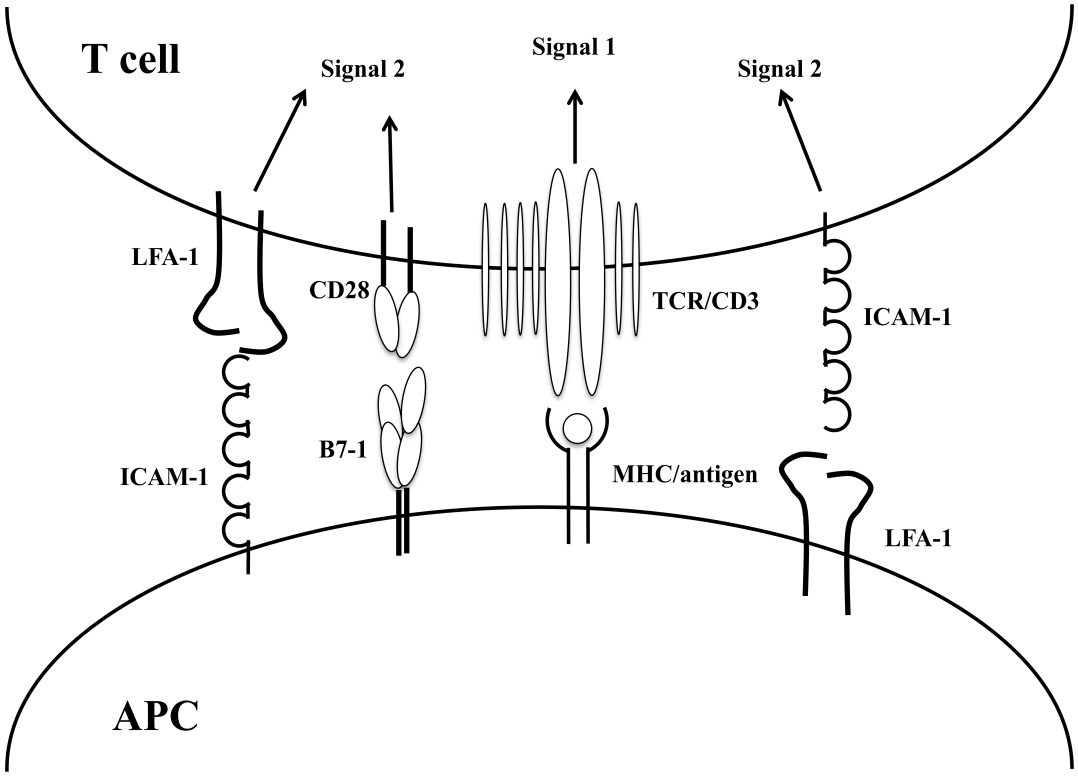
T cell
Signal 2
Signal 1
Signal 2
LFA-1
CD28
TCR/CD3
ICAM-1
B7-1
ICAM-1
MHC/antigen
LFA-1
APC

Figure 1.3. Model of T cell signal. Naïve T cells must receive two signals to become activated. The first signal is received through the TCR/CD3 complex by specific antigen bound to the MHC. The second signal may be received through, for example, CD28, LFA-1 or ICAM-1 on the T cell.

Signal 2: CD28

CD28 belongs to the immunoglobulin family of costimulatory molecules and is expressed as a glycosylated, disulfide-linked homodimer and is expressed on most T cells. The best-studied ligands for CD28 are B7.1 (CD80) and B7.2 (CD86) both of which send a signal through CD28 leading to phosphorylation of tyrosine residues and proline rich regions on the cytoplasmic tail that provide docking sites for src homology-2 (SH2) and src homology-3 (SH3) domain containing proteins (5). The binding of adaptor proteins to the cytoplasmic tail of CD28 allows for downstream activation of JNK, PLCγ1, PI 3-kinase (PI3K), NFAT and NFκB (5). Activation of the PI3K pathway induces the production of phosphatidylinositol (3,4)- bisphosphate (PIP2) and phosphatidylinositol (3,4,5)-trisphosphate (PIP3) which recruit phosphoinositide-dependent kinase 1 (PDK1) and PKB/Akt and lead to an increase in NFκB and NFAT transcription of Bcl-$X_{L,}$ IL-2 and other factors to promote cell survival and proliferation (6, 7). Costimulation through CD28 also promotes the development of both Th1 and Th2 subsets and differentiation to a memory phenotype (8) **(Table 1.1)**.

Signal 2: Leukocyte function-associated antigen-1 (LFA-1)

LFA-1 is a member of the β2 integrin family and is present on all leukocytes. The ligands for LFA-1 are adhesion molecules ICAM-1, ICAM-2 and ICAM-3. LFA-1 forms a heterodimeric complex of the α subunit (CD11a) and β subunit (CD18). On a resting cell surface, LFA-1 has an occluded conformation that changes to an open, active form in response to inside-out signaling and leads to the phosphorylation of the LFA-1 cytoplasmic domain. Signaling through LFA-1 has been linked to the tyrosine kinase

Table 1.1

	TCR(CD3)+CD28	TCR(CD3)+LFA-1	TCR(CD3)+ICAM-1
Proliferation	+	+	+
Activation of Th1 subset	+	+	+
Activation of Th2 subset	+	-	-
Protection from apoptosis	+	-	+
Memory cell development	+	-	+

phosphatidylinositol pathway that activates phospholipase C-γ1 (PLC-γ1) and induction of Ca^{2+} mobilization and to induce NFκB and NFAT transcription factors (9). The LFA-1 signal pathway leads to an initial burst of cell proliferation but limited IL-2 production or protection from apoptosis (10, 11). Cells costimulated through LFA-1 differentiate to a Th1 effector phenotype (12) but this does not lead to the development of immunological memory **(Table 1.1)**.

Signal 2: Intercellular adhesion molecule-1 (ICAM-1)

Relatively little is known about the signaling events that follow costimulation through ICAM-1. ICAM-1, also designated by CD54, is expressed on many cell types including endothelial cells, epithelial cells, monocytes and at low levels on naïve and resting T cells but becomes upregulated following activation (13). ICAM-1 binds to ligands LFA-1, Mac-1, p150/95 and CD43. Initially known for its role as a ligand to LFA-1 on leukocytes during immune cell extravasation into inflamed tissue, ICAM-1 has more recently been shown to be a costimulatory molecule on T cells (14, 15). ICAM-1 is a member of the immunoglobulin (Ig) superfamily. It has five glycosylated extracellular Ig domains that are formed by disulfide bridges, a transmembrane domain and a short cytoplasmic tail **(Fig. 1.4)** (16). The entire ICAM-1 molecule is 505 amino acids with only 28 of those amino acids making up the C-terminal cytoplasmic domain. The cytoplasmic tail contains a tyrosine residue that can be phosphorylated, an SH3 domain and many positively charged amino acids that could all possibly be utilized in binding or recruitment of signal proteins (17). Signaling of ICAM-1 on endothelial cells suggests that the cytoplasmic tail can interact with α-actinin, ezrin, moesin, β –tubulin and recruits

Figure 1.4

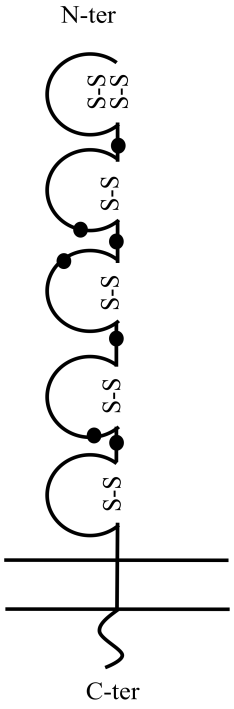

NRQRKIKKYRLQQAQKGTPMKPNTQATPP

Figure 1.4. Structure of the ICAM-1 molecule and amino acid sequence of the cytoplasmic tail. ICAM-1 contains 5 Ig extracellular domains at the N-terminus that are formed from disulfide bridges (S-S), a transmembrane region and a short cytoplasmic tail at the C-terminus. Circles on the extracellular portion indicate possible glycosylation sites. The amino acid sequence of the cytoplasmic tail is indicated below the ICAM-1 structure. The box indicates the SH3 domain.

Src-homology domain 2 containing phosphatase 2 (SHP-2) (18, 19). There is also evidence that ICAM-1 signalling initiates downstream activation of PKC, Src kinases, MAP kinases, Rho, and focal adhesion kinase (FAK) (18-20). Many members of our lab have worked on identifying the signaling proteins that associate with the ICAM-1 cytoplasmic tail on T cells when ICAM-1 is cross-linked in solution. Cdc2 and MAPK are constitutively associated with ICAM-1 and immediately after stimulation a complex that includes Zap-70, Fyn, P-Lck, TCRβ and CD3ζ chains becomes transiently associated (21, unpublished data) **(Fig. 1.5)**.

After a naïve T cell receives a costimulatory signal through ICAM-1 it undergoes activation that leads to proliferation and significant production of IL-2 slightly later than IL-2 secretion with CD28 costimulation (15). Costimulation through ICAM-1 also induces protection from apoptosis and cell differentiation to effector and memory phenotypes (15). Memory-like cells that were generated by costimulation through ICAM-1 were able to proliferate and secrete effector cytokines much quicker and with less signal that naïve T cells (15).

Figure 1.5

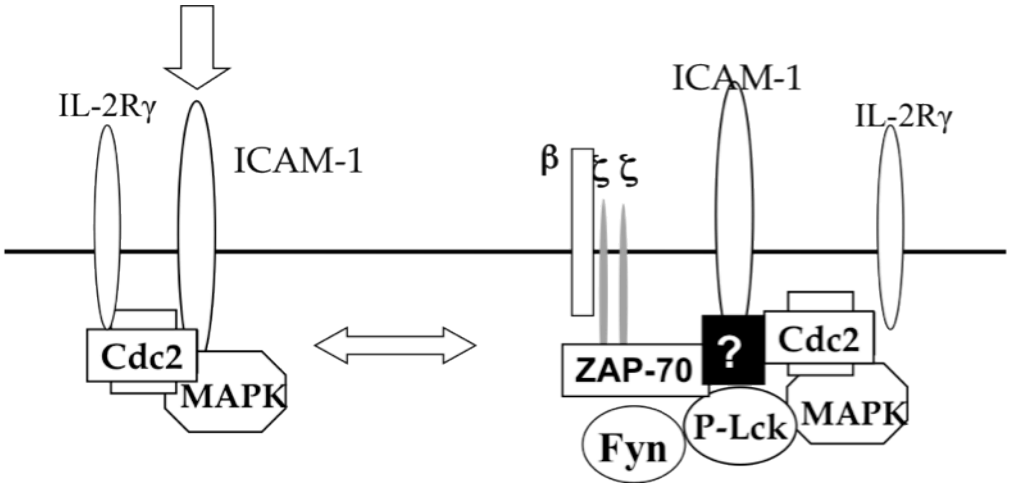
IL-2Rγ
ICAM-1
Cdc2
MAPK
β
ζ ζ
ICAM-1
IL-2Rγ
ZAP-70
?
Cdc2
Fyn
P-Lck
MAPK

Figure 1.5. ICAM-1 signaling complex. Cdc2 and MAPK are constitutively associated with the cytoplasmic tail of ICAM-1. Once a signal is sent into the T cell through ICAM-1, Zap-70, Fyn, P-Lck, TCRβ, CD3ζ and a not yet identified adaptor protein associate with the complex and disassociate within ten minutes. Cdc2 kinase becomes inactivated by phosphorylation and then reactivates by 10 minutes (21).

This dissertation

Chapters 3-6 will examine the role of ICAM-1 in the activation and differentiation of CD4+ naïve T cells to effector and memory cells. Specifically, we will evaluate the duration of signal needed to drive differentiation and homing ability of the differentiated cells and how different costimulatory signals impact differentiation. The affect that immunosenescence has on the ability of naïve T cells to respond to costimulatory signals will also determined. Finally, we will describe a method to differentiate murine CD4+ and naïve T cells to a central memory phenotype. Background information for each chapter will be given in more detail in their individual introductions.

T cells in Type I Diabetes

Autoimmune disease is the result of the loss of central or peripheral tolerance that allows the immune system to attack self-antigens. Auto-reactive T cells are eliminated before they mature and leave the thymus by mechanisms of central tolerance. T cells that escape the thymus and react to self antigens are controlled by peripheral tolerance using regulatory components of the immune system. When this balance malfunctions, auto-reactive cells can begin to attack and destroy self-tissue as is the case with type I diabetes (T1D). T1D is a T cell driven disease where self-reactive T cells attack β-cells in the islets of Langerhans within the pancreas. β-cells produce insulin that is necessary to maintain normal levels of glucose in the blood. Insulin, glucose and glucagon form a tightly regulated negative feedback loop that controls plasma glucose homeostasis. Glucagon is a hormone produced by islet α-cells that promotes gluconeogenesis, the production of glucose from carbon substrates, and glycogenolysis, the breakdown of glycogen (the stored form of glucose) to glucose (22). When the blood glucose level becomes elevated, it induces the secretion of insulin from the β-cells to promote glucose uptake by cells and the use of glucose for energy (22). The loss of blood glucose regulation can lead to ketoacidosis, hypoglycaemia, heart disease, blindness, kidney failure and other complications (23-26).

T cells involved in T1D respond to a number of islet self-antigens, including insulin, glutamic acid decarboxylase 65 (GAD65), insulinoma-associated protein 2 (IA2), zinc transporter 8 (ZnT8), and islet-specific glucose-6-phosphatase catalytic subunit-related protein (IGRP) (27). Initial recognition of islet autoantigens by T cells occurs in

the pancreatic lymph nodes. Destruction of β-cells during insulitis leads to the release of more autoantigens that can be presented by APCs and prime new T cells and result in additional islet destruction (28). Approaches to find therapies for T1D involve inducing specific tolerance to known autoantigens (29, 30), blocking of the immune response (31, 32) and suppressing autoreactivity with regulatory T cells (33). Some therapeutic approaches for T1D have met with limited success and the efficacy of others has yet to be determined.

This dissertation

Chapter two examines the use of peptides derived from the contact domains of ICAM-1 and LFA-1. These peptides block the interaction of ICAM-1:LFA-1 and are being developed by our lab as a therapy for type I diabetes. We have evaluated the effect that blocking the T cell second signal has on progression of the disease, maintenance of islet integrity and the ability of immune cells to respond to specific β-cell antigen or mitogenic stimulus. Specific background about the peptides and the role of T cells in T1D will be described in the next chapter.

References

1. Hara M, Kingsley CI, Niimi M, Read S, Turvey SE, Bushell AR, Morris PJ, Powrie F, Wood KJ. IL-10 is required for regulatory T cells to mediate tolerance to alloantigens in vivo. J Immunol. 2001;166(6):3789-96
2. Xuefang Cao, Sheng F. Cai, Todd A. Fehniger, Jiling Song, Lynne I. Collins, David R. Piwnica-Worms and Timothy J. Ley. Granzyme B and Perforin Are Important for Regulatory T Cell-Mediated Suppression of Tumor Clearance. Immunity. 2007; 27 (4): 635-646
3. Feito MJ, Jiménez-Periañez A, Ojeda G, Sánchez A, Portolés P, Rojo JM. The TCR/CD3 complex: molecular interactions in a changing structure. Arch Immunol Ther Exp (Warsz). 2002; 50(4):263-72
4. Lin J, Weiss A. T cell receptor signaling. J. Cell Sci. 2001; 114(Pt 2): 243-4.
5. Jonathan S. Boomer and Jonathan M. Green. An Enigmatic Tail of CD28 Signaling. Cold Spring Harb Perspect Biol. 2010;2:a002436
6. Sasaki T, Irie-Sasaki J, Jones RG, Oliveira-dos-Santos AJ, Stanford WL, Bolon B, Wakeham A, Itie A, Bouchard D, Kozieradzki I et al. Function of PI3Kg in thymocyte development, T cell activation, and neutrophil migration. Science. 2000; 287: 1040–1046
7. Vanhaesebroeck B, Alessi DR. The PI3K-PDK1 connection: more than just a road to PKB. Biochem. 2000; J 346: 561 – 576
8. Lenschow DJ, Walunas TL, Bluestone JA. CD28/B7 system of T cell costimulation. Annu Rev Immunol. 1996; 14:233–58

9. Kanner SB, Grosmaire LS, Ledbetter JA, and Damle NK. Beta 2-integrin LFA-1 signaling through phospholipase C-gamma 1 activation. Proc Natl Acad Sci U S A. 1993; 90(15): 7099–7103
10. Zuckerman LA, Pullen L, Miller J. Functional consequences of costimulation by ICAM-1 on IL-2 gene expression and T cell activation. J Immunol. 1998; 160(7):3259-68
11. Abraham C, Griffith J, Miller J. The dependence for leukocyte function-associated antigen-1/ICAM-1 interactions in T cell acti- vation cannot be overcome by expression of high density TCR ligand. J Immunol. 1999; 162:4399–405
12. Salomon B. and Bluestone J.A. Cutting Edge: LFA-1 interaction with ICAM-1 and ICAM-2 regulates Th2 cytokine production. J. Immunol. 1998; 161: 5138-5142
13. Roebuck K. and Finnegan A. Regulation of Intercellular Adhesion Molecule-1 (CD54) gene expression. J. Leukocyte Biol. 1999; 66: 876-888.
14. Chirathaworn C, Kohlmeier JE, Tibbetts SA, Rumsey LM, Chan MA, Benedict SH. Stimulation through intercellular adhesion molecule-1 provides a second signal for T cell activation. J Immunol. 2002; 168:5530–7
15. Kohlmeier JE, Chan MA and Benedict SH. Costimulation of naive human CD4+ T cells through intercellular adhesion molecule-1 promotes differentiation to a memory pheno- type that is not strictly the result of multiple rounds of cell division. Immunology. 2006; 118: 549–558

16. Stolpe, AV and PT Saag. Intercellular adhesion molecule - 1. Journal of Molecular Medicine. 1996; 74: 13-33.
17. Greenwood J, Amos CL, Walters CE, Couraud PO, Lyck R, Engelhardt B, Adamson P: Intracellular domain of brain endothelial intercellular adhesion molecule-1 is essential for T lymphocyte-mediated signaling and mi- gration. J Immunol. 2003; 171: 2099–2108.
18. Muro S. VCAM-1 and ICAM-1. Endothelial Biomedicine. New York: Cambridge University Press; 2007: 1058 – 1070.
19. Muro S. New biotechnological and nanomedicine strategies for treatment of lysosomal storage disorders. Wiley Interdiscip Rev Nanomed Nanobiotechnol. 2010;2(2):189-204.
20. Lawson C, Wolf S. ICAM-1 signaling in endothelial cells. Pharmacological Reports. 2009; 61: 22–32
21. Chirathaworn C, Tibbetts SA, Chan MA, Benedict SH. Cross-linking of ICAM-1 on T cells induces transient tyrosine phosphorylation and inactivation of cdc2 kinase. J Immunol. 1995;155(12):5479-82.
22. Aronoff SL, Berkowitz K, Shreiner B, Want L. Glucose Metabolism and Regulation: Beyond Insulin and Glucagon. Diabetes Spectrum. 2004; 17 (3): 183-190
23. Vauzelle-Kervroëdan F, Delcourt C, Forhan A, Jougla E, Hatton F, Papoz L. Analysis of mortality in French diabetic patients from death certificates: a comparative study. Diabete Metab. 1999; 25: 404–411

24. Maahs, D. M. & Rewers, M. Editorial: mortality and renal disease in type 1 diabetes mellitus—progress made, more to be done. J. Clin. Endocrinol. Metab. 2006; 91: 3757–3759

25. Steffes , M. W. et al. (EDIC Research Group). Sustained effect of intensive treatment of type 1 diabetes mellitus on development and progression of diabetic nephropathy: the Epidemiology of Diabetes Interventions and Complications (EDIC) study. J. Am. Med. Assoc. 2003; 290: 2159–2167

26. Bluestone JA, Herold K, Eisenbarth G. Genetics, pathogenesis and clinical interventions in type 1 diabetes. Nature. 2010;464(7293):1293-300.

27. Lieberman SM, DiLorenzo TP. A comprehensive guide to antibody and T-cell responses in type 1 diabetes. Tissue Antigens. 2003; 62: 359–377.

28. Turley S, Poirot L, Hattori M, Benoist C, Mathis D. Physiological beta cell death triggers priming of self-reactive T cells by dendritic cells in a type-1 diabetes model. J. Exp. Med. 2003; 198: 1527–1537

29. Skyler JS, Krischer JP, Wolfsdorf J, Cowie C, Palmer JP, Greenbaum C, Cuthbertson D, Rafkin-Mervis LE, Chase HP, Leschek E. Effects of oral insulin in relatives of patients with type 1 diabetes: the Diabetes Prevention Trial—Type 1. Diabetes Care. 2005;28(5):1068-76.

30. Ludvigsson J, Hjorth M, Chéramy M, Axelsson S, Pihl M, Forsander G, Nilsson NÖ, Samuelsson BO, Wood T, Aman J, Ortqvist E, Casas R. GAD treatment and insulin secretion in recent on set type 1 diabetes. N. Engl. J. Med. 2008; 359: 1909–1920

31. Herold KC, Hagopian W, Auger JA, Poumian-Ruiz E, Taylor L, Donaldson D, Gitelman SE, Harlan DM, Xu D, Zivin RA, Bluestone JA. Anti-CD3 monoclonal antibody in new-onset type 1 diabetes mellitus. N. Engl. J. Med. 2002; 346: 1692–1698

32. Keymeulen,B. Insulin needs after CD3-antibody therapy in new on set type1 diabetes. N. Engl. J. Med. 2005; 352: 2598–2608

33. Levings, M. K., Sangregorio, R. & Roncarolo, M. G. Human CD25(+)CD4(+) T regulatory cells suppress naive and memory T cell proliferation and can be expanded in vitro without loss of function. J. Exp. Med. 2001; 193: 1295–1302

Chapter 2

ICAM-1:LFA-1 blocking peptides eliminate the T cell response in the NOD mouse model for type I diabetes.

Introduction

The autoimmune disease, type I diabetes (T1D) is driven by T cells that are reactive against the pancreatic islets of Langerhans. These self-reactive T cells infiltrate islets and induce destruction of beta cells, gradually rendering the pancreas unable to control blood glucose levels [1]. Each self-reactive T cell is specific for an epitope of one beta cell antigen, of which there are several. In humans, the approximate number of T cell specificities at a given time is 100 million of which only a small percentage participates in T1D. A long sought approach to therapy has been to restore self-tolerance by inducing death or anergy only in the T cells that are attacking the pancreas while leaving the remainder of the uninvolved T cells free to function in defense of the organism.

The present work uses short peptides to block interaction of the counter receptor pair, lymphocyte function associated antigen-1 (LFA-1) and intercellular adhesion molecule-1 (ICAM-1), in NOD mice, as a therapeutic approach for T1D. The proposed mechanism is based on the long-standing concept of second signal blockade. Engagement of the T cell antigen receptor (TCR) by appropriately presented antigen (signal 1) represents the first decision point for the T cell [reviewed in 2, 3]. If the TCR has no specificity for the Ag, the complex dissociates and no signal is transmitted, but if the Ag is cognate, the T cell will initiate activation. This decision point provides the specificity of the T cell response and with T1D, only the disease relevant T cells will respond. To fully activate, the T cell requires a second signal, the most studied of which is received by resident CD28, although several additional T cell surface proteins have been classified as receivers for a second signal [rev, 3]. This includes both the proteins targeted in the present study, ICAM-1 [4] and LFA-1 [5]. With co-delivery of both

signals, the T cell activates, proliferates and begins to function. If signal 1 is delivered but signal 2 is prevented, the T cell dies or is rendered anergic. Thus, the proposed induction of tolerance is based on allowing signal 1 (antigen) and preventing signal 2, the result of which is to inactivate only the cells presently responding to Ag and have no effect on cells not being stimulated by their cognate Ag. The best of the early examples of blockade of LFA-1/ICAM-1 interactions in this manner was facilitation of heart transplants in mice [6] using antibodies against both proteins.

Both LFA-1 and ICAM-1, are resident on the T cell surface, and are known to have costimulatory function that can receive a second signal into an activating T cell [3, 4, 7]. Both LFA-1 and ICAM-1 participate in intercellular adhesion events associated with T cell activation and cytotoxic T cell function [8, 9], and both are important for adhesion, extravasation and migration of leukocytes. Migration is facilitated because LFA-1 is expressed on all leukocytes and ICAM-1 is expressed on many cell types including leukocytes, endothelial and epithelial cells. Thus, a potential second mechanism of action by interfering with interaction of these two is that migration of T cells and other leukocytes toward the site of attack may be transiently impaired as well. Because of their roles in cell contact, cell migration and T cell activation, LFA-1 and ICAM-1 play an important role in the development and maintenance of autoimmune disease [10, 11]. Over nearly two decades, antibody blockade of LFA-1 and ICAM-1 interactions has shown promise for treating T1D by tolerance induction [12-14] but the promise has not been fully realized.

Current approaches to induce tolerance in TID are directed toward inhibition of self-reactive lymphocytes or activation of regulatory components of the immune system,

including regulatory T cells; each of these approaches, however, has drawbacks [15, 16]. As examples, blockade of T cell costimulatory molecules such as CD28/B7, CD40/CD40L or ICAM-1/LFA-1 using antibodies has been explored as a possible therapy to treat T1D or assist in islet graft acceptance in NOD mice. These met with limited success because the therapy had to be initiated prior to insulitis or required blockade of multiple costimulatory pathways [17-20]. Also, administration of mAb to block costimulatory molecule activation can produce harmful side effects such as pruritis, urticaria, leucopenia [21, 22], complement-induced neutrophil activation [23] and allosensitization to the antibody [24].

We have generated peptides derived from human sequences of LFA-1 and ICAM-1 that block intercellular adhesion and inhibit human T cell function in a mixed lymphocyte reaction [25]. These human sequences are conserved in mice and work well in mouse assays *in vitro*. Here, we explore the hypothesis that use of these peptides in the treatment of T1D will induce tolerance to pancreatic auto-antigens. The non-obese diabetic (NOD) mouse is widely used to study T1D [26]. In the present study, our peptides were applied to early stage T1D in the NOD mouse model and islet infiltration and ability of T cells from treated animals to respond to pancreatic Ag was observed. Mechanism of action of the peptides was studied using mouse and human T cells *in vitro*.

Materials and Methods

Mice

Female NOD/ShiLtJ and NOD-SCID (Jackson Laboratories, Bar Harbor,ME) were obtained at 8 and 6 weeks of age, respectively, and were housed individually in barrier cages. Animal experiments were performed with approval from the University of Kansas Animal Care and Use Committee.

Peptides, chemicals and antibodies.

Peptides were prepared and cyclized essentially as we have described previously [25]. Cyclized peptides were purchased from American Peptide Company, Inc. (Sunnyvale, CA). Lyophilized peptides were stored desiccated at -20^{o}C until use when they were resuspended in normal saline at 1μg/μl. For i.v. injections, 50 μl c-IE-L and 50 μl cLAB-L, or 50 μl cIE-L and 50 μl c-LBE-L were mixed immediately prior to use. For *in vitro* experiments, peptides were used at 250 μM each in cell culture RPMI 1640.

Monitoring of diabetes and treatments.

Blood glucose levels (BGL) were monitored weekly before and after treatment and on alternate days during treatment using the OneTouch Ultra 2 glucometer and OneTouch Ultra Blue test strips from LifeScan, Inc. (Milpitas, CA). Mice were fasted 2 h before each BGL reading and mouse weight was determined on the same days as BGL monitoring. Saline, control peptides and therapeutic peptides were injected at 48 h intervals beginning at 13 weeks of age until 17.5 weeks of age. Mice were considered diabetic after two consecutive BGL readings >250 mg/dL. When severity of disease

indicated that mice needed to be terminated, BGL of 600 mg/dL was used thereafter in the calculations for those mice. More than five weeks (39 days) after cessation of injections, mice were sacrificed and pancreata and spleens were harvested for further analysis.

Splenocyte isolation, cell culture and pancreatic lysates.

Spleens were harvested from control or peptide treated NOD mice at 23.5 weeks of age, minced and repeatedly pressed with a 1cc syringe plunger through a sterile 70 μm nylon mesh cell strainer. Erythrocytes were cleared by a five-minute incubation of the cell suspension in ACK lysis buffer (0.15M NH_4Cl, 10mM $KHCO_3$, 0.1mM Na_2EDTA, pH 7.2) at 37^oC. Human T cells were isolated as we have described [27], from peripheral blood of healthy donors by Ficoll-Hypaque (Pharmacia, Piscataway, NJ) centrifugation followed by E-rosetting. T cell purity was verified by flow cytometric analysis. Total splenocytes and human T cells were cultured in complete RPMI 1640 (Mediatech, Herndon, VA) supplemented with 10% FBS (Atlanta Biologicals, Norcross, GA) as described [27]. Pancreatic lysates, used for antigenic stimulation of splenocytes, were made from pancreata of healthy NOD mice. Each pancreas was minced and digested in 1.1 mg/ml Collagenase P (Roche Diagnostics, Morristown, NJ) in HBSS containing 10mM HEPES for 15 minutes in a 37^oC shaking water bath. The digested material was resuspended in normal saline, frozen in liquid N_2 for 10 minutes, thawed at 37^oC and repeated for a total of 3 times to lyse the cells.

Cell stimulation and proliferation assay.

Splenocytes were stimulated via plate bound antibodies as we have described [7] or with 5 μg/ml pancreatic lysates. Antibodies in PBS were attached to 96 well tissue culture plates (Midwest Scientific, St. Louis, MO) by incubation at 37^{o}C for two hours and washed three times with PBS before the addition of splenocytes. Stimulations were performed with 0.5 μg/ml anti-CD3ε (clone 500A2). Human T cell stimulations were performed via the same plate bound procedure using 1 μg/ml anti-CD3 (clone OKT3), 10 μg/ml anti-ICAM-1 (clone R6.5). All cells were stimulated at a concentration of 2x10^{6} cells/ml. For samples cultured with peptides in vitro, cells were incubated with peptides in culture medium for 30 minutes prior to stimulation.

Flow cytometry.

Cell proliferation was measured with CFSE dilution as we have described [7]. Prior to stimulation, T cells were labeled with 2.5μM 5-(and 6)-Carboxyfluorescein diacetate succinimidyl ester (CFSE) from a 5mM stock in DMSO. Cells were incubated for 7 minutes at 37^{o}C in serum-free RPMI 1640. Cells were labeled for flow cytometry by following manufacturer's instructions of the antibody or reagent used. Cell apoptosis and death was analyzed by AnnexinV and 7-AAD (BD Pharmingen, San Jose, CA). For splenocyte surface protein staining, cells were incubated with CD4-PE (clone RM4-5) and CD8-PE-Cy5 (clone 53-6.7) from BD Pharmingen. Human T cells were stained with CD4-APC (clone OKT4) purchased from BioLegend, Inc. (San Diego, CA). All flow cytometry was performed using the Accuri C6 Flow Cytometer and data analysis was performed with CFlow (Accuri Cytometers, Inc., Ann Arbor, MI).

Pancreas imaging.

Pancreata were harvested from treated or control mice and frozen for sectioning. 10 μm planar slices were placed on slides and stained with hematoxylin and eosin (H&E). Islets were scored as pre-insulitis, peri-insulitis, intra-insular insulitus or complete islet destruction based on Bluestone et al., 2010 [1]. Pancreas sections were photographed at 20x using a Zeiss Axioscop photomicroscope (Carl Zeiss MicroImaging, LLC, Thornwood, NY).

Adoptive Transfer

T cells were magnetically isolated from spleens of peptide treated or saline treated mice using a total T cell negative selection separation kit (StemCell technologies, Vancouver, BC, Canada). $5X10^5$ cells were resuspended in 100 μl of sterile saline and injected via tail vein into NOD-SCID mice. BGL was monitored once a week for 40 days after adoptive transfer.

Statistical analysis.

All statistical analysis was performed using GraphPad Prism (GraphPad Software, La Jolla, CA.). Statistical tests and significance for individual figures are indicated in figure legends.

Results

Peptides.

Previous work by others using peptides designed from ICAM-1 demonstrated an ability to cause physical inhibition of LFA-1/ICAM-1 interactions [28, 29]. Our group designed a series of peptides from ICAM-1 and LFA-1 that inhibited the T cell response in a human mixed lymphocyte reaction (MLR) in a dose dependent manner and did not affect cell viability [27]. The peptides also were not agonistic in a T cell activation response. From those "parent" 20 amino acid peptides, short 10 amino acid peptides were synthesized in a more stable cyclic form as we have described [25]. Selected cyclic peptides inhibit T cell adhesion and function in a manner equivalent to the parent peptides and also are not toxic to the cells [25]. **Table 2.1** describes the cyclic peptides used in this study. cIE-L is derived from the first Ig domain of ICAM-1; cLAB-L is synthesized from I-domain of the LFA-1 α-subunit (CD11a); and cLBE-L is derived from the LFA-1 β-subunit (CD18). The therapeutic peptide combination used was cIE-L with cLAB-L and the negative peptide combination used was cIE-L with cLBE-L since the cyclic LBE-L peptide was not as effective in inhibiting T cell function as its parent peptide [25].

Peptide therapy caused a delay in increase of BGL and onset of diabetes.

Whether the peptides that block ICAM-1 and LFA-1 interactions *in vitro* could exert an effect on TID in mice, was addressed by injecting the peptides into female NOD mice beginning at week 13 of age. Mice were monitored for weight and BGL beginning at 11 weeks at which time their BGL averaged 90 mg/dL. By 13 weeks, the average BGL of

Table 2.1
Peptide sequences

Peptide	Derivation*	Sequence**
cIE-L [a,b]	ICAM-1 (26-35)	DQPKLLGIET
cLAB-L [b]	LFA-1α (237-246)	ITDGEATDSG
cLBE-L [a]	LFA-1β (112-122)	DLSYS-LDDLR

[a] Negative peptide combination [b] Therapeutic peptide combination

*Numbers represent specific amino acid residues.
** (-) indicates residue omitted because of synthesis difficulty.

all mice had risen to 130 mg/dL so it was concluded that diabetes had begun and the study was initiated. During BGL-matched grouping of mice, seven mice with an average BGL of 480 mg/dL, were excluded from the study because their disease had progressed well past the stage of early onset which was our target for initiation of therapy. The average BGL of the mice that were placed in the study was 115 mg/dL and it was concluded that diabetes in these animals was in the earliest stages of onset. This was supported by the documented initiation of insulitis at 3 to 4 weeks and the decrease in pancreatic insulin content that occurs at about 12 weeks of age [30], and by the fact that the mice averaged 90 mg/dL at intake.

Mice were placed into three equal groups by matching BGL levels, and injected with therapeutic peptides (cIE-L+cLAB-L), control peptides (cIE-L+cLBE-L) or saline at 48 h intervals; peptides were injected at 50 μg (each) per dose for a total of 100 μg/dose. BGL and weight assessments were recorded at the time of injection. Injections were continued for five weeks (17 injections) with the final injection on day 126. BGL and weight were monitored for an additional five weeks, until day 165 (**Fig. 2.1)**. Mice receiving control peptides exhibited elevated BGL starting at 120 days, about 17 weeks of age, followed shortly by the saline injected mice. The group receiving therapeutic peptides showed a delay in BGL elevation until 145 days, almost three weeks after onset in the controls. Incidence of diabetes as defined by two consecutive weekly BGL readings over 250 mg/dL (**Fig. 2.2**) also was delayed in the therapeutic peptide treated mice as compared with either control group. No difference was observed in mouse weight among the groups **(Fig. 2.3)**.

Figure 2.1

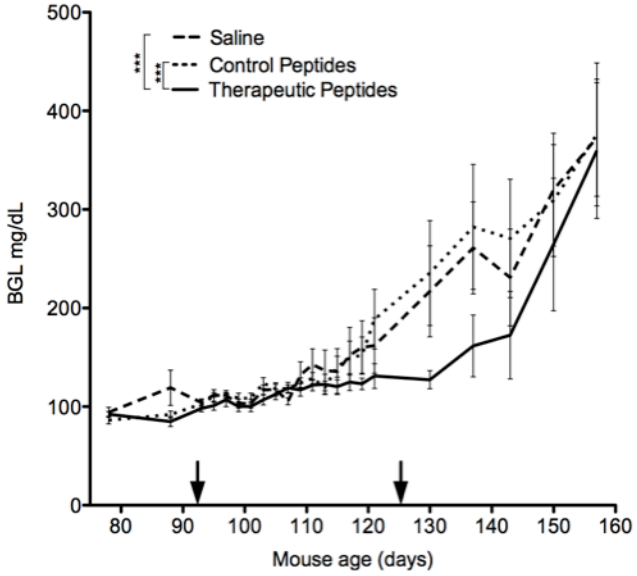

Figure 2.2

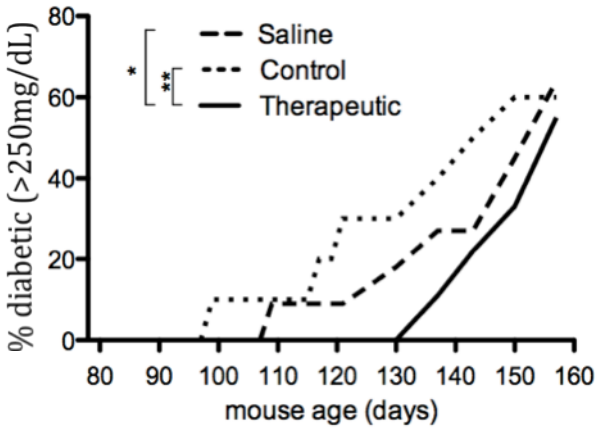

Figure 2.3

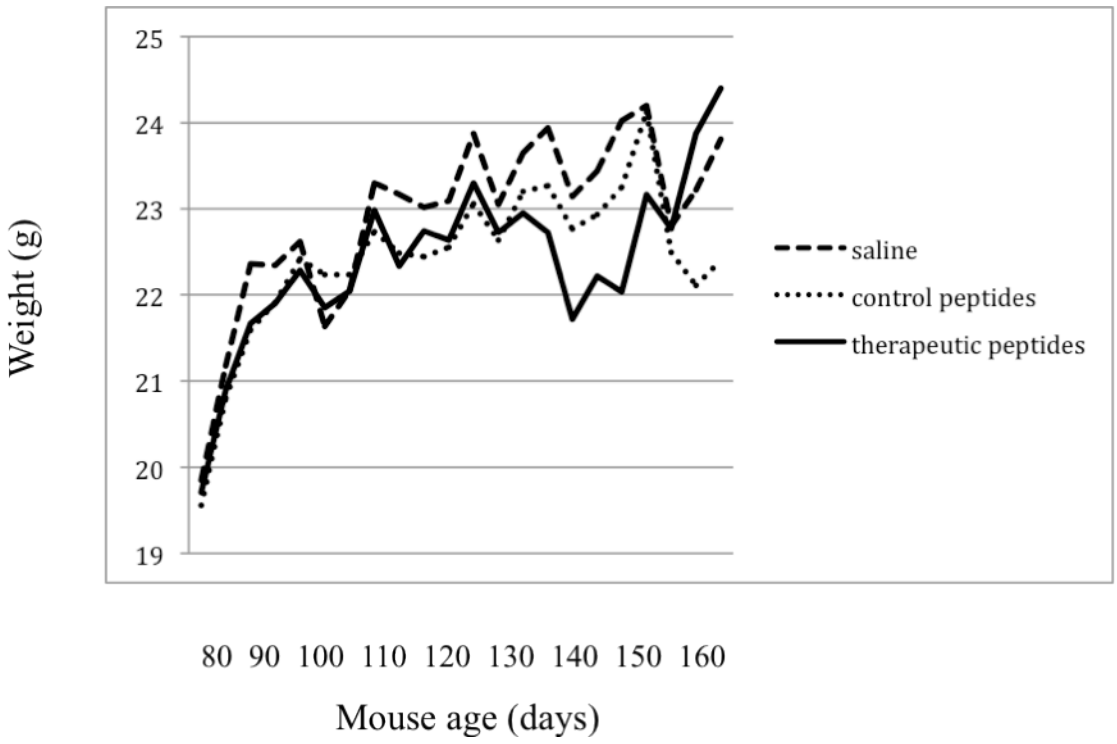
25
24
23
22
21
20
19
Weight (g)
saline
control peptides
therapeutic peptides
80 90 100 110 120 130 140 150 160
Mouse age (days)

Figure 2.1-2.3. Peptide therapy induced a delay in increase of BGL and onset of diabetes. **2.1)** NOD mice were injected on alternate days for five weeks with saline (dashed line), control peptides (dotted line) or therapeutic peptides (solid line). Arrows indicate start and finish of injections which began in week 13 (91 days of life) and ended in week 18 after 17 doses had been administered (126 days). Blood glucose levels (BGL) were monitored weekly and also on injection days from 11 to 22.5 weeks of age. Average BGL is shown for each group (n = 9 to 11 mice per group). **2.2)** Percentages of diabetic mice (>250 mg/dL) are shown over time (n = 9 to 11 mice per group). **2.3)** Average weight in grams over time (n = 9 to 11 mice per group). Statistical significance was determined using one-way ANOVA followed with a Bonferroni correction (A) or using Mann-Whitney test (B). *p<0.05, **p<0.01, ***p<0.001.

Islets in mice treated with therapeutic peptides showed greatly reduced infiltration by immune cells.

The counter receptors ICAM-1 and LFA-1 interact during leukocyte extravasation and thus potentially play a role in infiltration of islets in addition to their proposed role in T cell signaling. Histological examination of the pancreata was performed to estimate the degree of insulitis and leukocyte infiltration present at the end of the experiment. Five weeks after cessation of treatment, pancreata were harvested, paraffin fixed, sectioned and stained with hematoxylin and eosin. Islets were examined and scored for level of infiltration (**Fig. 2.4, 2.5**). Pancreata from saline injected mice exhibited a high level of leukocyte infiltration (**Fig. 2.4**) compared with therapeutically treated mice (**Fig. 2.5**).

The islets found in the tail section of the pancreas were scored for infiltration. Eighteen islets were observed in 3 control mice, and 17 islets were observed in 4 therapeutically treated mice. Infiltration was almost exclusively by mononuclear cells. When scored for level of infiltration (**Fig. 2.6)**, over half the islets from control treated mice had been completely infiltrated and another third were classified in the intra-insular infiltration category while only 5% scored as pre-insulitis indicating no infiltration. In contrast, the majority (almost 85%) of islets from therapeutic mice showed no infiltration. Thus, we conclude that mice treated with the therapeutic peptide combination were experiencing greatly reduced leukocyte infiltration at the time the experiment was terminated than were the mice treated with control treatments.

Figure 2.4

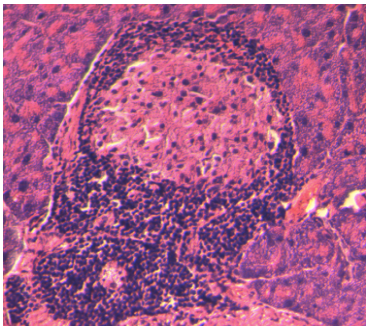

Figure 2.5

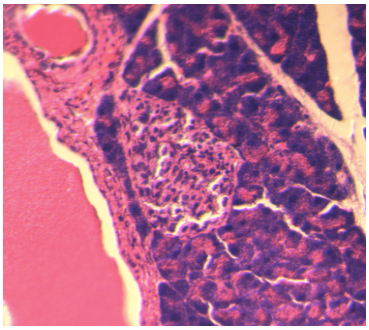

Figure 2.6

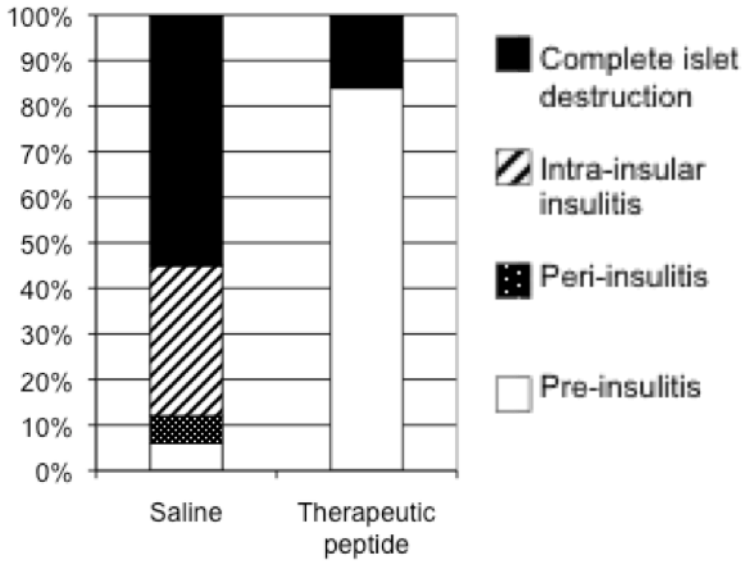

Figure 2.4-2.6. Islets in mice treated with therapeutic peptides showed greatly reduced infiltration. **2.4, 2.5)** Pancreata were isolated from saline control or therapeutic peptide treated mice, and pancreas sections stained with haematoxylin and eosin and scored for infiltration using the scoring system described in the materials and methods. Representative images are shown. **2.6)** Islets were quantified from control and treated mice and level of islet infiltration was determined. (n=18-19 islets per group)

T cells from peptide treated mice did not respond to islet antigen in a recall response.

The basic hypothesis under examination was that inhibition of the costimulatory events delivered by interaction of the counter receptors LFA-1 and ICAM-1 would lead to anergy or death of the antigen reactive T cells. If the hypothesis were to be supported, T cells reactive to pancreatic antigens would be present in the diabetic control mice but not in the therapeutically treated animals.

Splenocytes were harvested five weeks after cessation of therapy. Total splenocytes were stained with CFSE and incubated in culture with 5 μg/ml of pancreatic lysate antigen to induce the antigen specific response, or as a negative control, with medium alone. Proliferation of CD4+ and CD8+ T cells was measured after five days in culture (**Fig. 2.7-2.12**). CD4+ or CD8+ splenocytes from either the saline control mice or therapeutically treated mice (**Fig. 2.7, 2.7**) incubated in the absence of specific antigen underwent minimal spontaneous cell division. CD4+ and CD8+ T cells from saline injected mice responded to pancreatic antigen by proliferating (**Fig. 2.9**), indicating the presence of Ag-specific T cells in both the CD4 and CD8 populations. In contrast, no Ag-induced cell division was observed in cells taken from therapeutically treated mice (**Fig. 2.10**) suggesting that the recall response had been eliminated by the *in vivo* treatment with the therapeutic peptides. In individual experiments, the average increase in the number of dividing cells when stimulated with pancreatic antigen compared to cells with no stimulation was between 15 and 30 fold with the saline control mice. This was in contrast to no increase with the therapeutic peptide treated mice and this difference held true for both CD4+ and CD8+ T cells.

Proliferation indices were calculated by dividing the number of proliferating cells without antigen stimulation into the number of proliferating cells with antigen stimulation minus the number of proliferating cells without antigen; these were plotted for both CD4 and CD8 cells (**Fig. 2.11**). The proliferation index for cells from saline control mice was ~9 for CD4+ T cells and almost 5 for CD8+ T cells while both indices were 0 for cells from therapeutically treated animals. Fold increase of response by cells from individual mice also was plotted for CD4+ and CD8+ cells (**Fig. 2.12**). A value of 1 indicates no response. This approach exhibited the same trend of difference between treatment groups as did quantifying the average number of dividing cells and the proliferation index. It is also noteworthy that the ability to produce a recall response did not influence blood glucose level. **Figure 2.13** diagrams how fold recall would correlate with BGL if the two parameters influenced each other in our study. CD4+ and CD8+ splenocytic recall response did not seem to correlate with an elevation in BGL since the mice with the highest blood glucose did not necessarily exhibit the greatest recall response as measured by fold increase of proliferation with antigen **(Fig. 2.14)**. It is our hypothesis that this is caused by the irregularity of the genetics of the NOD mouse which is spontaneous and thought to have greater than 15 mutations, many of them undefined.

The inability of T cells from therapeutically treated mice to respond to pancreatic antigen suggests that the basic hypothesis was upheld and the Ag-responsive T cells were either rendered anergic or induced to die in response to the therapeutic peptides. However, the possibility that antigen-specific T cells had been induced by the peptide therapy to avoid the spleen and home elsewhere could not be formally ruled out by this experiment.

Figure 2.7

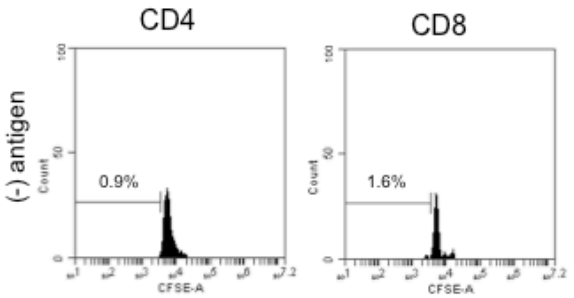

Figure 2.8

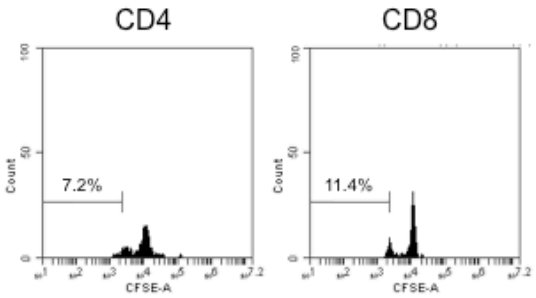

Figure 2.9

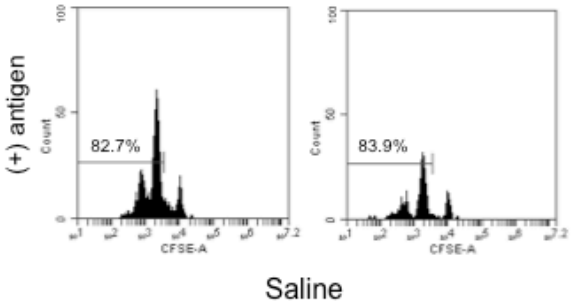

Figure 2.10

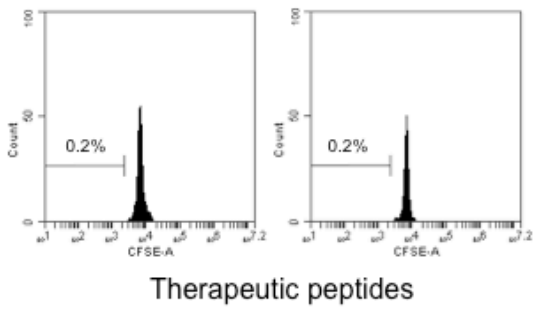

Figure 2.11

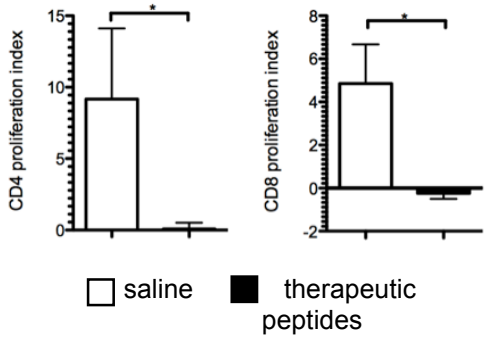

Figure 2.12

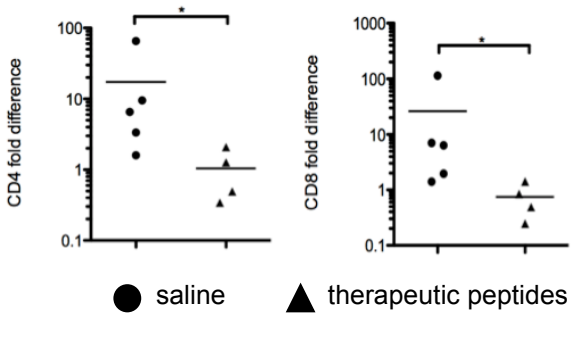

Figure 2.13

Correlation of increased BGL with recall response

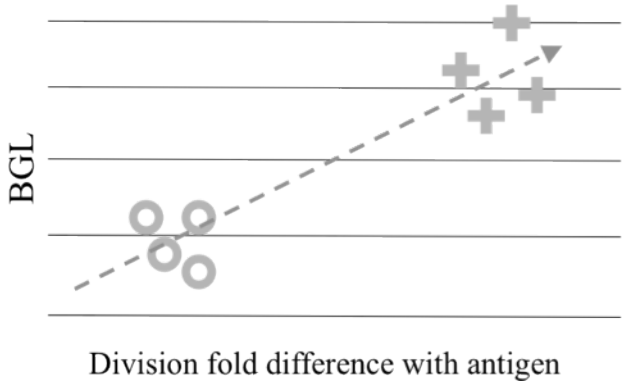

Figure 2.14

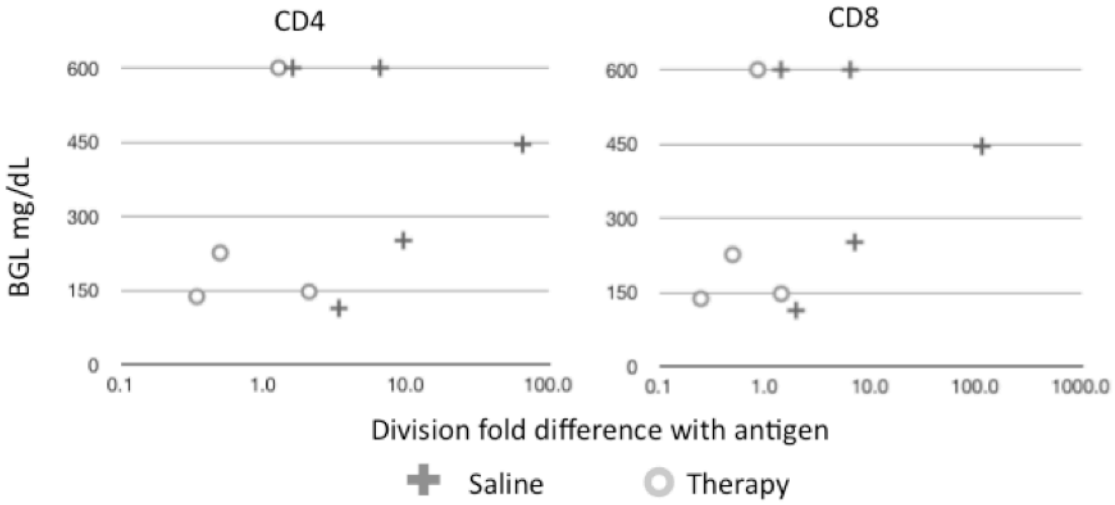

Figure 2.7-2.14. T cells from peptide treated mice did not respond to islet antigen in a recall response. Splenocytes were isolated from mice treated with saline or therapeutic peptides and cultured in medium alone or medium plus pancreatic lysate antigen. Cellular proliferative recall response was determined using a CFSE dilution proliferation assay. Representative flow cytometry histogram plots are shown of CD4+ and CD8+ T cell division without pancreatic antigen **(2.7 and 2.8)** or with antigen **(2.9 and 2.10)** from saline control **(2.7 and 2.9)** or therapeutic peptide treated **(2.8 and 2.10)** mice. **2.11)** Numbers of CD4 and CD8 mouse splenocytes after cell culture without or with antigen of cells from saline control (open bars) or therapeutic peptides (filled bars). **2.12)** Fold change of the response by dividing cells from antigen-stimulated versus nonstimulated CD4+ or CD8+ T cells for each control/treatment group. Circles represent saline and triangles represent therapeutically treated animals. **2.13)** Schematic diagram of fold recall and BGL correlation. **2.14)** Fold increase of the response by dividing cells from antigen-stimulated versus nonstimulated CD4+ or CD8+ T cells compared with final BGL of NOD mice. Data are shown as mean ± SEM (n = 4 to 5 per group). Statistical significance was determined using a Mann-Whitney test. *$p<0.05$.

Spleen-derived T cells from treated mice 7 weeks after cessation of therapy show no significant difference in proliferation compared to control mice.

The lack of recall response in splenocyte T cells five weeks following secession of treatment with therapeutic peptides led to an investigation of how long after treatment the recall response could be affected. Mice that received the same therapeutic peptide treatment regimen as seen in **Figure**s **2.7-2.12** or control mice that received saline injections were left for an additional two weeks and their splenocyte recall response to beta cell antigen was measured at seven weeks post therapy cessation. Proliferating cells in medium alone or with added beta cell antigen were quantified and there were no significant differences in the number of dividing CD4 and CD8 T cells **(Fig. 2.15)** or in the percent of dividing CD4 and CD8 T cells **(Fig. 2.16)** with either therapeutically treated or control saline mice. These data suggest that the peptide treatment will delay the activation of the autoimmune T cell response for five weeks but the recall response might eventually return.

Mouse T cells treated in vitro with peptides did not proliferate in response to mitogenic stimulus.

We also investigated whether a T cell response could be inhibited by exposure to therapeutic peptides *in vitro* immediately before TCR stimulation. Splenocytes from nontreated NOD mice ranging from 10 to 32 weeks of age, at various stages of the disease, were tested for effects of the peptides in an *in vitro* proliferation assay. The mice represented the pre-diabetic stage with BGL of 93, 87, 90; during onset of diabetes with BGL of 168, 179, 138; and frankly diabetic with BGL of 437. Cells were stained with

Figure 2.15

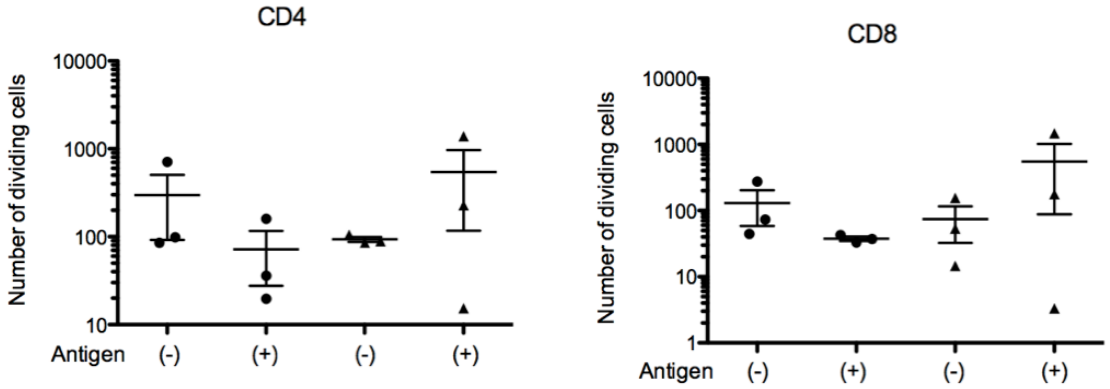

Figure 2.16

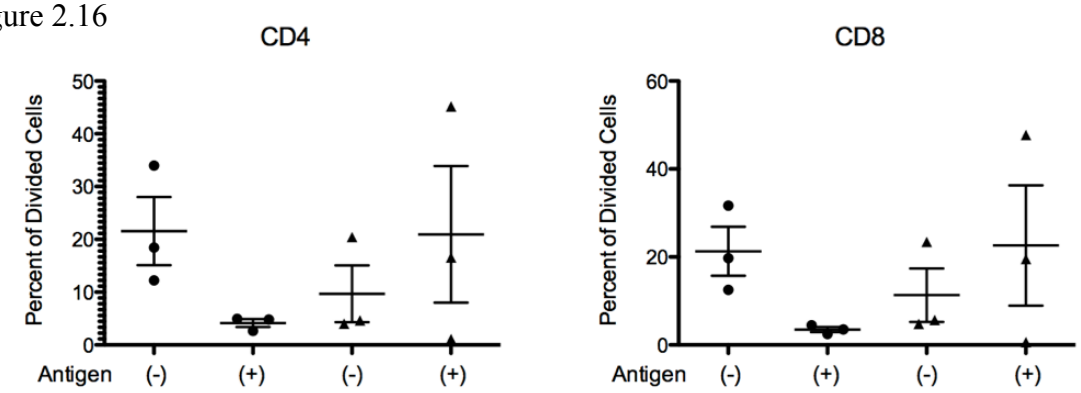

Figure 2.15, 2.16. Splenocyte T cells from treated mice 7 weeks after cessation of therapy show no significant difference in proliferation compared to control mice. Splenocytes were isolated from mice treated with saline or therapeutic peptides and cultured in medium alone or medium plus pancreatic lysate antigen. Cellular proliferative recall response was determined using a CFSE dilution proliferation assay. **2.15)** Numbers of dividing CD4 and CD8 splenocytes after cell culture without or with antigen from saline control (circles) or therapeutic peptides (triangles) injected mice. **2.16)** Percent of dividing CD4 and CD8 splenocytes after cell culture without or with antigen from saline control (circles) or therapeutic peptides (triangles) injected mice. Data are shown with mean ± SEM (n = 3 per group). Statistical significance was determined using a two-tailed Student's paired *t* test.

CFSE and pre-incubated in medium alone or in medium plus therapeutic peptides for thirty minutes. Cells were then cultured on plastic dishes coated with anti-CD3 to activate effector/memory T cells. Activation was determined by measuring CFSE dilution and cells were co-stained for CD4 or CD8 (**Fig. 2.17**). As expected, splenocytes left nonstimulated, with (2.3%) or without therapeutic peptides (5.2%) did not proliferate. Splenoctyes stimulated through CD3 in medium alone for 7 days proliferated (35.4%) whereas splenocytes stimulated through CD3 in the presence of therapeutic peptides did not proliferate (3.0%). Average percent division of stimulated total splenocytes with therapeutic peptides was significantly lower than percent division of splenocytes stimulated in medium alone and not significantly different from nonstimulated (**Fig. 2.18**) illustrating that the therapeutic peptides were able to inhibit proliferation of immune cells taken from healthy mice as well as from mice at early or late stages of disease. CD4+ and CD8+ T cells followed the same proliferation trend as total splenocytes (**Fig. 2.19**).

Peptide treatment ablated the response response to ICAM-1 costimulation in human T cells.

Although conclusions seemed clear with the mouse model, it was important to examine parts of the hypothesis in a human system as well. As mentioned, LFA-1 serves as a costimulatory molecule for T cells [5] and ICAM-1 also acts as a costimulatory molecule in human T cells [4]. When stimulated through the TCR plus ICAM-1, cells undergo multiple rounds of division, are protected from apoptosis and differentiate into a memory phenotype [31]. We investigated whether the therapeutic peptides have the same effect *in vitro* with human T cells as with murine cells by mitogenically stimulating human

Figure 2.17

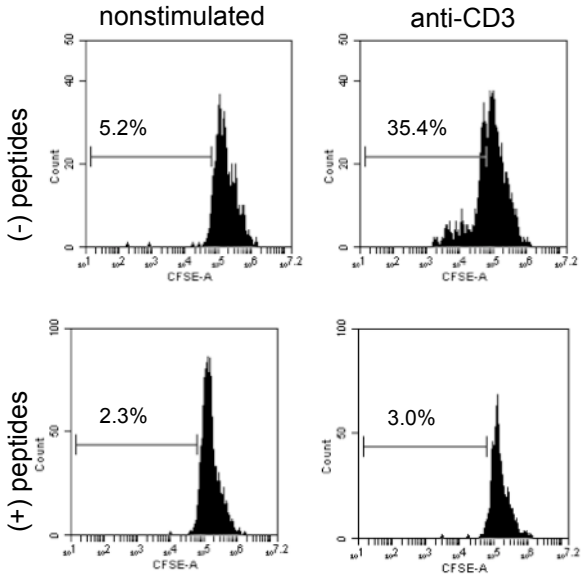

Figure 2.18

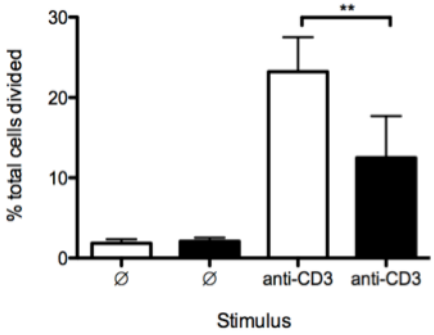

Figure 2.19

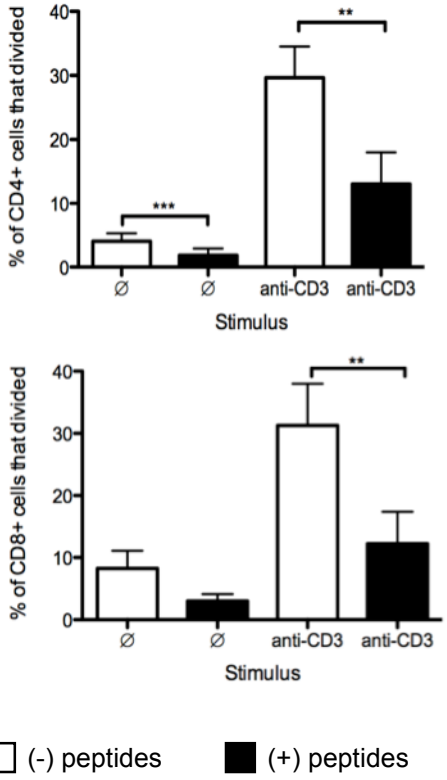

Figure 2.17-2.19. Mouse T cells treated *in vitro* with peptides did not proliferate in response to mitogenic stimulus. Total NOD splenocytes were isolated from nontreated animals at various levels of disease progression and left nonstimulated or stimulated with plate bound anti-CD3 for 7 days, with or without therapeutic peptides. **2.17)** Representative histogram plots of total splenic T cell CFSE dilution by nonstimulated and stimulated cells in the absence (upper panels) or presence (lower panels) of the peptides. **2.18)** Percent of divided splenic T cells without peptides (open bars) and with peptides (closed bars). **2.19)** Percent of CD4+ and CD8+ T cells that divided in the absence of peptides (open bars) and in the presence of peptides (closed bars). Values are presented as mean ± SEM (error bars) and represent data from 7 mice each done in triplicate. Statistical significance was determined using two-tailed Student's paired *t* test. $^{**}p<0.01$, $^{***}p<0.001$.

peripheral T cells in the presence of the therapeutic peptides. Total T cells were isolated from human peripheral blood, stained with CFSE and stimulated with a combination of plate bound antibodies against CD3 + ICAM-1 for 5 days as we have done many times [4]. Proliferation was determined by CFSE dilution and T cell populations were identified with an anti-CD4 co-stain. Results are presented in both dot plots and a histogram representing three separate experiments (**Fig. 2.20**). When cultured in medium alone, total T cells stimulated through CD3+ICAM-1 proliferated robustly (58.5%), undergoing multiple rounds of division (**Fig. 2.20** upper left panel), and this proliferation was ablated (2.1%) when cells were stimulated in the presence of therapeutic peptides (**Fig. 2.20,** upper right panel). When the purified T cells were stained for CD4, (**Fig. 2.20**, lower panels), we observed that the CD4+ cells proliferated robustly (41%) as did the CD4(-) (CD8+) T cells (17.4%) in response to the stimuli (left panel). In the presence of therapeutic peptides (right panel) neither the CD4+ nor CD8+ cells proliferated.

The average percent (**Fig. 2.21**) of total (left panel), CD4+ (center panel) and CD8+ (right panel) T cells that had undergone division when stimulated in the presence of therapeutic peptides was dramatically lower than cells stimulated without peptides. We conclude that the peptides were capable of inhibiting T cell activation induced by costimulation through CD3+ICAM-1 in human cells.

Figure 2.20

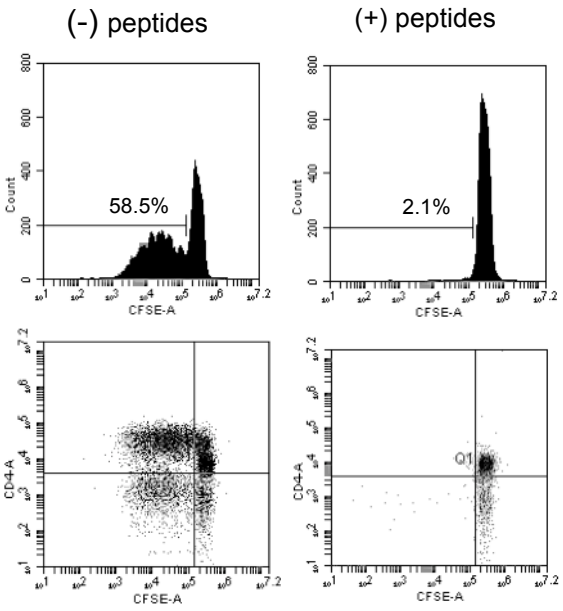

Figure 2.21

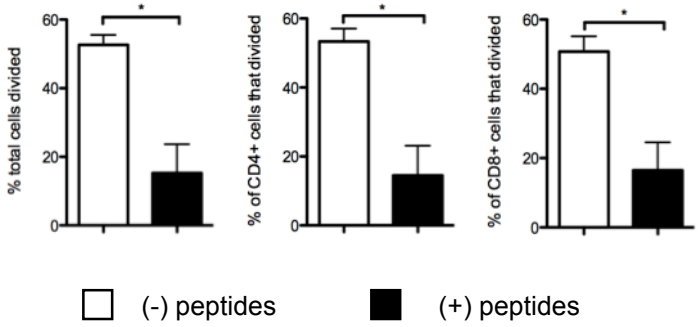

Figure 2.20, 2.21. Peptide treatment ablated the response and increased apoptosis in response to ICAM-1 costimulation in human T cells. Human T cells were isolated from peripheral blood and stimulated for five days with plate bound anti-CD3+anti-ICAM-1. **2.20)** Representative histogram plots of CFSE dilution by total T cells (upper panels) and dot plots of CFSE dilution (lower panels) of CD4+ and CD8+ [CD4(-)] T cells in the absence or presence of the therapeutic peptides. **2.21)** Percent of total T cells (left panel), CD4+ cells (center panel), or CD8+ cells (right panel) that divided in the absence (open bars) or in the presence (closed bars) of therapeutic peptides. Values are presented as mean ± SEM (error bars) and represent data from one subject done in triplicate. Statistical significance was determined using two-tailed Student's paired *t* test. **p*<0.05.

Preliminary data: NOD mice that receive a shorter duration of therapy are still protected from T1D up to 11 weeks after cessation of therapy and their splenic T cells do not cause T1D when injected into NOD-SCID mice.

The ability to achieve a therapeutic response with as few doses as possible is desirable from an economic standpoint as well for convenience to the recipient. This led us to investigate whether we could achieve the same therapeutic results with seven doses administered on alternate days as we observed using the seventeen such doses that were used in **Figures 2.1-2.14**. This study was done in collaboration with Courtney Gdowski. When NOD mice reached an average BGL of 107 mg/dL, mice were placed into two equal groups by matching BGL levels, and injected with either therapeutic peptides or saline for a series of seven injections that spanned over fourteen days. Mice receiving saline injections exhibited elevated BGL starting immediately after the termination of injections **(Fig. 2.22)**. The group receiving therapeutic peptides failed to exhibit an increase in BGL, even at eleven weeks after peptide treatment was stopped **(Fig. 2.22)**. The longevity of the health of the NOD mice receiving therapeutic treatment indicates that T1D symptoms were not only delayed, as in **Figure 2.1**, but also prevented in the longer term. To further determine the any autoreactive capabilities of the T cells from mice that received treatment, T cells from treated or saline mice were injected into NOD-SCID mice and they were observed for symptoms. NOD-SCID mice are a T cell-deficient NOD strain, therefore any signs of T1D must be induced by injected autoreactive T cells. T cells were isolated from the spleen of NOD mice nine weeks after termination of peptide therapy or saline injections and these cells were injected into NOD-SCID mice. The control mice that received T cells from saline injected mice began

to show an increase in BGL 20 days after adoptive transfer and had reached 600mg/dL by 35 days **(Fig. 2.23)**. NOD-SCID mice that were injected with T cells taken from therapeutically treated mice remained symptom free through 40 days post-adoptive transfer **(Fig. 2.23)**. The adoptive transfer data support our observations of the protection from disease after administration of seven therapeutic doses seen in **Figure 2.22**.

Figure 2.22

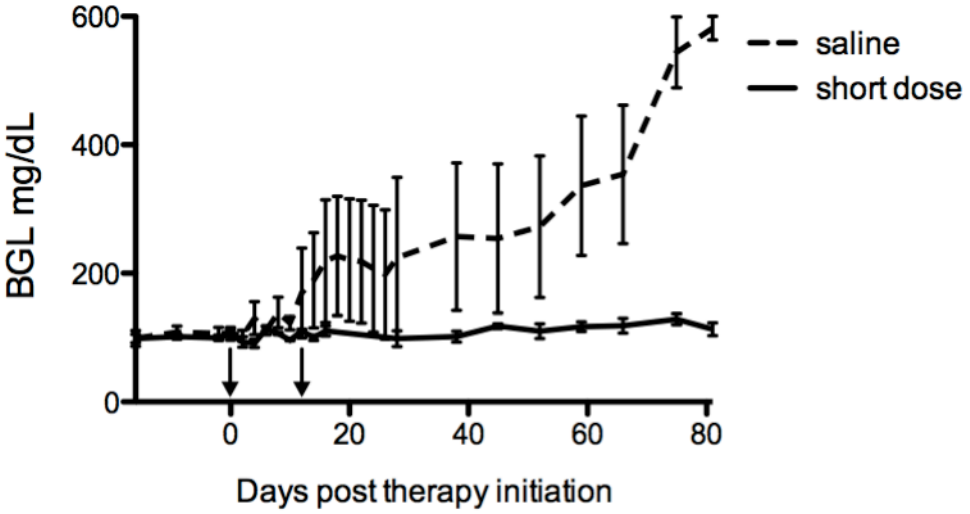

Figure 2.23

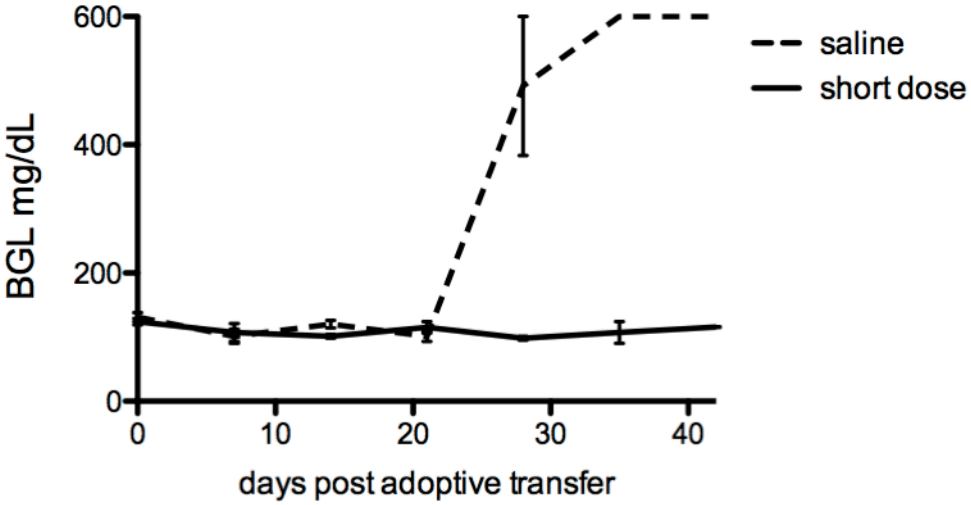

Figure 2.22, 2.23. Preliminary data: NOD mice that receive a shorter duration of therapy are still protected from T1D up to 11 weeks after cessation of therapy and their splenic T cells do not cause T1D when injected into NOD-SCID mice. **2.22)** NOD mice were injected on alternate days for two weeks (seven total doses) with saline (dashed line) or therapeutic peptides (solid line). Arrows indicate start and finish of injections. Blood glucose levels (BGL) were monitored on injection days and then weekly after treatment ended. Average BGL is shown for each group (n = 2-5 mice per time point for each group). **2.23)** NOD-SCID mice were injected with $5X10^5$ isolated T cells from spleens of saline control (dashed line) or therapy injected mice (solid line) from figure 7A. After adoptive transfer, blood glucose levels (BGL) were monitored weekly for 40 days. Average BGL is shown for each group (n = 2 mice per group).

Discussion

Type-1 diabetes is a T cell driven autoimmune disease that can lead to lifetime dependence on insulin as well as disease-related complications that can be very severe [32]. Interaction of the adhesion molecule, ICAM-1 with the integrin, LFA-1 likely plays an important role in the progression of the disease since ICAM-1 has been shown to be expressed at high levels on vascular endothelium, ductal epithelial cells and endothelial cells in NOD mouse pancreas and on infiltrating lymphocytes [14, 33, 34]. Since ICAM-1 is also a costimulatory molecule for T cells it could play a role in T cell activation in disease along with T cell migration. Our previous findings have identified short, cyclic peptides that inhibit ICAM-1:LFA-1 interactions, thereby arresting T cell activation [27]. In the present study, we examined the ability of our ICAM-1- and LFA-1-derived peptides to reduce the severity of T1D in the NOD mouse model and the mechanism by which this might happen.

As mentioned, costimulatory blockade has been examined by other investigators for treatment of diabetes and other autoimmune diseases. In one example, use of CTLA4Ig (which binds to B7 molecules on antigen presenting cells) and anti-B7.2 to interfere with the CD28/B7 pathway during the development of diabetes, inhibited the disease when administered at 2-4 weeks of age but not after 10 weeks in NOD mice [17]. Also, this therapy did not inhibit insulitis at any stage of administration; but treatment with anti-B7.1 actually accelerated the disease [17]. Inhibiting the CD40/CD40L interaction also ablates the disease in NOD mice when administered at 3 weeks of age but not after 9 weeks and the mechanism is not via a regulatory T cell pathway [18]. Blocking multiple costimulatory pathways does provide more efficient treatment of T1D in a mouse model

than blockade of a single costimulatory pathway. The combination of monoclonal antibodies against ICOS and CD40L significantly diminished disease in NOD mice compared with blockade of either pathway alone even when the treatment was given at 10 weeks of age [19]. Previous work with ICAM-1/LFA-1 blockade was conducted with monoclonal antibodies and reduced symptoms of T1D [13]. This was attributed to the inability of lymphocytes to enter islets, and was not considered to be due to a lymphocyte functional impairment. Our present data suggest that blocking the LFA-1/ICAM-1 interaction with our short cyclic peptides inhibits both T cell localization and T cell function.

When administered to NOD mice that had begun to undergo insulitis and experience elevated BGL, the therapeutic peptides were able to delay onset of diabetes by 3 to 4 weeks (from ~day 120 until day 145) as measured by blood glucose level compared to saline or control peptides. In addition, some of the mice that were not treated with therapeutic peptides did not survive until the conclusion of observations. The control mice began to show symptoms before cessation of injections whereas the therapeutically treated mice avoided symptoms for an additional three weeks. This delay also was evident when quantifying the percent of control versus therapeutically treated mice that are considered to be diabetic based on BGL.

The ICAM-1:LFA-1 interaction is important for autoreactive T cells to migrate into the pancreas and initiate β cell destruction [13, 14, 35]. Mice were sacrificed and organs harvested at day 165 of the experiment which is 5.6 weeks after injections were discontinued. Pancreata from therapeutic peptide treated mice showed much less infiltration compared with islets from saline treated mice which were highly infiltrated.

From the *in vivo* experiments, it formally remains unclear whether the autoreactive T cells were inactivated by the peptides *in vivo* or had been induced to migrate to a different location or not migrate at all. Islet specific T cell clones have been established from spleens of NOD mice [36, 37], suggesting that antigen-specific responses in the spleen are representative of the T cell response in T1D. To test this in our system, we examined spenocytes from our treated and control mice for islet-antigen-specific reactivity. Splenocytes isolated from saline control mice specifically responded to β cell antigen whereas splenocytes from therapeutically treated mice did not activate in the presence of specific antigen. This suggests that the therapeutic peptides rendered the mixed T cell population unable to respond to pancreatic antigens. Splenocytes from untreated NOD mice exhibiting varied levels of disease also did not respond to TCR stimulation when incubated with therapeutic peptides *in vitro*.

Our data suggest that the therapeutic peptides inactivated the T cell component of T1D, however, the mice still eventually did develop symptoms in the 17 dose experiment. One possibility is that the therapy was initiated too late after onset of insulitis. In these mice, insulitis begins around five weeks of age [26]. As early as three weeks of age dendritic cells and macrophages are found in insulitic infiltrates and thought to drive early autoreactive responses [38-40]. It is conceivable that islet destruction was too advanced for recovery from symptoms even though the therapy stopped infiltration and diminished T cell response. Also, insulin autoantibodies can reach peak levels in prediabetic mice, well before the onset of symptoms and elevated BGL [41, 42]. Although T1D is a T cell driven disease, insulin autoantibodies are a contributing factor

to disease progression and would have begun to be produced at elevated levels by the time of administration of the therapeutic peptides.

Introduction into a C57BL/6 background of an MHC haplotype known to be involved in development of T1D in NOD mice did not lead to disease [43]; hence, MHC autoreactivity alone is insufficient to induce T1D. This suggests that multiple genetic components are involved and even if some of the immune components can be diminished in the NOD mouse, disease progression may continue based on other predisposing genetic factors. The use of the NOD mouse model for T1D has many advantages when examining the immune reaction due to its similarity to the human immune process of disease [44], however, the usefulness of the model has come into question [45-47] and an alternative animal model as well as additional *in vitro* human studies with the therapeutic peptides are required.

Taken together, the data presented here suggest that peptide blockade of LFA-1:ICAM-1 interactions in NOD mice experiencing onset of diabetes could delay onset of symptoms. The delay was achieved by a mechanism that inhibited infiltration into the pancreas as well as eliminating T cells with reactivity to pancreatic antigens. *In vitro*, the peptides inhibited activation of both murine and human T cells that were under a mitogenic stimulus. The accumulated data suggest that a combination of LFA-1 and ICAM-1 blocking peptides may potentially provide a useful therapeutic model for autoimmune disease and organ transplantation.

References

1. Bluestone JA, Herold K, Eisenbarth G: Genetics, pathogenesis and clinical interventions in type 1 diabetes. Nature 2010;464:1293-1300.

2. Kwon E, Hurwitz A, Foster B, Madias C, Feldhaus A, Breenberg N, Burg M, Allison J. Manipulation of T cell costimulatory and inhibitory signals for immunotherapy of prostate cancer. Proc Natl Acad Sci. 1997; 94: 8099-8103.

3. Kohlmeier JE, Benedict SH: Alternate costimulatory molecules in T cell activation: differential mechanisms for directing the immune response. Histol Histopathol 2003;18:1195-1204

4. Chirathaworn C, Kohlmeier JE, Tibbetts SA, Rumsey LM, Chan MA, Benedict SH: Stimulation through intercellular adhesion molecule-1 provides a second signal for T cell activation. Journal of immunology 2002;168:5530-5537

5. Ni HT, Deeths MJ, Li W, Mueller DL, Mescher MF: Signaling pathways activated by leukocyte function-associated Ag-1-dependent costimulation. Journal of immunology 1999;162:5183-5189

6. Isobe M, Yagita H, Okumura K, Ihara A. Specific acceptance of cardiac allograft after treatment with anti-ICAM-1 and anti-LFA-1. Science 1992; 255:1125-1127.

7. Kohlmeier JE, Rumsey LM, Chan MA, Benedict SH: The outcome of T-cell costimulation through intercellular adhesion molecule-1 differs from costimulation through leukocyte function-associated antigen-1. Immunology 2003;108:152-157

8. Larson RS, Springer TA: Structure and function of leukocyte integrins. Immunol Rev 1990;114:181-217

9. van de Stolpe A, van der Saag PT: Intercellular adhesion molecule-1. J Mol Med 1996;74:13-33

10. Yagi N, Yokono K, Amano K, Nagata M, Tsukamoto K, Hasegawa Y, Yoneda R, Okamoto N, Moriyama H, Miki M, et al.: Expression of intercellular adhesion molecule 1 on pancreatic beta-cells accelerates beta-cell destruction by cytotoxic T-cells in murine autoimmune diabetes. Diabetes 1995;44:744-752

11. Linn T, Strate C, Federlin K, Papaccio G: Intercellular adhesion molecule-1 (ICAM-1) expression in the islets of the non-obese diabetic and low-dose streptozocin-treated mouse. Histochemistry 1994;102:317-321

12. Martin S, Heidenthal E, Schulte B, Rothe H, Kolb H: Soluble forms of intercellular adhesion molecule-1 inhibit insulitis and onset of autoimmune diabetes. Diabetologia 1998;41:1298-1303

13. Herold KC, Vezys V, Gage A, Montag AG: Prevention of autoimmune diabetes by treatment with anti-LFA-1 and anti-ICAM-1 monoclonal antibodies. Cellular immunology 1994;157:489-500

14. Hasegawa Y, Yokono K, Taki T, Amano K, Tominaga Y, Yoneda R, Yagi N, Maeda S, Yagita H, Okumura K, et al.: Prevention of autoimmune insulin-dependent diabetes in non-obese diabetic mice by anti-LFA-1 and anti-ICAM-1 mAb. Int Immunol 1994;6:831-838

15. Luo X, Herold KC, Miller SD: Immunotherapy of type 1 diabetes: where are we and where should we be going? Immunity 2010;32:488-499

16. Castro CN, Barcala Tabarrozi AE, Noguerol MA, Liberman AC, Dewey RA, Arzt E, Morelli AE, Perone MJ: Disease-modifying immunotherapy for the management of autoimmune diabetes. Neuroimmunomodulation 2010;17:173-176

17. Lenschow DJ, Ho SC, Sattar H, Rhee L, Gray G, Nabavi N, Herold KC, Bluestone JA: Differential effects of anti-B7-1 and anti-B7-2 monoclonal antibody treatment on the development of diabetes in the nonobese diabetic mouse. J Exp Med 1995;181:1145-1155

18. Balasa B, Krahl T, Patstone G, Lee J, Tisch R, McDevitt HO, Sarvetnick N: CD40 ligand-CD40 interactions are necessary for the initiation of insulitis and diabetes in nonobese diabetic mice. Journal of immunology 1997;159:4620-4627

19. Nanji SA, Hancock WW, Luo B, Schur CD, Pawlick RL, Zhu LF, Anderson CC, Shapiro AM: Costimulation blockade of both inducible costimulator and CD40 ligand induces dominant tolerance to islet allografts and prevents spontaneous autoimmune diabetes in the NOD mouse. Diabetes 2006;55:27-33

20. Rigby MR, Trexler AM, Pearson TC, Larsen CP: CD28/CD154 blockade prevents autoimmune diabetes by inducing nondeletional tolerance after effector T-cell inhibition and regulatory T-cell expansion. Diabetes 2008;57:2672-2683

21. Kavanaugh AF, Davis LS, Nichols LA, Norris SH, Rothlein R, Scharschmidt LA, Lipsky PE: Treatment of refractory rheumatoid arthritis with a monoclonal antibody to intercellular adhesion molecule 1. Arthritis Rheum 1994;37:992-999

22. Haug CE, Colvin RB, Delmonico FL, Auchincloss H, Jr., Tolkoff-Rubin N, Preffer FI, Rothlein R, Norris S, Scharschmidt L, Cosimi AB: A phase I trial of

immunosuppression with anti-ICAM-1 (CD54) mAb in renal allograft recipients. Transplantation 1993;55:766-772; discussion 772-763

23. Vuorte J, Lindsberg PJ, Kaste M, Meri S, Jansson SE, Rothlein R, Repo H: Anti-ICAM-1 monoclonal antibody R6.5 (Enlimomab) promotes activation of neutrophils in whole blood. Journal of immunology 1999;162:2353-2357
24. Turgeon NA, Avila JG, Cano JA, Hutchinson JJ, Badell IR, Page AJ, Adams AB, Sears MH, Bowen PH, Kirk AD, Pearson TC, Larsen CP: Experience with a novel efalizumab-based immunosuppressive regimen to facilitate single donor islet cell transplantation. Am J Transplant 2010;10:2082-2091
25. Tibbetts SA, Seetharama Jois D, Siahaan TJ, Benedict SH, Chan MA: Linear and cyclic LFA-1 and ICAM-1 peptides inhibit T cell adhesion and function. Peptides 2000;21:1161-1167
26. Van Belle TL, Taylor P, von Herrath MG: Mouse Models for Type 1 Diabetes. Drug Discov Today Dis Models 2009;6:41-45
27. Tibbetts SA, Chirathaworn C, Nakashima M, Jois DS, Siahaan TJ, Chan MA, Benedict SH: Peptides derived from ICAM-1 and LFA-1 modulate T cell adhesion and immune function in a mixed lymphocyte culture. Transplantation 1999;68:685-692
28. Fecondo JV, Kent SB, Boyd AW: Inhibition of intercellular adhesion molecule 1-dependent biological activities by a synthetic peptide analog. Proc Natl Acad Sci U S A 1991;88:2879-2882
29. Ross L, Hassman F, Molony L: Inhibition of Molt-4-endothelial adherence by synthetic peptides from the sequence of ICAM-1. J Biol Chem 1992;267:8537-8543

30. Anderson MS, Bluestone JA: The NOD mouse: a model of immune dysregulation. Annual review of immunology 2005;23:447-485

31. Kohlmeier JE, Chan MA, Benedict SH: Costimulation of naive human CD4 T cells through intercellular adhesion molecule-1 promotes differentiation to a memory phenotype that is not strictly the result of multiple rounds of cell division. Immunology 2006;118:549-558

32. Atkinson MA, Eisenbarth GS: Type 1 diabetes: new perspectives on disease pathogenesis and treatment. Lancet 2001;358:221-229

33. Lee MS, Sarvetnick N: Induction of vascular addressins and adhesion molecules in the pancreas of IFN-gamma transgenic mice. Journal of immunology 1994;152:4597-4603

34. McMurray RW: Adhesion molecules in autoimmune disease. Semin Arthritis Rheum 1996;25:215-233

35. Saravia-Fernandez F, Durant S, el Hasnaoui A, Dardenne M, Homo-Delarche F: Environmental and experimental procedures leading to variations in the incidence of diabetes in the nonobese diabetic (NOD) mouse. Autoimmunity 1996;24:113-121

36. Faveeuw C, Gagnerault MC, Lepault F: Expression of homing and adhesion molecules in infiltrated islets of Langerhans and salivary glands of nonobese diabetic mice. Journal of immunology 1994;152:5969-5978

37. Haskins K, Portas M, Bradley B, Wegmann D, Lafferty K: T-lymphocyte clone specific for pancreatic islet antigen. Diabetes 1988;37:1444-1448

38. Verdaguer J, Schmidt D, Amrani A, Anderson B, Averill N, Santamaria P: Spontaneous autoimmune diabetes in monoclonal T cell nonobese diabetic mice. J Exp Med 1997;186:1663-1676

39. Jansen A, Homo-Delarche F, Hooijkaas H, Leenen PJ, Dardenne M, Drexhage HA: Immunohistochemical characterization of monocytes-macrophages and dendritic cells involved in the initiation of the insulitis and beta-cell destruction in NOD mice. Diabetes 1994;43:667-675

40. Bouma G, Coppens JM, Mourits S, Nikolic T, Sozzani S, Drexhage HA, Versnel MA: Evidence for an enhanced adhesion of DC to fibronectin and a role of CCL19 and CCL21 in the accumulation of DC around the pre-diabetic islets in NOD mice. European journal of immunology 2005;35:2386-2396

41. Delovitch TL, Singh B: The nonobese diabetic mouse as a model of autoimmune diabetes: immune dysregulation gets the NOD. Immunity 1997;7:727-738

42. Greeley SA, Katsumata M, Yu L, Eisenbarth GS, Moore DJ, Goodarzi H, Barker CF, Naji A, Noorchashm H: Elimination of maternally transmitted autoantibodies prevents diabetes in nonobese diabetic mice. Nat Med 2002;8:399-402

43. Yui MA, Muralidharan K, Moreno-Altamirano B, Perrin G, Chestnut K, Wakeland EK: Production of congenic mouse strains carrying NOD-derived diabetogenic genetic intervals: an approach for the genetic dissection of complex traits. Mamm Genome 1996;7:331-334

44. Thayer TC, Wilson SB, Mathews CE: Use of nonobese diabetic mice to understand human type 1 diabetes. Endocrinology and metabolism clinics of North America 2010;39:541-561

45. Atkinson MA, Leiter EH: The NOD mouse model of type 1 diabetes: as good as it gets? Nat Med 1999;5:601-604

46. Roep BO, Atkinson M: Animal models have little to teach us about type 1 diabetes: 1. In support of this proposal. Diabetologia 2004;47:1650-1656

47. Roep BO, Atkinson M, von Herrath M: Satisfaction (not) guaranteed: re-evaluating the use of animal models of type 1 diabetes. Nat Rev Immunol 2004;4:989-997

Chapter 3

Early development of a memory T cell phenotype with costimulation through ICAM-1 that is not influenced by additional costimulation

Introduction

Immunological memory is a defining characteristic of the adaptive immune system. Memory T cells are an essential component of the immune response because they can provide long-term protection against foreign antigens, activate rapidly into effector cells following secondary stimulus and require less signal than naïve T cells to become activated. CD4+ memory T cells are especially important because they confer longer immunological protection than antibody or CD8+ memory cells (1,2) and are essential for initiating secondary B cell and cytotoxic T cell responses.

CD4+ memory T cells exhibit multiple protective functions in the body. After activation, resting memory cells begin to produce effector cytokines within hours, whereas naïve cells require days to activate in response to antigen (3,4). Activated memory T cells can rapidly secrete proinflammatory cytokines and chemokines to recruit leukocytes to sites of inflammation and initiate the innate immune response much quicker than naïve cells (5,6). Activated CD4+ T cells influence the adaptive immune response by producing Th1 cytokines to initiate the cytotoxic T cell response or by producing Th2 cytokines and expressing additional cell surface molecules such as CD40L to activate the humoral response (7-9). The secondary T helper response generated from memory cells is superior to the primary effector response from naïve cells due primarily to the prompt nature of the response as well as the ability to produce more effector molecules (10). This is demonstrated, in part, by the fact that secondary effector CD4+ T cells could protect mice from influenza better than primary effectors without antiviral CD8+ T cell or B cell components (11).

Memory T cells can be defined as CD45RO+, CDlla+ and CD27(-) (12). Central memory T cells (T_{CM}) also express CCR7 and CD62L, which allow the cells to circulate into the peripheral lymph nodes (PLNs) for immunosurveillance (13). While IL-15 is necessary for CD8+ memory cell survival, IL-7 and TCR:MHC II engagement are more important for CD4+ memory cell generation, survival and homeostasis (14-19). Memory cells have less strict requirements for activation compared to naïve cells. Lower doses of antigen, reduced levels of costimulation and/or shorter duration of signal is needed for memory T cells to activate than naïve (20,21). Upon reactivation, CD4+ memory T cells can alter their effector response (depending on TCR stimulus) from its initial effector response and this functional plasticity is thought to have multiple advantages in adjustment of the immune response (22).

When CD4+ naïve T cells encounter their cognate antigen in a primary immune response, they undergo proliferation and differentiation into effector cells with specialized functions (23). The effector population is short lived and eventually dies by apoptosis leaving only the memory phenotype. The progression to a memory cell phenotype is proposed to happen in one of two ways. The theory of linear progression supports that memory cells are generated from effector precursors whereas the proposed divergent pathway indicates that the memory population emerges in parallel with the effector population from a predestined precursor (24-26). The pathway that a differentiating T cell takes from naïve to memory can be influenced by many factors and may differ depending on how the naïve T cell is signaled. Factors that have been found to influence memory cell development include: precursor frequency, TCR affinity, antigen dose, antigen duration, cytokines and costimulation (10). It has been suggested that since

relatively few signals are needed for effector-to-memory transition after optimal priming of naïve CD4+ T cells, the memory cell fate is determined early in activation (10). This concept is supported by a rapid effector-to-memory transition observed when memory phenotype cells are seen after primed effector cells were rested only three days in vitro and away from antigen (27,28).

Differences in the outcomes of activation and differentiation of T cells with various costimulatory molecules indicates the importance of costimulation in the progression of CD4+ naïve T cells to an effector or memory phenotype. Of the costimulatory molecules that are on the surface of CD4+ naïve T cells, CD28 and ICAM-1 have been shown to generate phenotypic and functional memory populations (29). Costimulation through CD28 or ICAM-1 both lead to proliferation, IL-2 production and protection from apoptosis, however, they differ in their outcomes in that CD28 will generate both Th1 and Th2 subsets while ICAM-1 generates a Th1 population (29).

The mechanisms of memory cell generation and the factors that regulate their development are not fully understood and some of the aspects are still being elucidated. This chapter will examine the kinetics of differentiation of CD4+ naïve cells, the minimum stimulation required to achieve a memory cell phenotype, and whether differentiation can be modulated when signals change after initial activation. Our goal is to provide some insight to how quickly memory cells develop from naïve cells and whether memory T cells arise from effector cells or are induced from a naïve precursor. We also will examine the differences in activation and memory cell development with costimulation through ICAM-1 or CD28 and ask whether removing one signal or

exchanging it will alter the end population. With this approach, we hope to help elucidate the presence of a precursor population following initial signal.

Materials and methods

Antibodies and Reagents

Anti-CD54 (R6.5D6) was purchased from BioXCell (West Lebanon, NH), anti-CD28 (clone ANC28.1) was purchased from Ancell (Minneapolis, MN) and anti-CD3 (OKT3) was purchased from eBioscience (San Diego, CA). Anti-CD11a-FITC, anti-CD27-PE, anti-CD45RA-FITC and anti-CD45RO-TriColor were purchased from Caltag Laboratories (Burlingame, CA).

Cell Purification

Naïve human CD4+ T cells were isolated from peripheral blood of multiple donors by negative selection using a naïve T cell enrichment kit (Stem Cell Technologies, Vancouver, BC, Canada). All magnetically selected naïve CD4+ T cell populations were of >98% purity as assessed by flow cytometry (30). In the present work, purified naïve human T cells represents cells that are CD4(+) CD45RA(+)RO(-) CD11a^{lo} CD27(+).

T cell Stimulation

Antibodies in PBS were attached to tissue culture-treated plates (Midwest Scientific, St. Louis, MO) by incubation at 37°C for 2 hours or overnight at 4°C, and wells were washed three times with PBS to remove unbound antibody. Naïve CD4+ T cells were added at a concentration of $1x10^6$-2×10^6 / ml, and stimulated with 1 μg/ml anti-CD3 plus 10 μg/ml anti-ICAM-1, or 5 μg / ml anti-CD28. For experiments in which cells were removed from stimulation or switched to new stimulation, cells were pippetted using a 1000ul pipette and tip to minimize cell damage and then transferred to a clean well or a

new well with freshly attached stimulating antibodies, respectively. Optimal antibody concentrations were determined based on the minimum dose that led to maximum T cell proliferation (not shown).

Flow Cytometry

Flow cytometry was performed using the FACScan (Becton Dickenson, San Jose CA) or the Accuri C6 Flow Cytometer System (Accuri Cytomoters, Ann Arbor MI). The FACScan was calibrated using CaliBRITE beads (Becton Dickinson), and the Accuri C6 was calibrated using Sphero APC Calibration Particles (Spherotech, Inc. Lake Forest, IL). This was supplemented by compensation using singly stained cells. Data were analyzed using Cell Quest (Becton Dickenson), FlowJo (Tree Star Inc, Ashland, OR) and CFlow (Accuri Cytometers).

Luminex Assay

Cell culture supernatants were collected at 1, 3, 5, 7, 10, 14 and 21 days following stimulation. 25 plex human cytokine panel luminex (LHC0009) was purchased from Biosource. Samples were diluted 1:1 and assay was performed according to manufacturer's protocol. Samples were analyzed with the Luminex100 multiplex system and xPONENT® software.

Statistical analysis.

Statistical analysis was performed using GraphPad Prism (GraphPad Software, La Jolla, CA.) or SigmaStat (Systat Software Inc. San Jose, CA). Statistical tests and significance for individual figures are indicated in figure legends.

Results

Costimulation through ICAM-1 induces naïve T cell differentiation to a memory phenotype but delays induction of CD45R0 expression compared to CD28

CD45 is a protein tyrosine phosphatase belonging to the common leukocyte antigen family and is required for T cell receptor signal transduction (31, 32). CD45 is expressed as different isoforms on T cells, and as naïve T cells become activated they lose expression of the CD45RA isoform and express a CD45RO isoform (33). Our lab has shown that costimulation through ICAM-1 leads to production of a memory phenotype after 12-14 days of stimulation. We investigated the rate at which naïve T cells began to downregulate CD45RA and upregulate CD45RO expression to indicate cell differentiation and if that change varied with costimulation through ICAM-1 or CD28. Five days after costimulation through ICAM-1, CD4+ T cells remained mostly CD45RA+ (76%) and only a small fraction of the cells had progressed to single positive CD45RO+ (4%) leaving the rest of the cells in a transitional CD45RA(+)CD45RO(+) stage of differentiation **(Fig. 3.1)**. Day 7 showed that 53% of cells costimulated through ICAM-1 were still CD45RA+ and 24% were CD45RO+, however, by day 11 only 21% of cell expressed CD45RA and 60% expresses CD45RO indicative of rapid differentiation after day 7 **(Fig. 3.1)**. When CD4+ naïve T cells were costimulated through CD28 for five days, the percent of CD45RA had dropped to 47% but the population expressing CD45RO was only 21% indicating a transitional population of double positive cells **(Fig. 3.1)**. By day 7, 38% of cells costimulated through CD28

Figure 3.1

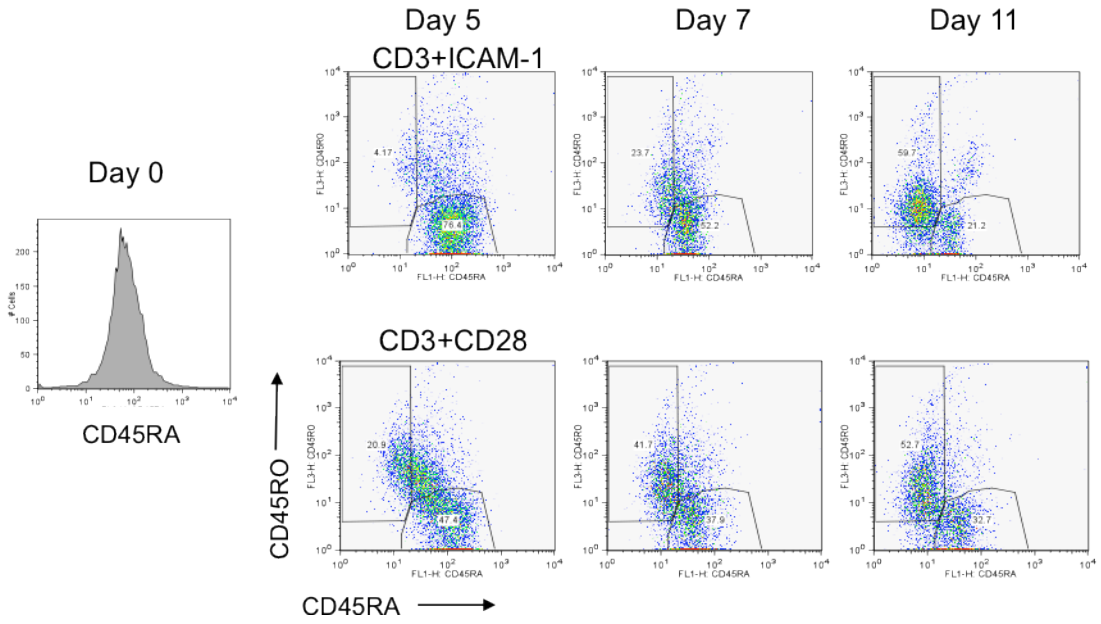
Day 0
CD45RA
Day 5
CD3+ICAM-1
Day 7
Day 11
CD3+CD28
CD45RO
CD45RA
FL1-H: CD45RA
FL3-H: CD45RO
4.17
76.6
23.7
52.2
59.7
21.2
20.9
47.4
41.7
47.9
52.7
32.7

Figure 3.1. Costimulation through ICAM-1 induces naïve T cell differentiation to a memory phenotype but delays induction of CD45R0 expression compared to CD28. Percent CD45RA positive of isolated CD4+ naïve T cells at day 0 was determined by flow cytometry. Naïve cells were stimulated through CD3+ICAM-1 or CD3+CD28 for 5, 7, or 11 days. Expression of CD45RA vs. CD45RO was determined by flow cytometry. n=3.

expressed CD45RA with 42% expressing CD45RO and the remaining cells were double positive **(Fig. 3.1)**. After 11 days of CD28 costimulation, 33% of cells expressed CD45RA and 53% expressed CD45RO, indicating a progressive decrease in CD45RA+CD45RO(-) and CD45RA(+)CD45RO(+) transitional cells after the day 5 time point **(Fig. 3.1)**. Together, these data suggest that costimulation of CD4+ naïve T cells through CD28 initiates activation quicker than ICAM-1 with over half of the cells being positive for CD45RO or double positive for CD45RA/RO by day five and which is similar to what is seen with costimulation through ICAM-1 at day 7. However, the cells costimulated through ICAM-1 quickly caught up to CD28 between days 7 and 11 exhibiting population of CD45RO positive cells even greater than CD28 at day 11.

During long term costimulation of naïve human T cells through ICAM-1, memory T cells appear by days 5 - 7

Previous depictions of the rapid nature by which effector cells can transition to memory were described using *in vitro* or *in vivo* primed effector cells that exhibited a memory phenotype shortly following antigen clearance *in vivo* or after 3 days of rest *in vitro* (27,28). The efficiency of memory cell generation shown by other groups led us to question the timeframe in which memory T cells were able to differentiate from naïve cell activation using our *in vitro* stimulation protocol. We also wanted to examine any differences in the time it took to differentiate naïve T cells to effector and memory when costimulated through ICAM-1 or CD28, given the differences we observed in CD45RO expression. CD4+ naïve T cells were stimulated in vitro for 3, 5, 7, and 12 days. **Figure 3.2** illustrates the kinetics of progression from the naïve phenotype [CD27(+)CD11a(-)

(upper left quadrant)] to effector cells [CD27(+)CD11a(+) (upper right quadrant)] and a memory phenotype [CD27(-)CD11a(+) (lower right quadrant)]. Costimulation of CD4+ naïve T cells through ICAM-1 or CD28 leads to the apperance of effector cells after 3 days of stimulation and we begin to see cells displaying a memory phenotype as rapidly as 5 days after stimulation **(Fig. 3.2)**. The number of effector and memory cells at each time point were quantified. As expected, effector cell numbers were at their highest between 5 and 7 days after costimulation through either ICAM-1 or CD28, contracting to far fewer cells by day 12 **(Fig. 3.3)**. Cells that were costimulated through ICAM-1 began to exhibit detectable memory T cell numbers at 5 days of stimulation with robust cell numbers appearing at 7 and 12 days of stimulation **(Fig. 3.4)**. Costimulation of CD4+ naïve T cells through CD28 generated more memory cells than ICAM-1 at day 5 of stimulation and those cell numbers plateau to 7 and 12 days of stimulation **(Fig. 3.4)**. Examining the data together, we can observe that costimulation through ICAM-1 produces more robust activation and differentiation compared to CD28, giving a greater number of effector cells at each day of stimulation and far more memory cells by days 7 and 12. The efficiency of differentiation with ICAM-1 is interesting considering the delay in CD45RO expression we observed in figure 1.1. Also, the appearance of a memory phenotype by 5-7 days of stimulation through either ICAM-1 or CD28 is far earlier than expected. This observation may be supportive of a precursor memory population or the hypothesis that weak signal after initial stimulation is required for differentiation.

Figure 3.2

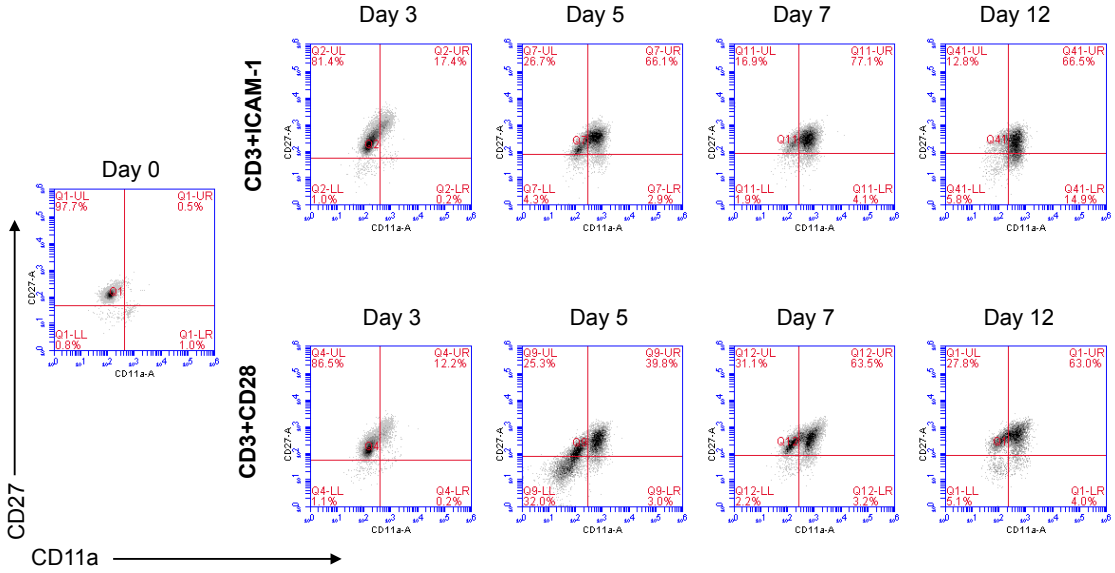
Day 0
Day 3
Day 5
Day 7
Day 12
CD3+ICAM-1
CD3+CD28
CD27
CD11a
CD27-A
CD11a-A
Q1-UL 97.7%
Q1-UR 0.5%
Q1-LL 0.8%
Q1-LR 1.0%
Q2-UL 81.4%
Q2-UR 17.4%
Q2-LL 1.0%
Q2-LR 0.2%
Q7-UL 26.7%
Q7-UR 66.1%
Q7-LL 4.3%
Q7-LR 2.9%
Q11-UL 16.9%
Q11-UR 77.1%
Q11-LL 1.9%
Q11-LR 4.1%
Q41-UL 12.8%
Q41-UR 66.5%
Q41-LL 5.8%
Q41-LR 14.9%
Q4-UL 86.5%
Q4-UR 12.2%
Q4-LL 1.1%
Q4-LR 0.2%
Q9-UL 25.3%
Q9-UR 39.8%
Q9-LL 32.0%
Q9-LR 3.0%
Q12-UL 31.1%
Q12-UR 63.5%
Q12-LL 2.2%
Q12-LR 3.2%
Q1-UL 27.8%
Q1-UR 63.0%
Q1-LL 5.1%
Q1-LR 4.0%

Figure 3.3

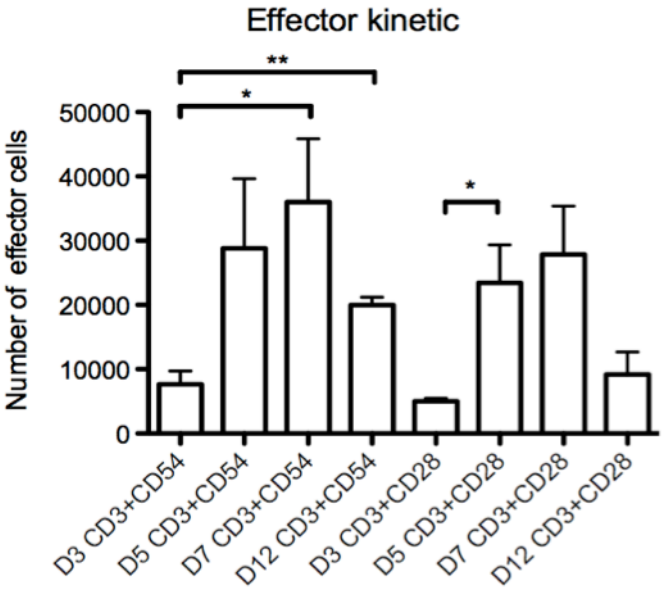

Figure 3.4

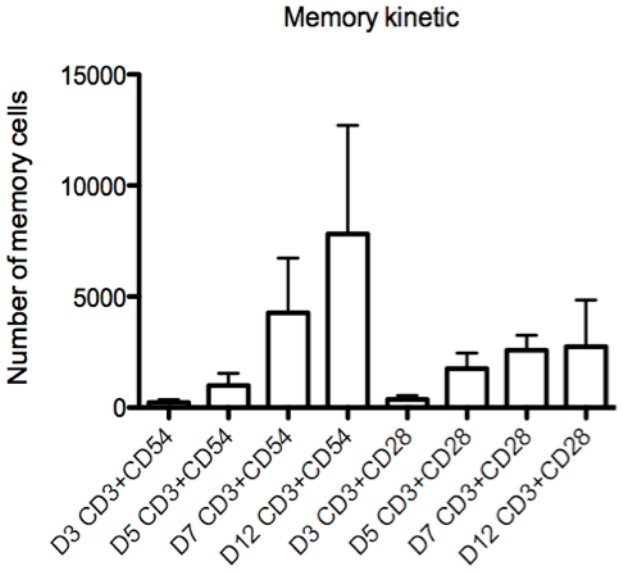

Figure 3.2-3.4. During long term costimulation of naïve human T cells through ICAM-1, memory T cells appear by days 5 – 7. Naïve cells were stimulated through CD3+ICAM-1 or CD3+CD28 for 3, 5, 7 and 12 days. Figure **3.2)** Cell phenotype was assessed by CD11a and CD27 expression to be naïve ($CD11a^{lo}$, CD27+), effector (CD11a+, CD27+) or memory (CD11a+, $CD27^{lo}$) by flow cytometry. Figure **3.3, 3.4)** Total number of effector cells **(3.3)** or memory cells **(3.4)** was determined by CFlow software. Data are presented as mean ± SEM, *$p<0.05$, **$p<0.01$ using paired two tailed t-Test. n=4.

Costimulation of naïve T cells through ICAM-1, when interrupted before days 5 - 7 leads to reduced memory cell differentiation compared with continuous costimulation

Since we see memory cells develop early after costimulation through ICAM-1 or CD28, we wanted to determine if a memory fate was set early after stimulation or if more continual stimulation was needed. CD4+ naïve T cells were stimulated for 1, 3, 5, 7, and 10 days before they were removed from stimulating antibodies and transferred to a clean 96 well plate where they remained with no additional stimulation until 12 total days following initial stimulation before being analyzed for phenotype **(Fig. 3.5)**. When CD4+ naïve T cells costimulated through ICAM-1 were removed from stimulating antibodies after one day (D1), we did not see activation or differentiation of cells at day 12 indicated by a mostly naïve phenotype **(Fig. 3.6)** and very low effector cell numbers **(Fig. 3.7)**. Cells taken off CD3+ICAM-1 stimulatory antibodies at day 3 (D3) or 5 (D5) did exhibit some differentiation but were slightly impaired in activation to an effector phenotype by day 12 **(Fig. 3.6)** and number of effector cells **(Fig. 3.7)** compared to cells not removed from stimulation. Cells that had been costimulated through ICAM-1 for 7 days before resting to day 12 exhibited differentiation to an effector phenotype that resembled cells not removed from stimulus **(Fig. 3.6)**, as well, they produced numbers of effector cells that were not significantly different from the day 12-14 cells **(Fig. 3.7)**. When examining the differentiation of CD4+ naïve T cells to a memory phenotype after costimulation through ICAM-1 for various days, we see that a very small memory population does develop after 1, 3 or 5 days of stimulation before resting with more defined memory populations generated at 7 days of stimulation **(Fig. 3.6)**, however these populations are not reflected when looking at total memory cell numbers **(Fig. 3.8)**.

Costimulation of CD4+ naïve T cells through ICAM-1 for 1 to 7 days before resting produced memory cells numbers that were significantly different than the number of memory cells after 12-14 days of constant stimulation **(Fig. 3.8)** indicating a considerably more favorable memory cell expansion occurred with constant ICAM-1 costimulation.

To compare the duration of costimulation needed for activation by ICAM-1, we applied the same stimulation parameters to CD28. Costimulation of CD4+ naïve T cells through CD28 for 1 or 3 days prior to interruption did initiate a small amount of activation, as we can observe an effector phenotype beginning to emerge from naïve cells **(Fig 3.9)** but the number of effector cells is significantly different from cells left on continual stimulation **(Fig. 3.10)**. However, unlike costimulation through ICAM-1, at 5 days of costimulation through CD28 before rest a more substantial effector population is observable in phenotype **(Fig. 3.9)** as well as cell number **(Fig. 3.10)**. By 7 days of costimulation through CD28, the differentiation to an effector phenotype **(Fig. 3.9)** and activation to produce a sizable number of differentiated cells **(Fig. 3.10)** closely resembles that of cells that were left on stimulation for 12-14 days. When examining memory cell generation with short-term costimulation through CD28 **(Fig. 3.11)**, we see that much like ICAM-1 a small but noticeable memory phenotype develops after just one day of stimulation **(Fig. 3.9)**. However, memory cell numbers do not resemble those of constantly stimulated cells until after 5 days of stimulation **(Fig. 3.11)**. As a control, the same procedures were applied to stimulation through the TCR (CD3) alone, which should not be able to induce full activation/differentiation of naïve cells. As expected, stimulation through CD3 did not activate or differentiate cells to an effector or memory phenotype **(Fig. 3.12, 3.13)**.

Figure 3.5

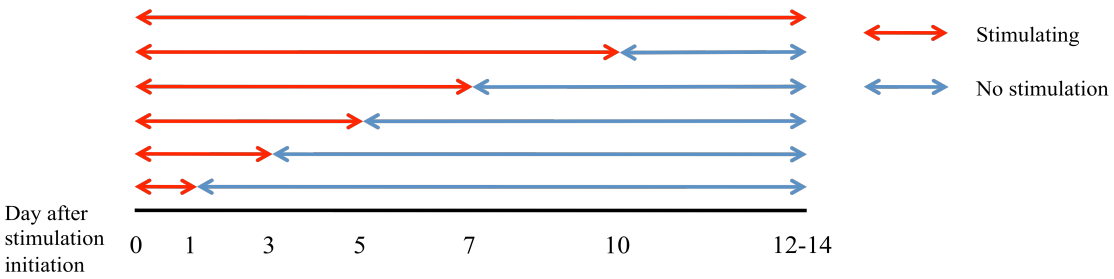
Stimulating
No stimulation
Day after stimulation initiation
0
1
3
5
7
10
12-14

Figure 3.6

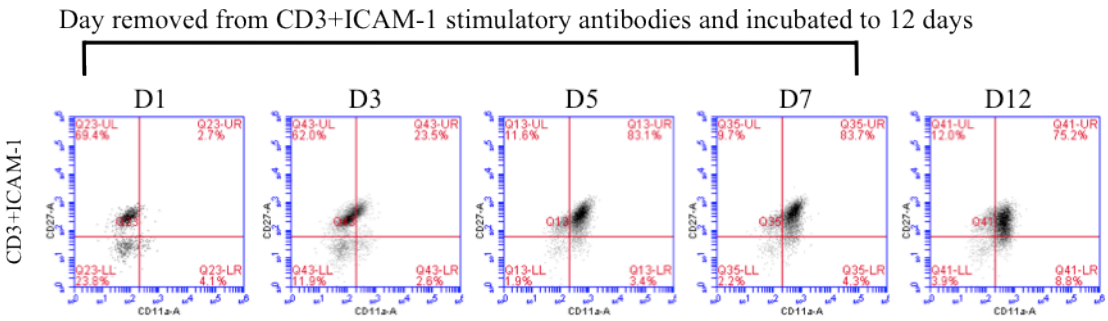
Day removed from CD3+ICAM-1 stimulatory antibodies and incubated to 12 days
D1
D3
D5
D7
D12
CD3+ICAM-1
CD27-A
CD11a-A
Q23-UL 89.4%
Q23-UR 2.7%
Q23-LL 23.8%
Q23-LR 4.1%
Q43-UL 52.0%
Q43-UR 23.5%
Q43-LL 11.9%
Q43-LR 2.6%
Q13-UL 11.6%
Q13-UR 83.1%
Q13-LL 1.9%
Q13-LR 3.4%
Q35-UL 9.7%
Q35-UR 83.7%
Q35-LL 2.2%
Q35-LR 4.3%
Q41-UL 12.0%
Q41-UR 75.2%
Q41-LL 3.9%
Q41-LR 8.9%

Figure 3.7

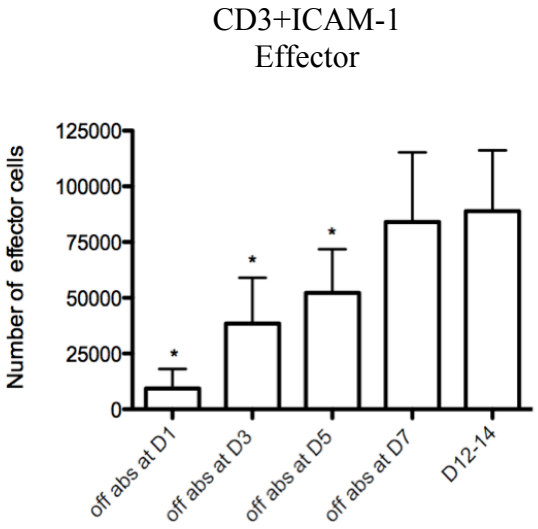

Figure 3.8

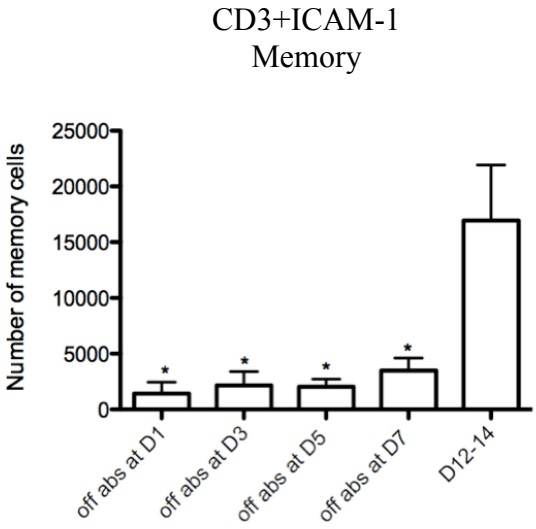

Figure 3.9

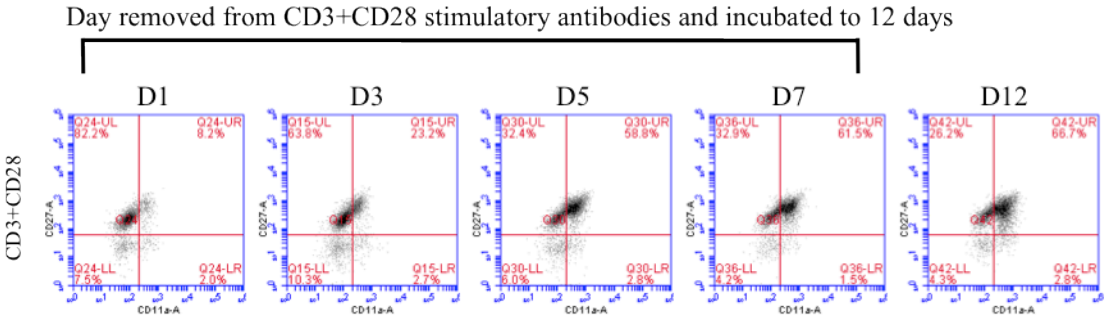
Day removed from CD3+CD28 stimulatory antibodies and incubated to 12 days
D1
D3
D5
D7
D12
CD3+CD28
CD27-A
CD11a-A
Q24-UL 82.2%
Q24-UR 8.2%
Q24-LL 7.5%
Q24-LR 2.0%
Q15-UL 63.8%
Q15-UR 23.2%
Q15-LL 10.3%
Q15-LR 2.7%
Q30-UL 32.4%
Q30-UR 58.8%
Q30-LL 6.0%
Q30-LR 2.8%
Q36-UL 32.9%
Q36-UR 61.5%
Q36-LL 4.2%
Q36-LR 1.5%
Q42-UL 26.2%
Q42-UR 66.7%
Q42-LL 4.3%
Q42-LR 2.8%

Figure 3.10

CD3+CD28
Effector

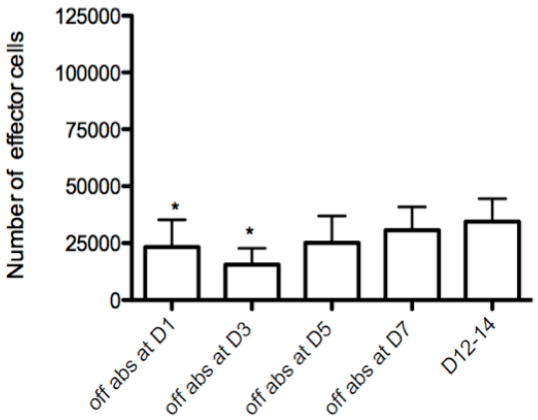

Figure 3.11

CD3+CD28
Memory phenotype

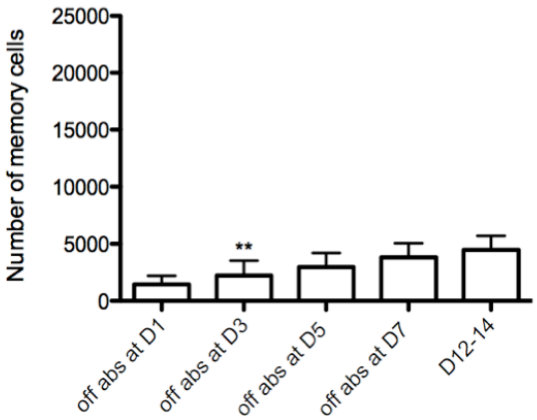

Figure 3.12

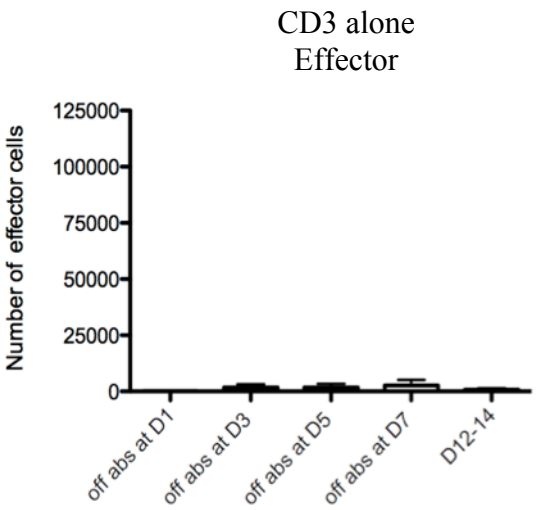

Figure 3.13

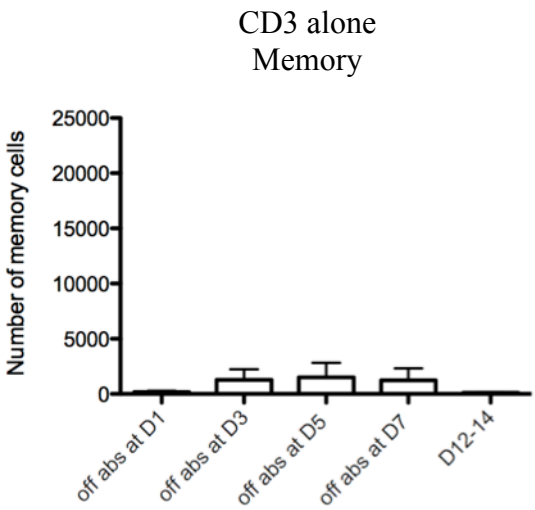

Figure 3.5-3.13. Costimulation of naïve T cells through ICAM-1, when truncated before days 5 - 7 leads to reduced memory cell differentiation compared with continuous costimulation. Naïve cells were stimulated through CD3 alone, CD3+ICAM-1 or CD3+CD28 for 1, 3, 5 or 7 days before being removed from stimulation until day 12-14 or left on constant stimulation for 12-14 days. 12-14 days were used interchangeably with identical results. **Figure 3.5)** Schematic of the duration of stimulation or rest for each time point. **Figures 3.6, 3.9)** Cell phenotype was assessed by CD11a and CD27 expression to be naïve ($CD11a^{lo}$, CD27+), effector (CD11a+, CD27+) or memory (CD11a+, $CD27^{lo}$) by flow cytometry. **Figures 3.7, 3.8, 3.10, 3.11, 3.12, 3.13)** Total number of effector cells (**3.7, 3.10, 3.12**) or memory cells (**3.8, 3.11, 3.13**) was determined by CFlow software. Samples were tested for significance with day 12-14 effector or memory cell numbers. Data are presented as mean ± SEM, *$p<0.05$, **$p<0.01$ using paired two tailed t-Test. CD3+ICAM-1: day 1 n=7; days 3, 5, 7 n=11; day 12-14 n=10. CD3+CD28: day 1 n=8; days 3, 5, 7 n=12; day 12-14 n=11. CD3: day 1 n=3; days 3, 5, 7 n=6; day 12-14 n=5.

Although it seems that CD4+ naïve T cells costimulated through ICAM-1 needed longer stimulation than costimulation through CD28 to develop differentiated cells, the total number of differentiated cells with constant ICAM-1 stimulation was so much higher than CD28 that the effector and memory cell numbers from interrupted stimulation through ICAM-1 are very similar, if not greater, when compared to that of CD28. It is also interesting that the early interrupted stimulation of ICAM-1 or CD28 led to a small subpopulation of cells that differentiated to memory phenotype even in the absence of effector cell production **(Fig. 3.6 and 3.9, days 1 and 3)**. The memory phenotype seems to originate from a CD11a, CD27 double negative population and not an effector population. This phenomenon was observed to various degrees in flow cytometry dot plots from multiple subjects. It is possible that the small memory population developed from precursors that needed brief stimulation and little, if any, proliferation to differentiate.

The effects observed with using interruption costimulation through ICAM-1 or CD28 were due to removal of stimulus, not disruption of cell culture

To verify that the differentiation results seen in **Figures 3.6-3.11** were from truncation of signal and not simply an artifact of disrupting the cells in culture we mimicked the removal procedure of cells from stimulating antibodies while leaving the cells on continual stimulating antibodies. CD4+ naïve T cells were costimulated through ICAM-1 or CD28 and at 1, 3, 5, or 7 days after initial stimulation, cells were mixed by pipetting but left in the stimulating well for the remainder of the 12 days and analyzed for phenotype. Cells that were mixed in culture at various time points following

costimulation through ICAM-1 or CD28 displayed a very similar differentiation pattern of CD11a and CD27 expression as cells that were stimuated undisturbed for 12 days **(Fig. 3.14)**. As well, the number of resulting memory cells was not statistically different with cells mixed at each time point or stimulated for 12 day without disruption for either ICAM-1 or CD28 **(Fig. 3.15, 3.16)**. This indicates that the reduction in memory cells seen with early interruption of stimulus in **Figures 3.6-3.11** was due to the removal from signal and not simply disruption of cells in culture.

Change of costimulatory signal does not modulate differentiation to a memory phenotype at various times following initial costimulation through ICAM-1 or CD28

Our system of *in vitro* stimulation allows for the elimination of variables by isolating initial signals being sent into cells. This permits us to effectively observe the effect that each individual costimulatory signal has on activation and differentiation of the cell. However, during an immune response *in vivo* it is less likely that T cells receive only one costimulatory signal. In this section, we examine the effect that multiple costimulatory signals have on differentiation of naïve T cells. Specifically, we wanted to see if switching the costimulatory signal at different times after initial costimulation would have any impact on memory phenotype generation. The goal is to determine whether we can modulate the effect of stimulation during the activation process or if the initial stimulus determines fate of the cell. **Figure 3.17** depicts the stimulation switching system used. Naïve CD4+ T cells were initially stimulated through CD3 alone, CD3+ICAM-1 or CD3+CD28. At 1, 3, 5 and 7 days after stimulation, cells were removed from stimulation completely as a control or transferred to a single stimulus of

Figure 3.14

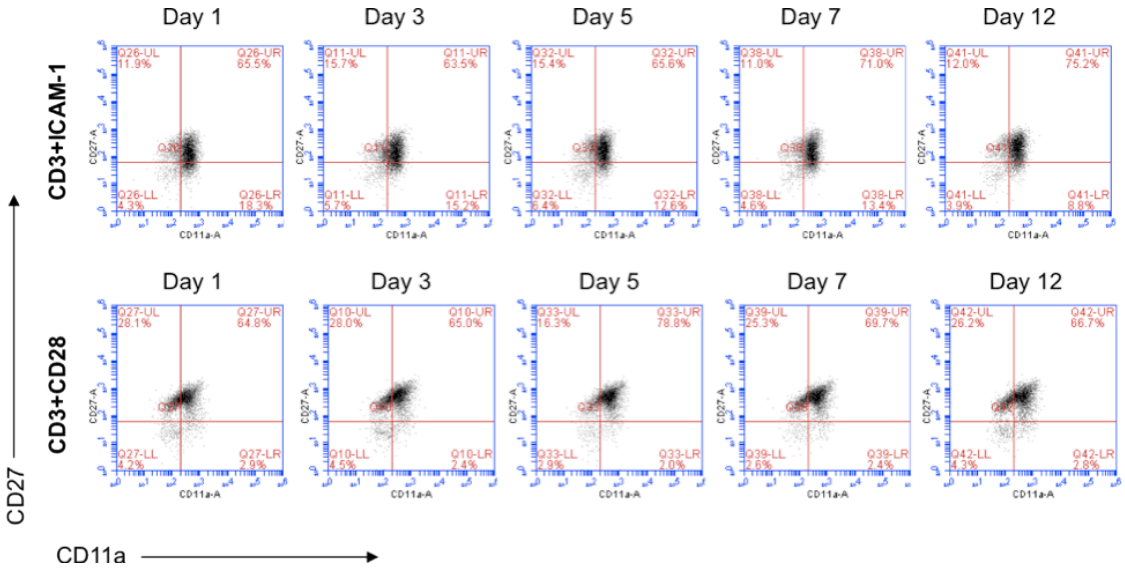
Day 1
Day 3
Day 5
Day 7
Day 12
CD3+ICAM-1
CD3+CD28
CD27
CD11a
Q26-UL 11.9%
Q26-UR 65.5%
Q26-LL 14.3%
Q26-LR 18.3%
Q11-UL 15.7%
Q11-UR 63.5%
Q11-LL 5.7%
Q11-LR 15.2%
Q32-UL 15.4%
Q32-UR 65.6%
Q32-LL 6.4%
Q32-LR 12.6%
Q38-UL 11.0%
Q38-UR 71.0%
Q38-LL 4.6%
Q38-LR 13.4%
Q41-UL 12.0%
Q41-UR 75.2%
Q41-LL 3.9%
Q41-LR 8.8%
Q27-UL 28.1%
Q27-UR 64.8%
Q27-LL 4.2%
Q27-LR 2.9%
Q10-UL 28.0%
Q10-UR 65.0%
Q10-LL 4.5%
Q10-LR 2.4%
Q33-UL 16.3%
Q33-UR 78.8%
Q33-LL 2.9%
Q33-LR 2.0%
Q39-UL 25.3%
Q39-UR 69.7%
Q39-LL 2.6%
Q39-LR 2.4%
Q42-UL 26.2%
Q42-UR 66.7%
Q42-LL 4.3%
Q42-LR 2.8%

Figure 3.15

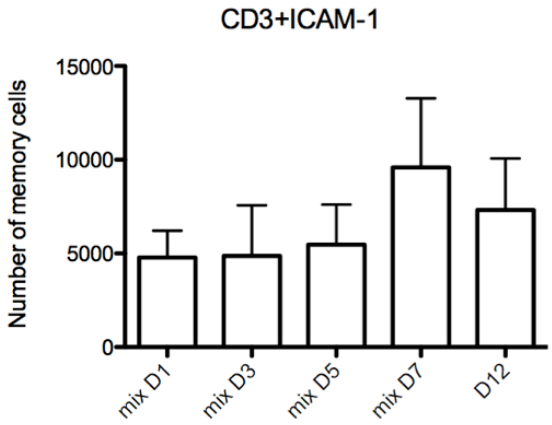

Figure 3.16

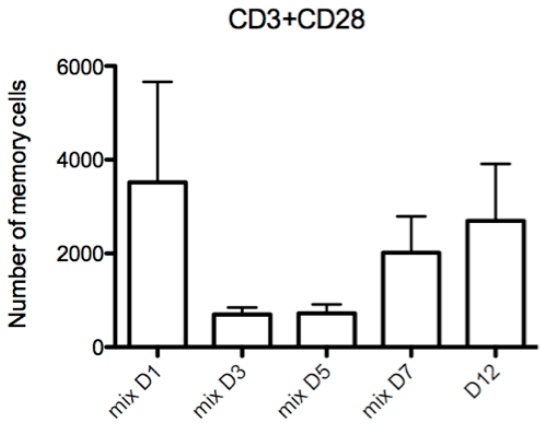

Figure 3.14-3.16. The effects observed with interruption of costimulation through ICAM-1 or CD28 were due to removal of stimulus, not mechanical disruption of cell culture. As a control, cells were mixed in culture at days 1, 3, 5 and 7 to mimic cell transfer and left to rest in the same well as primary stimulation until day 12. **Figure 3.14)** Cell phenotype was assessed by CD11a and CD27 expression to be naïve ($CD11a^{lo}$, CD27+), effector (CD11a+, CD27+) or memory (CD11a+, $CD27^{lo}$) by flow cytometry. **Figure 3.15, 3.16)** Total number of memory cells costimulated through ICAM-1 **(3.15)** or CD28 **(3.16)** was determined by CFlow software. All samples were tested for significance with day 12 memory cell numbers. Data are presented as mean ± SEM, significance was assessed using paired two tailed t-Test. n=4

either CD3, ICAM-1, CD28 where they would remain for 14 total days of stimulation. When naïve cells were initially costimulated through CD3+ICAM-1 and transferred to CD3, ICAM-1 or CD28 at day 1, 3, 5, or 7 the number of cells displaying a memory phenotype was not modulated compared to the control of cells taken off of stimulating antibodies altogether **(Fig. 3.18)**. Also, cells that received only signal 1, CD3, for 1, 3, 5 or 7 days before getting ICAM-1 costimulation did not produce significant memory cells numbers. This indicates that after naïve CD4+ T cells receive initial stimulation through CD3+ICAM-1, they are not easily modulated by or cannot receive additional costimulation from another legitimate costimulatory receptor such as CD28. These data could argue for early determination of cell fate for a small population of naïve cells as well as need for constant costimulation for efficient memory cell production of cells costimulated through ICAM-1. One exception was observed when cells stimulated through CD3+ICAM-1 were transferred to additional CD3 at day 7 of initial stimulation **(Fig. 3.18)**. It is interesting that cells could be modulated so late after stimulation, however, it could be conceivable that the high number of effector cells seen at 7 days following stimulation through CD3+ICAM-1 **(Fig. 3.3)** were able to receive additional signal 1 to further propagate cell differentiation.

When CD4+ naïve T cells were initially stimulated through CD3+CD28 before switching costimulatory signals at days 1, 3, 5 or 7, we observed a slightly different pattern of memory cell numbers compared with CD3+ICAM-1. The majority of stimulation treatments in **figure 3.19** did not show a statistically significant difference from cells that were continuously costimulated through CD28. Much like in **figure 3.11** we can assume that this is because of the lower total number of memory cells generated

Figure 3.17

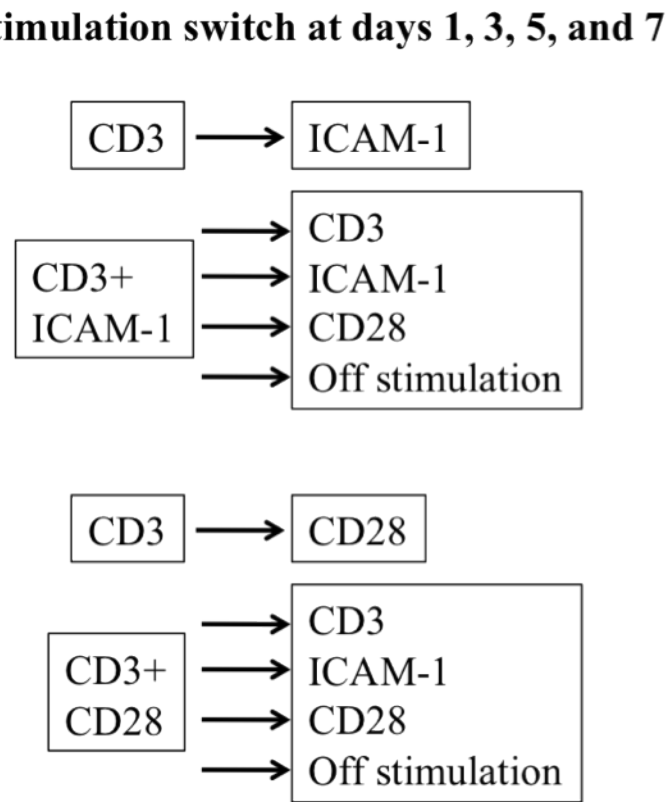
Stimulation switch at days 1, 3, 5, and 7
CD3
ICAM-1
CD3+
ICAM-1
CD3
ICAM-1
CD28
Off stimulation
CD3
CD28
CD3+
CD28
CD3
ICAM-1
CD28
Off stimulation

Figure 3.18

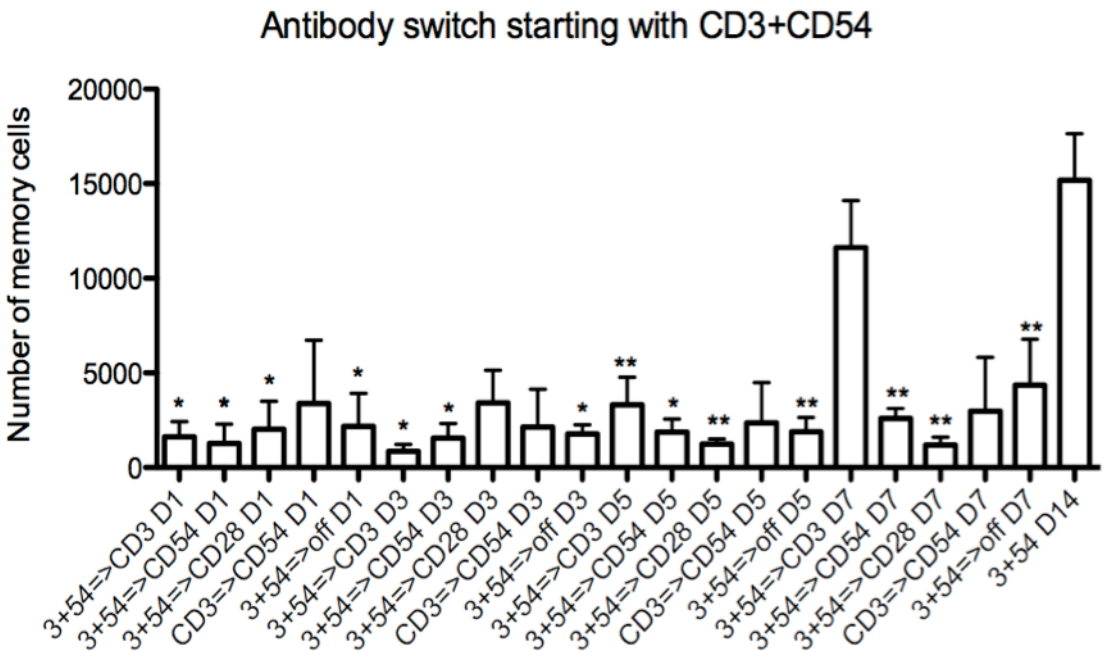
Antibody switch starting with CD3+CD54
Number of memory cells
20000
15000
10000
5000
0
3+54=>CD3 D1
3+54=>CD54 D1
3+54=>CD28 D1
CD3=>CD54 D1
3+54=>off D1
3+54=>CD3 D3
3+54=>CD54 D3
3+54=>CD28 D3
CD3=>CD54 D3
3+54=>off D3
3+54=>CD3 D5
3+54=>CD54 D5
3+54=>CD28 D5
CD3=>CD54 D5
3+54=>off D5
3+54=>CD3 D7
3+54=>CD54 D7
3+54=>CD28 D7
CD3=>CD54 D7
3+54=>off D7
3+54 D14

Figure 3.19

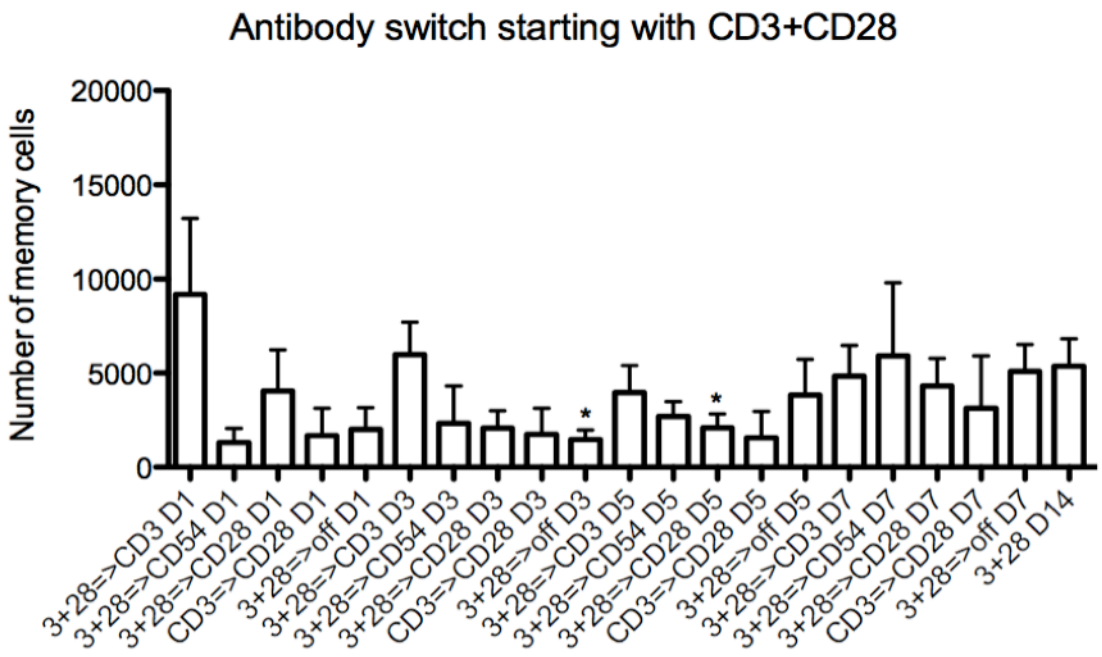
Antibody switch starting with CD3+CD28
Number of memory cells
20000
15000
10000
5000
0
*
*
3+28=>CD3 D1
3+28=>CD54 D1
3+28=>CD28 D1
CD3=>CD28 D1
3+28=>off D1
3+28=>CD3 D3
3+28=>CD54 D3
3+28=>CD28 D3
CD3=>CD28 D3
3+28=>off D3
3+28=>CD3 D5
3+28=>CD54 D5
3+28=>CD28 D5
CD3=>CD28 D5
3+28=>off D5
3+28=>CD3 D7
3+28=>CD54 D7
3+28=>CD28 D7
CD3=>CD28 D7
3+28=>off D7
3+28 D14

Figures 3.17-3.19. Change of costimulatory signal does not modulate differentiation to a memory phenotype at various times following initial costimulation through ICAM-1 or CD28. **Figure 3.17)** Schematic of the stimulation transfer procedure. **Figure 3.18)** Number of memory cells generated with stimulation through CD3+ICAM-1 before transfer to indicated stimulation or removal from stimulation at days 1, 3, 5 or 7. Memory cell number was analyzed at day 14. **Figure 3.19)** Number of memory cells generated with stimulation through CD3+CD28 before transfer to indicated stimulation or removal from stimulation at days 1, 3, 5 or 7. All memory cell numbers were analyzed at day 14. All samples were tested for significance with day 14 memory cell numbers. Data are presented as mean ± SEM, *$p<0.05$, **$p<0.01$ and no asterisk indicates no significant difference to day 14 using paired two tailed t-Test. CD3+ICAM-1: n=3-4. CD3+CD28:n=4-5.

by constant costimulation through CD28 compared to constant costimulation through ICAM-1 for 12-14 days. Much like in **figure 3.18**, naïve cells that were initially costimulated through CD3+CD28 and transferred to CD3, ICAM-1 or CD28 (or switched from CD3 alone to CD28) at any time point did not differ in the number of cells displaying a memory phenotype compared to the control activity of cells removed from stimulating antibodies altogether **(Fig. 3.19)**. One trend of interest is that at early transfer times (days 1, 3, and 5), cells that go from CD3+CD28 to CD3 alone exhibit a greater memory cell number than other stimulation treatments **(Fig. 3.19)**. This observation could support the hypothesis that duration of antigen signal can influence differentiation and memory cell development (21,22).

Preliminary data: Costimulation of CD4+ naïve T cells through ICAM-1 or CD28 induces the generation memory cells in the presence of effector cytokines.

Previous studies have indicated that the switch from effector to memory T cells happens rapidly in the absence of antigen and effector cytokines (27, 34, 35). We have observed that in our *in vitro* stimulation system, we do not observe creation of a substantial memory population after removal from stimulation **(Fig. 3.6-3.11)**, therefore we looked at the cell culture supernatants to determine effector cytokine presence during differentiation of naïve T cells following costimulation through ICAM-1 or CD28. All of the cytokine profiling was done in collaboration with Kelli Williams in the Benedict lab. Pro-inflammatory cytokines, IL-1β, IL-6 and TNF-α, were present in culture during effector and memory stages of differentiation (days 7-21) **(Fig. 3.20)**. Th1 effector cytokines IFN-γ and IL-12 but not IL-2 were abundant during differentation stages **(Fig.**

3.21), as well, Th2 cytokines IL-4, IL-5 and IL-10 were all detected in various amounts at effector and memory development phases (days 7-21) **(Fig. 3.22)**. Our preliminary findings suggest that we can develop large numbers of memory phenotype cells with constant costimulation through ICAM-1 without the removal of inflammatory or effector cytokines.

Figure 3.20

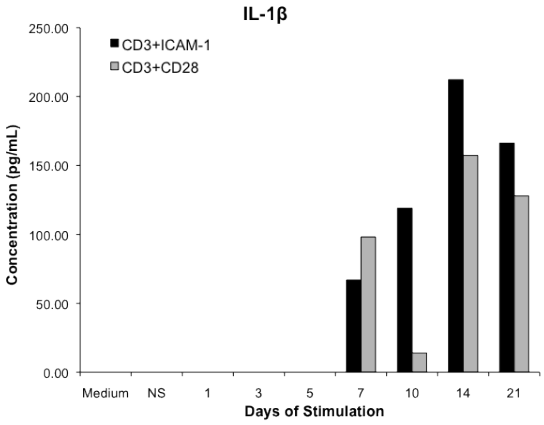
IL-1β
CD3+ICAM-1
CD3+CD28
Concentration (pg/mL)
250.00
200.00
150.00
100.00
50.00
0.00
Medium
NS
1
3
5
7
10
14
21
Days of Stimulation

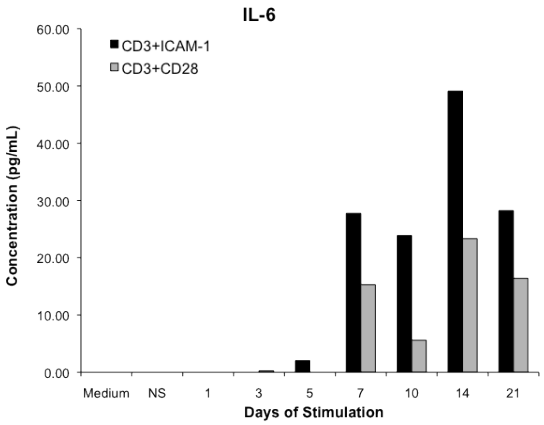
IL-6
CD3+ICAM-1
CD3+CD28
Concentration (pg/mL)
60.00
50.00
40.00
30.00
20.00
10.00
0.00
Medium
NS
1
3
5
7
10
14
21
Days of Stimulation

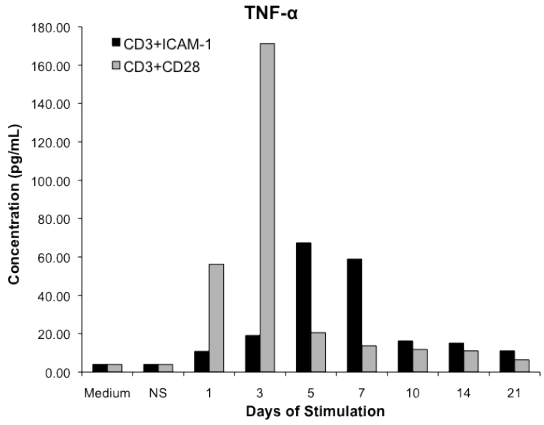
TNF-α
CD3+ICAM-1
CD3+CD28
Concentration (pg/mL)
180.00
160.00
140.00
120.00
100.00
80.00
60.00
40.00
20.00
0.00
Medium
NS
1
3
5
7
10
14
21
Days of Stimulation

Figure 3.21

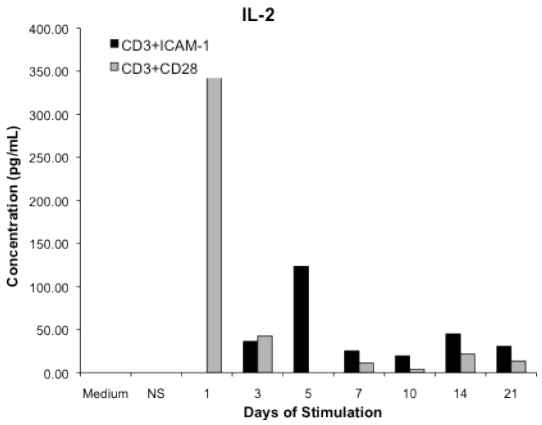
IL-2
CD3+ICAM-1
CD3+CD28
Concentration (pg/mL)
400.00
350.00
300.00
250.00
200.00
150.00
100.00
50.00
0.00
Medium
NS
1
3
5
7
10
14
21
Days of Stimulation

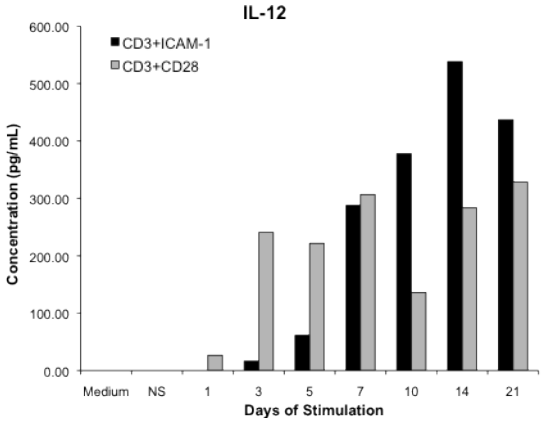
IL-12
CD3+ICAM-1
CD3+CD28
Concentration (pg/mL)
600.00
500.00
400.00
300.00
200.00
100.00
0.00
Medium
NS
1
3
5
7
10
14
21
Days of Stimulation

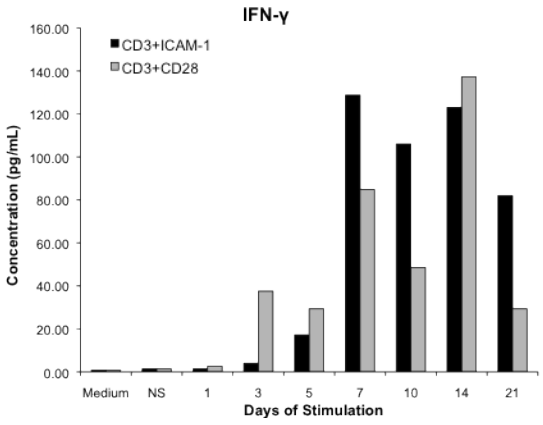
IFN-γ
CD3+ICAM-1
CD3+CD28
Concentration (pg/mL)
160.00
140.00
120.00
100.00
80.00
60.00
40.00
20.00
0.00
Medium
NS
1
3
5
7
10
14
21
Days of Stimulation

Figure 3.22

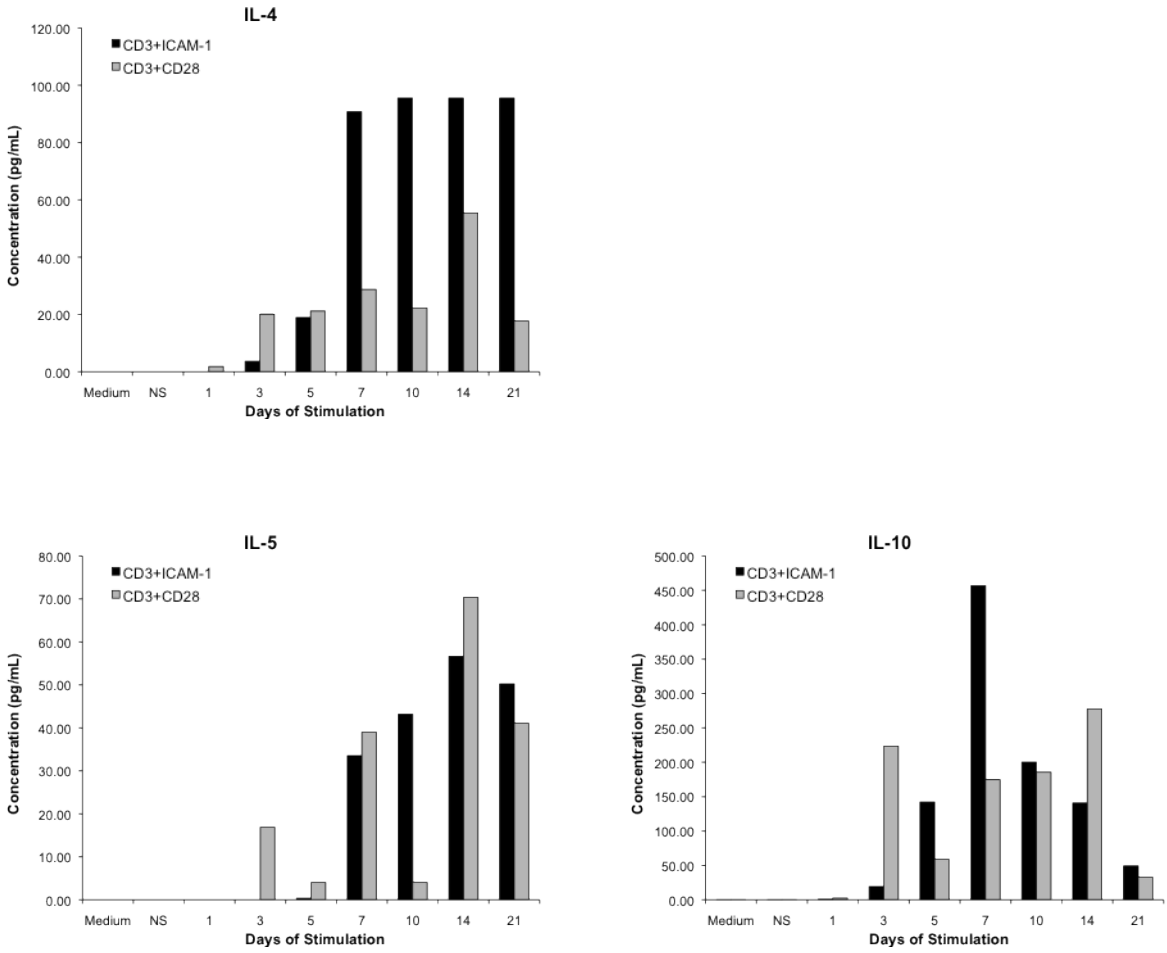
IL-4
CD3+ICAM-1
CD3+CD28
Concentration (pg/mL)
120.00
100.00
80.00
60.00
40.00
20.00
0.00
Medium
NS
1
3
5
7
10
14
21
Days of Stimulation
IL-5
CD3+ICAM-1
CD3+CD28
Concentration (pg/mL)
80.00
70.00
60.00
50.00
40.00
30.00
20.00
10.00
0.00
Medium
NS
1
3
5
7
10
14
21
Days of Stimulation
IL-10
CD3+ICAM-1
CD3+CD28
Concentration (pg/mL)
500.00
450.00
400.00
350.00
300.00
250.00
200.00
150.00
100.00
50.00
0.00
Medium
NS
1
3
5
7
10
14
21
Days of Stimulation

Figures 3.20-3.22. Preliminary data: Costimulation of CD4+ naïve T cells through ICAM-1 or CD28 induces the generation memory cells in the presence of effector cytokines. Cell culture supernatants were analyzed at days 1, 3, 5, 7, 10, 14 and 21 for the presence of inflammatory cytokines **(3.20)**, Th1 cytokines **(3.21)** and Th2 cytokines **(3.22)**. NS= nonstimulated. n=1.

Discussion

Upon antigenic stimulation, naïve T cells undergo clonal expansion that leads to the apperance of an effector cell population followed by clonal contraction. The resulting cell phenotype is a highly differentiated memory population. CD4+ memory T cells are an extremely important part of the immune response because they allow the body to induce an immune reaction days before a primary response would be able to take effect. Memory cells can signal to activate the innate and other arms of the adaptive immune response in the same amount of time that takes naïve cells to begin expansion because memory cells require weaker antigenic dose and shorter duration for activation (3, 4, 10). The specific factors required for efficient memory cell generation remain unclear and the ability to define those parameters could provide useful tools for disease treatment and modulation of the immune response. Here we aim to define the duration of stimulation needed for differentiation of CD4+ naïve T cells into memory and the degree to which costimulation plays a deciding factor in that differentiation.

Cosimulatory molecules can differentially affect the outcome of T cell differentiation. Not all costimulatory molecules on the surface of CD4+ naïve T cells are able to generate a memory phenotype. Costimulation through leukocyte function antigen-1 (LFA-1) activates CD4+ naïve T cells to proliferate but does not protect them from apoptosis or generate a memory population (29, 36, 37). ICAM-1 costimulation of CD4+ naïve T cells was shown by our lab to generate a memory population, however, we knew little about the process or timing of this differentiation. CD28 is thought to be the dominant costimulatory molecule, leading to protection from apoptosis and memory cell

production (38). Since CD28 is the most widely accepted costimulatory molecule for differentiation into memory, it is an appropriate control to compare with ICAM-1.

Costimulation of CD4+ naïve T cells through ICAM-1 led to an apparent delay in expression of differentiation molecule CD45RO compared to stimulation through CD28, however no delay was observed in the appearance of an effector or memory phenotype. In fact, memory cells were observed after only 5-7 days of costimulation through either ICAM-1 or CD28, during the height of the expansion in the effector population. When examining the duration of signal needed for differentiation to effector and memory cells, we observed that naïve cells needed 5-7 days of stimulation through either CD3+ICAM-1 or CD3+CD28 to allow detection of a differentiated population by flow cytometry at day 12. However, costimulation through ICAM-1 required longer stimulation time to increase numbers of effector or memory cells to similar numbers observed with continual stimulus. Costimulatory signal did not seem to exert a large influence on differentiation of naïve cells into a memory phenotype since switching costimulatory molecules at various time points of stimulation showed similar effects to removing the cells from stimulation altogether. However, it is noteworthy that early switching of CD3+CD28 stimulated cells to CD3 alone showed a trend of increasing the memory cell number by day 14. Finally, we detected high levels of inflammatory and effector cytokines in supernatants at later times of cell culture indicating that the differentiation to a memory phenotype occured in the presence of activating molecules.

The debate about which path of differentiation cells take to memory is ongoing and there seems to be evidence to support multiple mechanisms of differentiation. As mentioned earlier, there are two main proposed methods of memory generation, linear

and divergent, although there are also many proposed variations of each (39). **Figure 3.23** illustrates each pathway. Linear generation of memory hypothesizes that memory T cells arise from antigen induced, highly activated effector cells after the effector response has occurred and as the effector population undergoes contraction. Research done by Joseph Opferman, et al. states that the CD8+ cells require at least 5 divisions following antigenic stimulation *in vitro* to produce a significant memory population, indicating linear memory development (40). Other labs have supported the linear pathway into memory using antigen specific CD4+ cells and adoptive transfer. Susan Swain generated antigen specific effector cells *in vitro* that gave rise to long-lived memory cells after transfer to adoptive hosts (41) and Sylvie Garcia, et al. reported that following the transfer of CD4+ naïve T cells into adoptive hosts, memory T cells were generated from activated T cells that had undergone at least 8 cell divisions (23). The divergent pathway of memory T cell development suggests that memory cells appear independent of effector cell differentiation after initial naïve cell activation. Murine CD8+ naïve cells cultured with high concentrations of IL-2 during antigen activation differentiate into cells with effector functions (42). However, naïve cells activated in culture with low concentrations of IL-2 never developed an effector phenotype but did differentiate into a memory-like cell, suggesting the cells took the divergent pathway to memory (42).

As demonstrated in the previous paragraph, much of the known research on memory T cell production has been done in mice and with CD8+ T cells. The goal of the present research was not only to examine the role that costimulation played in the differentiation of CD4+ naïve T cells into a memory phenotype, but also to give more

Figure 3.23

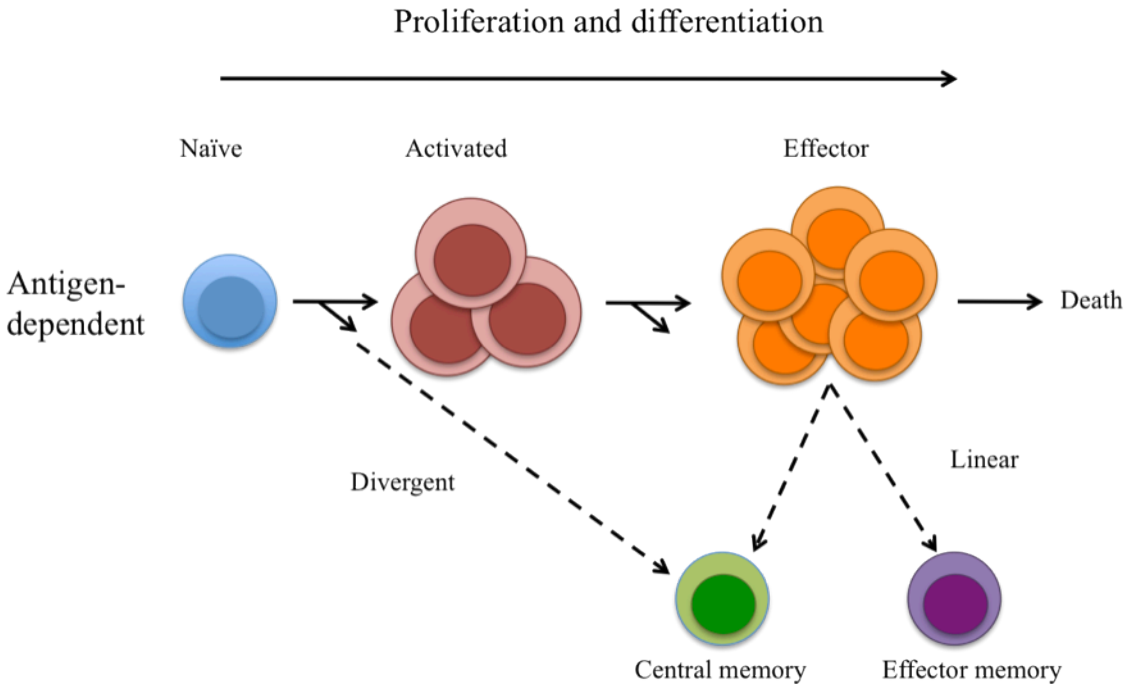
Proliferation and differentiation
Naïve
Activated
Effector
Antigen-dependent
Death
Divergent
Linear
Central memory
Effector memory

Figure 3.23. Shematic diagram of the linear and divergent pathways into memory cell generation during differentiation. The linear pathway generates memory cells after activation and differentiation into effector cells. The divergent pathway generates memory cells without differentiation into effector cells. Figure is adapted from Moulton and Farber, 2006 (39).

insight into how memory cells are generated. We have demonstrated that unlike previous findings (27, 28, 33, 34), CD4+ memory T cells can appear within days of primary stimulation, without rest or removal of inflammatory and effector cytokines. When cells are removed from stimulation early, we see a decrease in the number of memory T cells produced but there is still a small subpopulation able to differentiate into memory. Based on the late kinetic of CD45RO expression that we see with naïve T cell costimulation through ICAM-1, we can speculate that these cells have not undergone full activation or proliferation in these early time points. At the same time, it seems that the small memory population that appears after CD4+ naïve T cells are removed from either ICAM-1 or CD28 costimulation at 1-3 days is derived from the CD11a, CD27 double negative quadrant of the flow dot plot, whereas the robust memory population generated from cells that were stimulated continuously for 7-12 days seem to be derived from the CD11a, CD27 double positive effector quadrant. Together, these data may indicate that a weak or short stimulus could lead to memory cell, but not effector cell generation. This hypothesis is supported by Yang Liu, et al. who reported that costimulation through CD28 and heat-stable antigen (HSA or CD24) could lead to production of effector and memory T cells but costimulation through CD24 alone led to only memory cell production since CD24 gives rise to a much weaker stimulation signal than CD28 (43).

A final aspect to be examined is whether the differentiation process can be modulated at any point following primary stimulation. With our stimulation system we see that at any time point following the initial costimulatory signal being sent into the cell, the differentiation fate of that cell apparently is not changed with additional or alternate costimulatory signal. This was demonstrated when switching the activated cells

to the same singular costimulatory molecule or a different costimulatory led to an effect similar to simply taking the cells off stimulation altogether. One exception was that with cells that were stimulated through CD3+CD28 and transferred to CD3 alone at early time points, a slight increase memory cell number was observed. It is conceivable that at those early times following stimulation, the costimulatory signal was no longer needed and that the continued CD3 stimulation mimicked a prolonged antigen signal, therefore increasing activation and differentiation through the linear pathway to memory.

In the perspective of previous research, the present study may support the hypothesis that multiple pathways exist whereby CD4+ naïve T cells differentiate into a memory phenotype. In our stimulation system, continual, long term signaling appears to support the linear pathway where memory cell generation is derived from activated effector cells. However, brief stimulation generates a small memory population without activation, supporting the divergent pathway of memory differentiation from precursor naïve T cells. Finally, our data may also support the hypothesis that initial signal determines cell fate and that late, exogenous or environmental factors are not as influential as previously thought. Taken together, the present data may indicate that memory cells can develop in multiple ways depending on the stimulatory signal.

1. Hammarlund E, Lewis MW, Hansen SG, Strelow LI, Nelson JA, Sexton GJ, Hanifin JM, Slifka MK. Duration of antiviral immunity after smallpox vaccination. Nat Med 2003; 9:1131–7.
2. Amara RR, Nigam P, Sharma S, Liu J, Bostik V. Long-lived poxvirus immunity, robust CD4 help, and better persistence of CD4 than CD8 T cells. J Virol 2004; 78:3811–6.
3. Kaech, S.M., E.J. Wherry & R. Ahmed. Effector and memory T-cell differentiation: implications for vaccine development. Nat. Rev. Immunol. 2002; 2: 251–262.
4. Chandok, M.R. & D.L. Farber. Signaling control of memory T cell generation and function. Semin. Immunol. 2004; 16: 285–293.
5. Strutt TM, McKinstry KK, Swain SL. Control of innate immunity by memory CD4 T cells. Adv Exp Med Biol. 2011;780: 57-68.
6. Strutt TM, McKinstry KK, Dibble JP, Winchell C, Kuang Y, Curtis JD, Huston G, Dutton RW, Swain SL. Memory CD4+ T cells induce innate responses independently of pathogen. Nat Med. 2010;16(5):558-64
7. Bevan MJ. Helping the CD8(+) T-cell response. Nat Rev Immunol. 2004; 4:595–602.
8. Abbas AK, Burstein HJ, Bogen SA. Determinants of helper T cell-dependent antibody production. Semin Immunol. 1993; 5:441–7.
9. Banchereau J, Bazan F, Blanchard D et al. The CD40 antigen and its ligand. Annu Rev Immunol. 1994; 12:881–922.

10. McKinstry KK, Strutt TM and Swain SL. The potential of CD4 T-cell memory. Immunology. 2010; 130: 1–9.
11. McKinstry KK, Strutt TM, Swain SL. Hallmarks of CD4 T cell immunity against influenza. J Intern Med. 2011; 269(5):507-18
12. Schiött A, Lindstedt M, Johansson-Lindbom B, Roggen E, Borrebaeck CA. CD27– CD4+ memory T cells define a differentiated memory population at both the functional and transcriptional levels. Immunology. 2004; 113: 363–370
13. Lisa M. Ebert, Patrick Schaerli, Bernhard Moser. Chemokine-mediated control of T cell traffic in lymphoid and peripheral tissues. Molecular Immunology. 2005; 42: 799–809.
14. Purton JF, Tan JT, Rubinstein MP, Kim DM, Sprent J, Surh CD. Antiviral CD4+ memory T cells are IL-15 dependent. J Exp Med. 2007; 204:951–61.
15. Li J, Huston G, Swain SL. IL-7 promotes the transition of CD4 effectors to persistent memory cells. J Exp Med. 2003; 198:1807–15.
16. Kondrack RM, Harbertson J, Tan JT, McBreen ME, Surh CD, Bradley LM. Interleukin 7 regulates the survival and generation of memory CD4 cells. J Exp Med. 2003; 198:1797–806.
17. De Riva A, Bourgeois C, Kassiotis G, Stockinger B. Noncognate interaction with MHC class II molecules is essential for maintenance of T cell metabolism to establish optimal memory CD4 T cell function. J Immunol. 2007; 178:5488–95.
18. Kassiotis G, Garcia S, Simpson E, Stockinger B. Impairment of immunological memory in the absence of MHC despite survival of memory T cells. Nat Immunol. 2002; 3:244– 50.

19. Seddon B, Tomlinson P, Zamoyska R. Interleukin 7 and T cell receptor signals regulate homeostasis of CD4 memory cells. Nat Immunol. 2003; 4:680–6.

20. Berard M, Tough DF. Qualitative differences between naive and memory T cells. Immunology. 2002; 106:127–38.

21. MacLeod MK, Kappler JW and Marrack P. Memory CD4 T cells: generation, reactivation and re-assignment. Immunology. 2010; 130: 10–15

22. Lees JR and Farber DL. Generation, persistence and plasticity of CD4 T-cell memories. Immunology. 2010; 130: 463–470

23. Garcia S, DiSanto J, Stockinger B. Following the development of a CD4 T cell response in vivo: from activation to memory formation. Immunity. 1999; 11:163–71.

24. Ahmed R, Gray D. Immunological memory and protective immunity: understanding their relation. Science. 1996; 272(5258):54-60.

25. Farber, D.L. Differential TCR signaling and the generation of memory T cells. J. Immunol. 1998; 160: 535–539.

26. Bushar ND and Farber DL. Recalling the Year in Memory T Cells. Ann. N.Y. Acad. Sci. 2008; 1143: 212–225

27. McKinstry KK, Golech S, Lee WH, Huston G, Weng NP, Swain SL. Rapid default transition of CD4 T cell effectors to functional memory cells. J Exp Med 2007; 204:2199–211.

28. McKinstry KK, Strutt TM, Swain SL. The effector to memory transition of CD4 T cells. Immunol Res. 2008; 40:114–27.

29. Kohlmeier JE, Chan MA, Benedict SH. Costimulation of naïve human CD4+ T cells through intercellular adhesion molecule-1 promotes differentiation to a memory phenotype that is not strictly the result of multiple rounds of cell division. Immunology. 2006; 118(4): 549-58.

30. De Rosa SC, Herzenberg LA, Herzenberg LA, Roederer M. 11-color, 13-parameter flow cytometry. identification of human naive T cells by phenotype, function, and T-cell receptor diversity. Nat Med 2001; 7:245–8.

31. Clark E.A. and Ledbetter J.A. Leukocyte surface enzymology: CD45 (LCA, T200) is a protein tyrosine phosphatase. Immunol. Today.1989; 10: 225-228.

32. Kung, C., Pingel, J.T., Heikinheimo, M., Klemola, T., Varkila, K., Yoo, L.I., Vuopala, k., Poyhonen, M., Rogers, M., Speck, S.H., Chatilla, T.A., and T.M. Matthews. Mutations in the tyrosine phosphotase CD45 genes in child with sever combine immunodeficiency disease. Nat Med. 2000; 6(3):343-5

33. A.N. Akbar, L. Terry, P.C.L. Beverley and G. Janossy, Loss of CD45R and gain of UCHLI reactivity is a feature of primed T cells. J. Immunol. 1988; 140: 2171-2178.

34. Harbertson J, Biederman E, Bennett KE, Kondrack RM, Bradley LM. Withdrawal of stimulation may initiate the transition of effector to memory CD4 cells. J Immunol 2002;168:1095–102.

35. Hu H, Huston G, Duso D, Lepak N, Roman E, Swain SL. CD4(+) T cell effectors can become memory cells with high efficiency and without further division. Nat Immunol 2001; 2:705–10.

36. Kohlmeier J.E., Rumsey L.M., Chan M.A. and Benedict S.H. The outcome of T cell costimulation through ICAM-1 differs from costimulation through LFA-1. Immunology. 2003; 108: 152-157.

37. Ragazzo J.L., Ozaki M.E., Karlsson L., Peterson P.A. and Webb S.R. Costimulation via lymphocyte function-associated antigen-1 in the absence of CD28 ligation promotes anergy of naïve CD4+ T cells. Proc. Natl. Acad. Sci. USA. 2001; 98: 241-246.

38. Boise L.H., Minn A.J., Noel P.J., June C.H., Accavitti M.A., Lindsten T. and Thompson C.B. CD28 costimulation can promote T cell survival by enhancing the expression of Bcl-xL. Immunity1995; 3: 87-98.

39. Moulton, V.R. & D.L. Farber. Committed to memory: lineage choices for activated T cells. Trends. Immunol. 2006; 27: 261–267.

40. Opferman JT, Ober BT, Ashton-Rickardt PG. Linear differentiation of cytotoxic effectors into memory T lymphocytes. Science 1999; 283: 1745–1748

41. Swain,S.L. Generation and in vivo persistence of polarized Th1 and Th2 memory cells. Immunity. 1994; 1: 543–552

42. Manjunath N, Shankar P, Wan J, Weninger W, Crowley MA, Hieshima K, Springer TA, Fan X, Shen H, Lieberman J, von Andrian UH. Effector differentiation is not prerequisite for generation of memory cytotoxic T lymphocytes. J. Clin. Invest. 2001; 108: 871–878

43. Liu, Y., R. H. Wenger, M. Zhao, and P. J. Nielsen. Distinct costimulatory molecules are required for the induction of effector and memory cytotoxic T lypmphocytes. J. Exp. Med. 1997; 185:251.

Chapter 4

Homing potential of differentiated cells generated with ICAM-1 costimulation

Introduction

Chemokines are chemotactic cytokines that range from 6 to 14kDa in mass. There have been approximately 50 different chemokines identified (1). Chemokines can be classified into four groups depending on the positioning of their conserved cysteine residues near the N-terminus (4-6). C chemokines contain one cysteine near its N-terminus, CC chemokines contain two, and CXC or CX3C have cysteine residues separated by one or three amino acids, respectively (1). Chemokine receptors are seven transmembrane GTP-binding protein (G-protein) coupled receptors (GPCR)(2,3). The classification of chemokine receptors is dependent on the class of chemokine that it binds. There are currently 19 known chemokine receptors and the majority are classified as CCR or CXCR (3). Chemokines and their engagement of chemokine receptors are responsible for mediating cell adhesion and chemotaxic migration of leukocytes. Once triggered, G proteins signal phospholipase Cβ (PLCβ) isoforms, phosphatidylinositol 3-kinase-γ (PI3Kγ), Serine /Threonine-kinases and c-Src-related non-receptor tyrosine kinases (4,7,8).

Chemokines, and thus chemokine receptors, are also grouped by function. Homeostatic chemokines are constitutively expressed in particular microenvironments and responsible for maintaining circulation of leukocytes (specifically lymphocytes) between periphery and secondary lymphoid organs in order to look for cognate antigen (9-12). This chemokine function is essential for immune surveillance by naïve and memory T cells which can lead to their specific activation and ability to travel to a secondary site of immune response. Another function of chemokines is referred to as inflammatory or inducible. This function occurs following leukocyte activation or

stimulation by pro-inflammatory cytokines and directs cells to inflamed tissue where their effector function can be brought into play (9-12). Chemokines can also induce activation of integrins present on leukocyte cell surface; this is an essential step in initiating the cell migration process. This process begins with leukocyte tumbling over the endothelial cell surface as a part of blood flow and low affinity interactions between selectins on leukocytes and endothelial cells lining the vessel. Tumbling, or rolling, allows leukocyte exposure endothelial cell surface chemokines (13). Binding to the chemokine receptor leads to high affinity integrin interactions with adhesion molecules on the surface of the endothelial cells and arrests the leukocyte tumbling. Finally, leukocytes are able to extravasate through vascular endothelial junctions into surrounding tissue. A similar process is used for lymphocytes migrating through high endothelial venule (HEV) cells into secondary lymphoid organs.

Differential chemokine receptor expression on T cells is indicative of which chemokines that particular cell can respond to and, in turn, where that cell can go in the body. Also, subsets of T cells at various stages of activation or differentiation will express particular chemokine receptors that can direct those cells to specific locations in the body. In this chapter we will examine the phenotype of CD4+ naïve T cells before and following differentiation induced by different costimulatory molecules and whether that phenotype can be modulated with the addition of external factors. Our hypothesis is that T cell activation through specific costimulatory molecules can differentially affect the homing patterns of the differentiated cell.

Materials and Methods

Antibodies and Reagents

Anti-CD54 (R6.5D6) was purchased from BioXCell (West Lebanon, NH), anti-CD28 (clone ANC28.1) was purchased from Ancell (Minneapolis, MN) and anti-CD3 (OKT3) was purchased from eBioscience (San Diego, CA). Anti-CCR7-PE, anti-CCR5-PE, anti-CXCR5-PE and anti-CCR9-PE were purchased from R&D Systems (Minneapolis, MN). Anti-CD62L-TriColor, anti-CXCR4-PE, anti-CD45RO-FITC/APC and flagellin from *S. typhimurium* were purchased from Caltag Laboratories of Invitrogen (Burlingame, CA). Anti-CD127-PE, and anti-β7-PECy5 were purchased from Becton Dickinson (San Jose CA). anti-CD45RO-FITC Caltag (Burlingame, CA). Anti α4-PE was purchased from eBioscience (San Diego, CA) and retinoic acid was purchased from Sigma-Aldrich (St. Louis, MO).

Cell Purification

Naïve human CD4+ T cells were isolated from peripheral blood or tonsil of multiple donors by negative selection using a naïve T cell enrichment kit (Stem Cell Technologies, Vancouver, BC, Canada). All magnetically selected naïve CD4+ T cell populations were of >98% purity as assessed by flow cytometry. In the present work, purified naïve human T cells represents cells that are CD4(+) CD45RA(+)RO(-) CD11a^{lo} CD27(+).

T cell Stimulation

Antibodies in PBS were attached to tissue culture-treated plates (Midwest Scientific, St. Louis, MO) by incubation at 37°C for 2 hours or overnight at 4°C, and wells were

washed three times with PBS to remove unbound antibody. Naïve CD4+ T cells were added at a concentration between 1-2×10^6 / ml, and stimulated with 1 μg/ml anti-CD3 plus 10 μg/ml anti-ICAM-1, or 2 μg / ml anti-CD28. Retinoic acid or bacterial flagellin protein was added at the start of cell culture and used at a concentration of 1 nM or 5 nM for retinoic acid and 1 nM for flagellin. Optimal antibody concentrations were determined based on the minimum dose that led to maximum T cell proliferation (not shown).

Flow Cytometry

Flow cytometry was performed using the FACScan (Becton Dickinson, San Jose CA) and the Accuri C6 Flow Cytometer System (Accuri Cytomoters, Ann Arbor MI). The FACScan was calibrated using CaliBRITE beads (Becton Dickinson), and the Accuri C6 was calibrated using Sphero APC Calibration Particles (Spherotech, Inc. Lake Forest, IL). This was supplemented by compensation using singly stained cells. Data were analyzed using Cell Quest (Becton Dickenson), FlowJo (Tree Star Inc, Ashland, OR) and CFlow (Accuri Cytometers).

Statistical analysis.

Statistical analysis was performed using GraphPad Prism (GraphPad Software, La Jolla, CA.) or SigmaStat (Systat Software Inc. San Jose, CA). Statistical tests and significance for individual figures are indicated in figure legends.

Results

CCR7 expression is maintained following activation of CD4+ naïve T cells costimulated through ICAM-1 or CD28

CCR7 is the classic chemokine receptor that directs naïve and memory T cells to the lymph nodes where they can encounter cognate antigen to undergo activation (14,15). The process of naïve and memory T cell recirculation between the periphery and lymph nodes is essential to initiate immune responses. The chemokines that bind to CCR7 are CCL21 and CCL19 and are expressed on HEVs in the venule lumen (16-19). Mice that lack either expression of CCR7 or its chemokines have been found to be defective in chemokine regulated homing illustrating their importance in lymphocyte migration and entry into the lymph node (20-22). As expected, almost all of CD4+ naïve T cells express CCR7 **(Fig. 4.1, 4.2)**. Following stimulation through CD3+ICAM-1 effector/memory cells (cells that express CD45RO) exhibited a decrease of CCR7 **(Fig. 4.1, 4.2)**. This would be expected knowing that activated/effector cells do not completely retain ability to home to the lymph node (23). The subset of memory T cells known as "central memory" or T_{CM} has been characterized to be CCR7 and CD62L positive (24). After costimulation of CD4+ naïve T cells through ICAM-1, the percent of CD45RO+ cells that expressed CCR7 was slightly higher than cells costimulated through CD28 (60% versus 50% CCR7 positive, respectively) **(Fig. 4.1, 4.2)**.

Figure 4.1

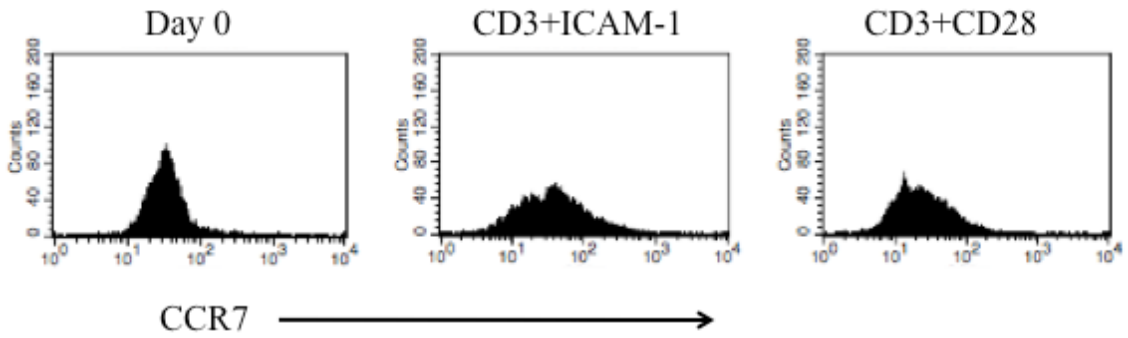

Figure 4.2

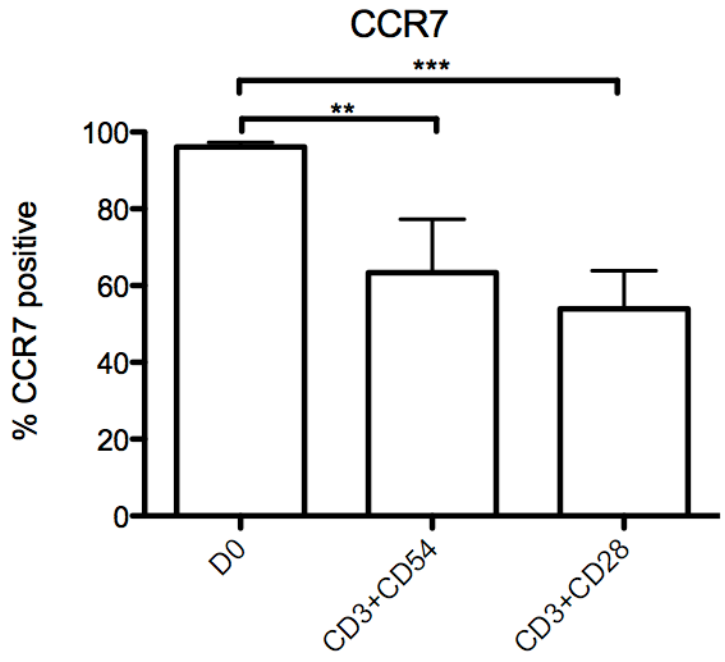

Figure 4.1, 4.2. CCR7 expression is maintained following activation of CD4+ naïve T cells costimulated through ICAM-1 or CD28. Percent CCR7 positive of isolated CD4+ naïve T cells was determined by flow cytometry. Naïve cells were stimulated through CD3+ICAM-1 or CD3+CD28 for 14 days. Cells were gated on CD45RO and CCR7 positive cells were determined by flow cytometry. Representative flow plots **(4.1)** and cumulative data **(4.2)** are shown. Data are presented as mean ± SEM, **p<0.01, ***p<0.001 using two tailed t-Test. n=9, naïve cells; n=5, CD3+CD54; n=6, CD3+CD28.

Costimulation of CD4+ naïve T cells through ICAM-1 results in a decreased CD62L expression compared to costimulation through CD28.

L-selectin (CD62L) is present on the surface of many leukocyte subsets including naïve T cells and some effector and memory T cells. They bind to peripheral-node GlyCAM-1 on HEVs to facilitate entry into lymph nodes (25). Studies have shown that impairment CD62L expression in mice will lead to a massive depletion of T cells in the peripheral lymph nodes (26). L-selectin can also mediate homing to the gut by binding mucosal vascular cell-adhesion molecule-1 (MAdCAM-1) on the HEVs of the gut-associated lymphoid tissue (GALT) (27). After activation, Effector T cells and effector memory T cells (T_{EM}) decrease the L-selectin on their cell surface in order to allow activated T cells to migrate to sights of inflammation, and to the gut (via integrin $\alpha_4\beta_7$) and skin to carry out effector functions where needed (25,28). Much like CCR7, the CD4+ naïve T cells that we isolated were positive for CD62L **(Fig. 4.3, 4.4)**. As expected, after costimulation the activated/differentiated cells did downregulate CD62L expression, however, the CD4+ naïve T cells stimulated with CD3+ICAM-1 decreased surface expression (about 45% CD62L positive) more so than the cells stimulated through CD3+CD28 (about 55% CD62L positive) but the difference was not significant **(Fig. 4.3, 4.4).**

IL-7 receptor α subunit is expressed at low levels on mature T cells following costimulation through either ICAM-1 or CD28

The IL-7 receptor α subunit (CD127) is not involved in directing T cell homing, however like CCR7 and CD62L, CD127 can be used as a marker for naïve and central memory T cell subsets. CD127 is present on the surface of naïve T cells and its

Figure 4.3

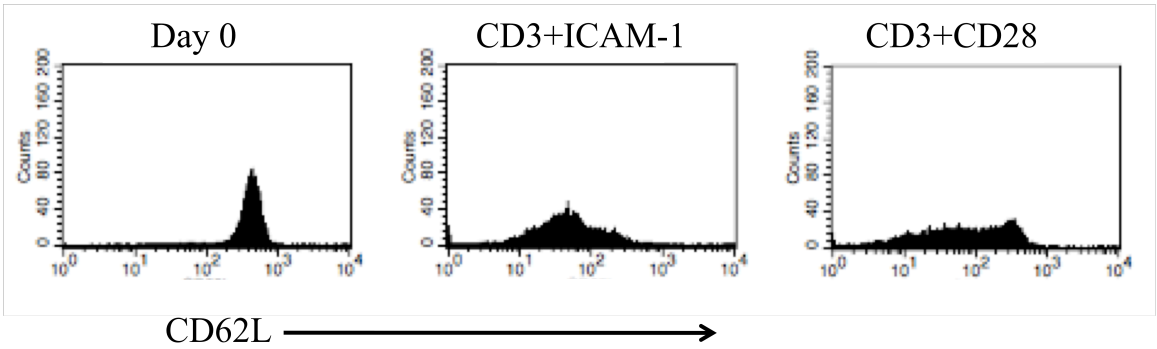

Figure 4.4

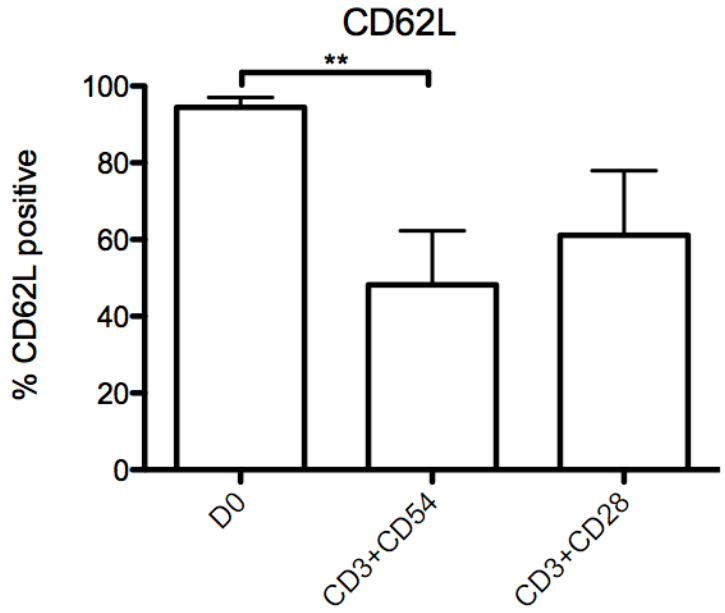

Figure 4.3, 4.4. Costimulation of CD4+ naïve T cells through ICAM-1 results in a decreased CD62L expression compared to costimulation through CD28. Percent CD62L positive of isolated CD4+ naïve T cells was determined by flow cytometry. Naïve cells were stimulated through CD3+ICAM-1 or CD3+CD28 for 14 days. Cells were gated on CD45RO and CD62L postitve cells were determined by flow cytometry. Representative flow plots **(4.3)** and cumulative data **(4.4)** are shown. Data are presented as mean ± SEM, **p<0.01 using two tailed t-Test. n=6, naïve cells; n=4, CD3+CD54; n=5, CD3+CD28.

expression is downregulated soon after activation of the cell (29,30). T cells that maintain or upregulate CD127 following activation can transition to a memory cell phenotype (31-35). CD127 is expressed on naïve and memory T cells because it is necessary for long-term cell survival by increasing expression of anti-apoptotic proteins, Bcl-2 and Glut1 (36-38). As with CCR7 and CD62L, CD127 was expressed on our isolated CD4+ naïve cells **(Fig. 4.5, 4.6)**. Following costimulation of the naïve cells through ICAM-1 or CD28, the expression of CD127 was dramatically reduced on CD45RO+ T cells, however, a small population remained CD127 positive for both sets of costimualtion (20% CD127 positive with ICAM-1 and 30% positive for CD28) **(Fig. 4.5, 4.6)**. Since CD127 is not expressed on effector cells, it seems logical that the cells retaining expression of CD127 after 14 days of stimulation would correlate to a central memory T cell population because CD45RA positive naïve cells were gated out of the analyzed population.

Inflammatory chemokine receptor expression does not significantly change following T cell activation through ICAM-1 or CD28

CCR5 is known to be an inflammatory chemokine receptor and is not expressed on the surface of resting T cells (39). Expression of inflammatory chemokine receptors allows effector T cells to directly enter sites of inflammation. CCR5 can respond to multiple chemokines including RANTES, MIP-1α, MIP-1β and MCP-2 (12). Upon naïve or resting T cell activation, CCR5 can be upregulated preferentially on Th1 cells and generally 5-15 percent of peripheral blood T cells are CCR5 positive (40,41). Expression of CCR5 has also been associated with autoimmune diseases that are largely

Figure 4.5

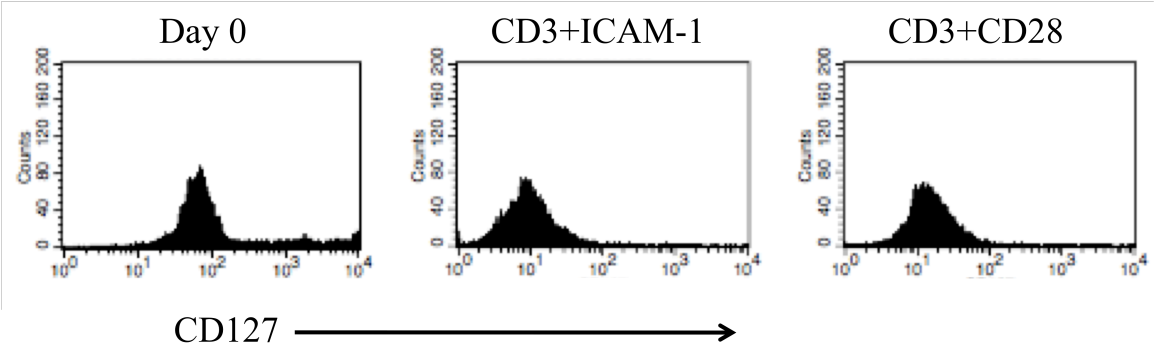

Figure 4.6

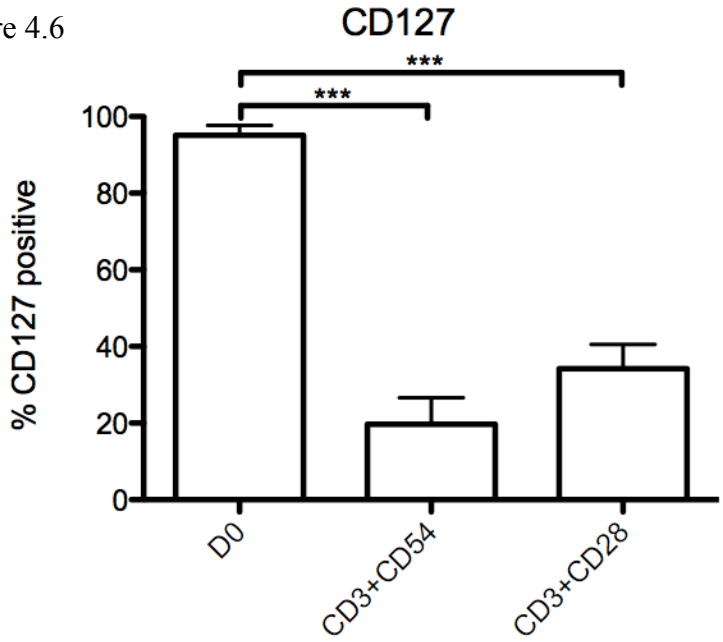

Figure 4.5, 4.6. IL-7 receptor is expressed at low levels on mature T cells following costimulation through either ICAM-1 or CD28. Percent CD127 (IL-7Rα) positive of isolated CD4+ naïve T cells was determined by flow cytometry. Naïve cells were stimulated through CD3+ICAM-1 or CD3+CD28 for 14 days. Cells were gated on CD45RO and CD127 positive cells were determined by flow cytometry. Representative flow plots **(4.5)** and cumulative data **(4.6)** are shown. Data are presented as mean ± SEM, ***$p<0.001$ using two tailed t-Test. n=3, naïve cells; n=3, CD3+CD54; n=3, CD3+CD28.

Th1 driven since nearly all of the auto-reactive T cells are found to be CCR5 positive (42,43). CCR5 was expressed at very low levels (under 5%) on our isolated CD4+ naïve T cells **(Fig. 4.7, 4.8)**. Costimulation through ICAM-1 or CD28 slightly increased CCR5 expression to 12% positive for ICAM-1 and 9% positive for CD28 **(Fig. 4.7, 4.8)**. The increase in CCR5 expression with cells costimulated through ICAM-1 as opposed to CD28 is justified since costimulation through ICAM-1 gives a mainly Th1 population and costimulation through CD28 leads to both Th1 and Th2 populations (44). These data conflict with previous findings from Dr. Jake Kohlmeier (unpublished data) taken at 5 and 10 days after stimulation looking at total T cells. However, different time points of analysis, thus, different T cell populations examined shows that CCR5 expression changes with differentiation. The present data fall in line nicely with the known percent expression of CCR5 by resting peripheral T cells and could be expected from cells analyzed 14 days after stimulation when the effector phenotype would be contracting. It is of considerable interest to use this system to identify what determines which of the naïve T cell population responds to signals by turning on CCR5, and why.

Preliminary data: CXCR4 expression mimics CCR7 expression in CD4+ naïve T cells and following costimulation through ICAM-1 or CD28

CXCR4 is broadly expressed on many leukocytes and during all T cell developmental stages. The ligand for CXCR4 is stromal cell-derived factor- 1 (SDF-1) or CXCL12. SDF-1 is widely expressed throughout the body in primary and secondary lymphoid tissue and peripheral tissues (12). The ubiquitous expression of SDF-1 and CXCR4 suggests multiple roles in leukocyte homing, function and homeostasis (45-48).

Figure 4.7

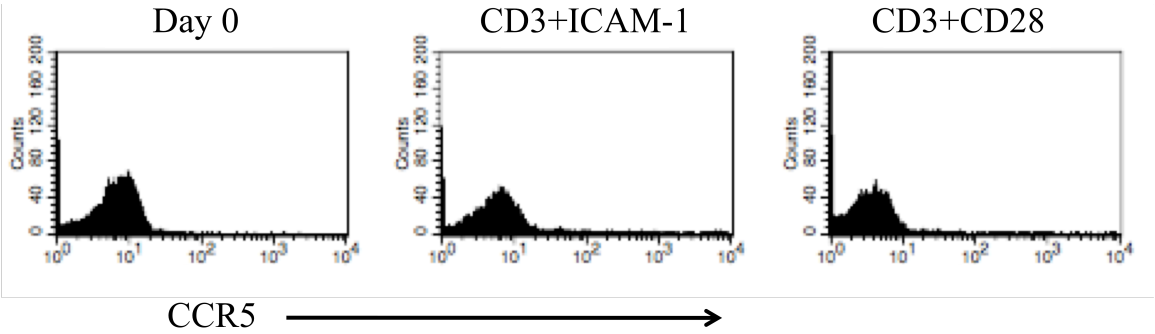

Figure 4.8

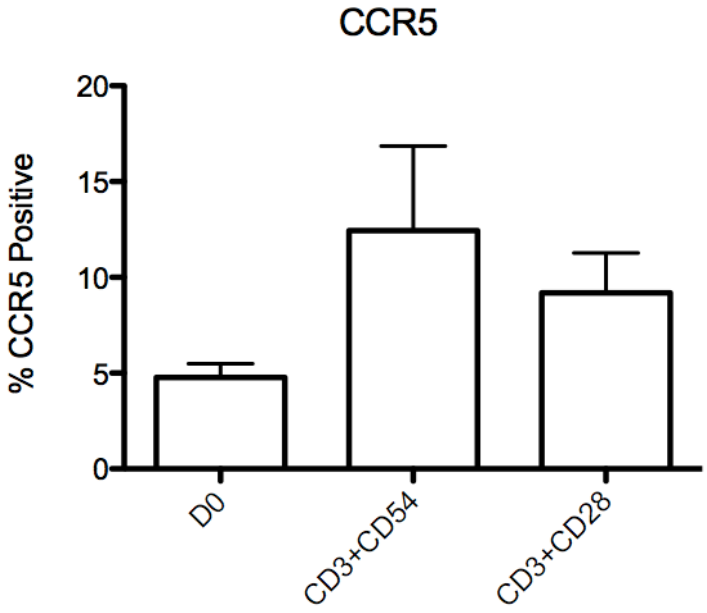

Figure 4.7, 4.8. Inflammatory chemokine receptor expression does not significantly change following T cell activation through ICAM-1 or CD28. Percent CCR5 positive of isolated CD4+ naïve T cells was determined by flow cytometry. Naïve cells were stimulated through CD3+ICAM-1 or CD3+CD28 for 14 days. Cells were gated on CD45RO and CCR5 postitve cells were determined by flow cytometry. Representative flow plots **(4.7)** and cumulative data **(4.8)** are shown.Data are presented as mean ± SEM and significance was determined using a two tailed t-Test. n=5, naïve cells; n=5, CD3+CD54; n=6, CD3+CD28.

Studies have shown that CXCR4 also contributes to central memory T cell entry into the peripheral lymph nodes (PLN) (49). Our isolated CD4+ naïve T cells exhibited nearly 100 percent expression of CXCR4. After costimulation of naïve cells, the resulting activated/memory cells costimulated through ICAM-1 showed about 60 percent and cells costimulated through CD28 retained 50 percent **(Fig. 4.9, 4.10)**. Figure 5 illustrates a pattern of CXCR4 expression that is similar to expression of CCR7 on naïve CD4+ T cells and on cells stimulated through ICAM-1 or CD28 suggesting that in our stimulation system, CXCR4 could assist CCR7 in T cell migration to the PLNs.

Preliminary data: CXCR5 may define a small subset of memory T cells generated by costimulation through ICAM-1 or CD28

CXCR5 binds BCA-1 (B cell–activating chemokine 1) in secondary lymphoid tissue; is not expressed on CD4+ naïve T cells but is present on a subset called follicular helper T cells (T_{FH}) that help form follicles in secondary lymphoid tissue (50,51). CXCR5 expression is unique in that it is rapidly induced (2-3 days after stimulation) before T cell differentiation, and subsequently lost during proliferation (52). Long term CXCR5 expression can characterize a subset of memory T cells, the vast majority being CD4+, where peripheral CXCR5+ T cells coexpress CCR7 and tonsillar CXCR5+ T cells do not (53). Therefore expression of CXCR5 represents a subpopulation of central memory T cells with B cell helper function (53). CXCR5 was not expressed on our isolated CD4+ naïve T cells, as expected, and only slightly expressed on cells stimulated for 14 days through CD3+ICAM-1 or CD3+CD28 only at about 4% and 5% positive, respectively **(Fig. 4.11,12)**. Since CXCR5 is rapidly lost from activated/dividing cells, it

Figure 4.9

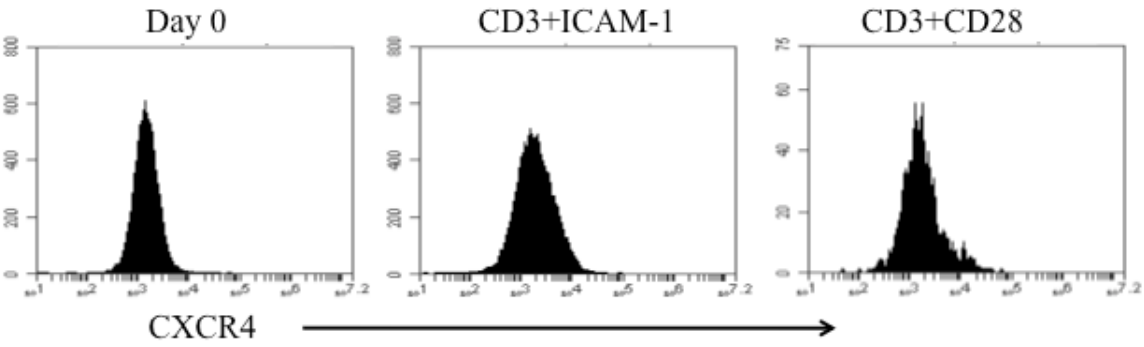

Figure 4.10

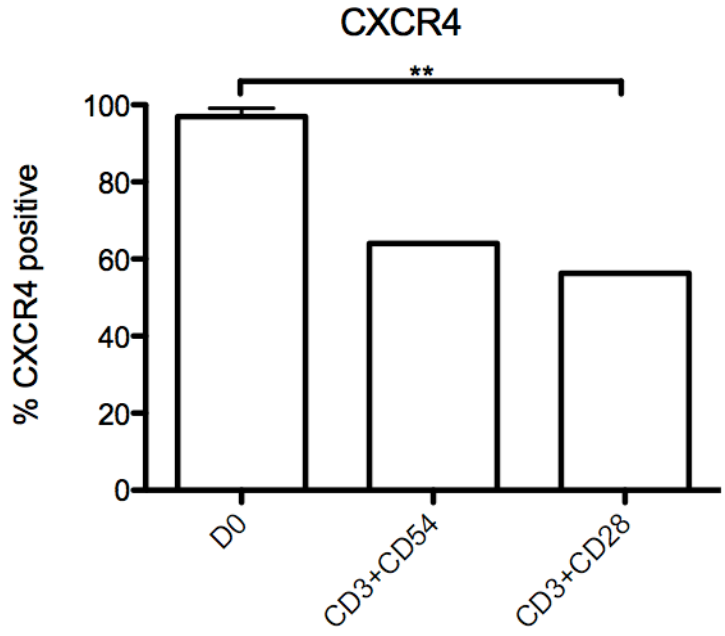

Figure 4.9, 4.10. Preliminary data: CXCR4 expression mimics CCR7 expression in CD4+ naïve T cells and following costimulation through ICAM-1 or CD28. Percent of isolated CD4+ naïve T cells that were positive for CXCR4 was determined by flow cytometry. Naïve cells were stimulated through CD3+ICAM-1 or CD3+CD28 for 14 days. Cells were gated on CD45RO and CXCR4 postitve cells were determined by flow cytometry. Representative flow plots **(4.9)** and cumulative data **(4.10)** are shown. Data are presented as mean ± SEM, **$p<0.01$ using two tailed t-Test. n=2, naïve cells; n=1, CD3+CD54; n=2, CD3+CD28.

Figure 4.11

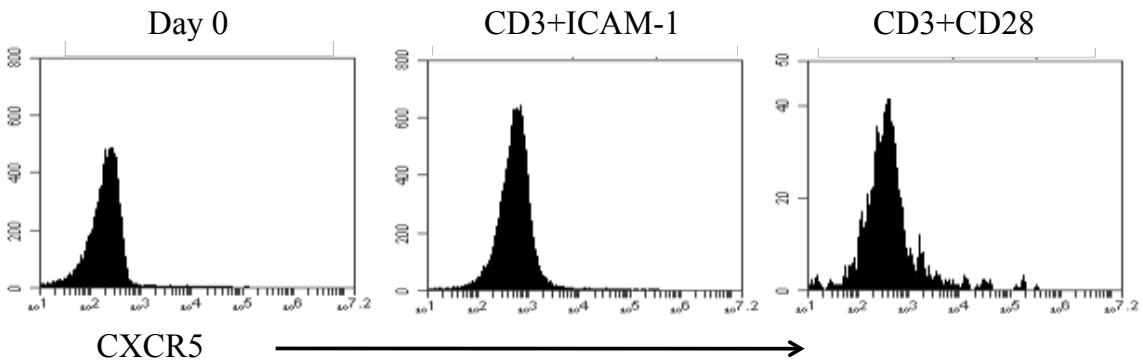

Figure 4.12

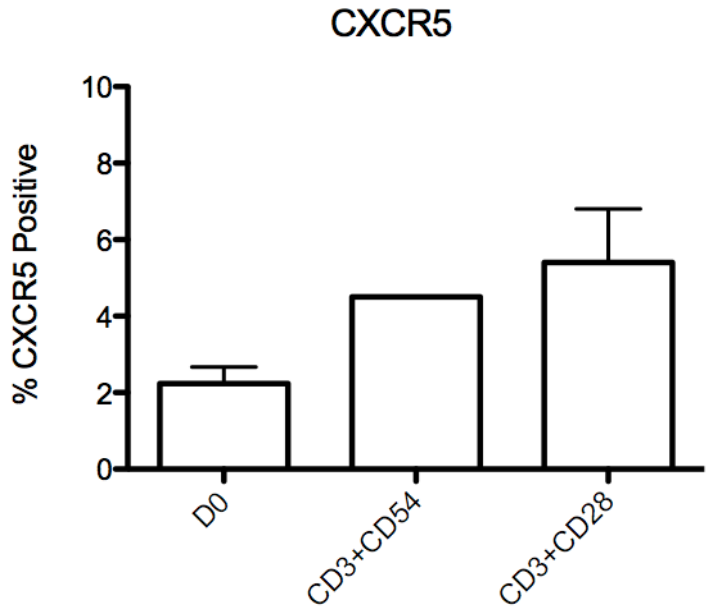

Figure 4.11, 4.12. Preliminary data: CXCR5 may define a small subset of memory T cells generated by costimulation through ICAM-1 or CD28. Percent of isolated CD4+ naïve T cells positive for CXCR5 was determined by flow cytometry. Naïve cells were stimulated through CD3+ICAM-1 or CD3+CD28 for 14 days. Cells were gated on CD45RO and CXCR5 postitve cells were determined by flow cytometry. Representative flow plots **(4.11)** and cumulative data **(4.12)** are shown. Data are presented as mean ± SEM and significance was determined using a two tailed t-Test. n=3, naïve cells; n=1, CD3+CD54; n=2, CD3+CD28.

seems possible that CXCR5 may define a small subset of central memory T cells in response to costimulation through ICAM-1 or CD28 *in vitro*. It is interesting that the baseline percentage did not really vary over the 14 days. This seems to suggest some sort of homeostatic necessity for a low percentage of these cells.

Costimulation of naïve CD4+ T cells through ICAM-1 or CD28 drastically increases expression of gut homing integrin α4β7 when the cells are co-cultured with retinoic acid

Migration to lymphoid tissue in the gut, particularly under non-inflamed conditions, is mediated in part by the integrin α4β7 on the surface of T cells (54). α4β7 binds to its ligand MAdCAM-1 expressed in gut lamina propria venules (55,56). α4β7 expression on our freshly isolated CD4+ naïve T cells was just over 50% **(Fig. 4.13, 4.14)**. The integrin expression seems slightly elevated considering that naïve cells are thought to express low levels of α4β7. However, naïve T cells use α4β7-MAdCAM-1 interactions to enter the Peyer's patches and mesenteric lymph nodes as they circulate throughout the body (58), possibly explaining our observations. By day 14 the CD45RO+ cells that had been stimulated through either CD3+ICAM-1 or CD3+CD28 displayed a decrease in α4β7 expression and therefore gut homing potential **(Fig. 4.13, 4.14)**. Due to the expression of possible lymph node homing molecules, CCR7, CD62L and CXCR4, on the differentiated cells at day 14 it seems likely that a larger subset of these cells would preferentially home to the peripheral lymph nodes (PLNs) as opposed to secondary lymphoid tissue in the gut.

Retinoic acid is a metabolite of vitamin A. The role of retinoic acid in gut homing by T cells was characterized by others using vitamin A deficient mice that lacked

Figure 4.13

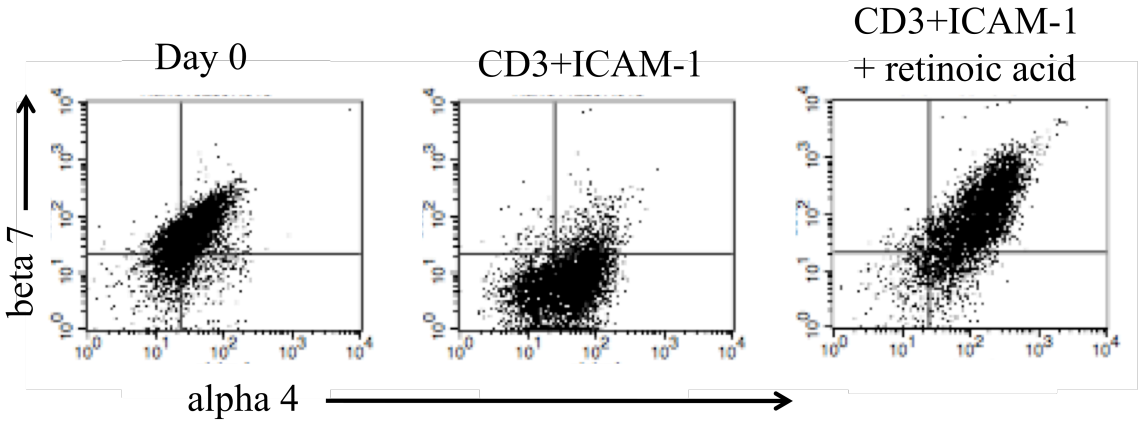

Figure 4.14

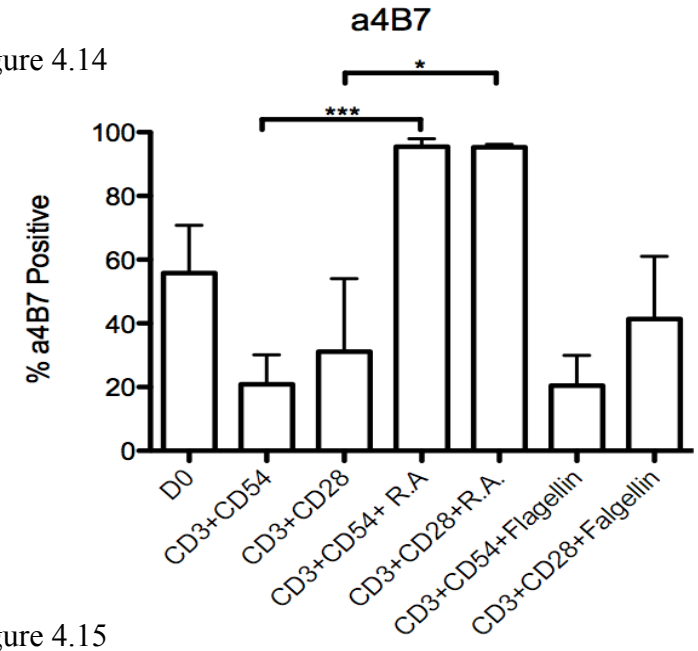

Figure 4.15

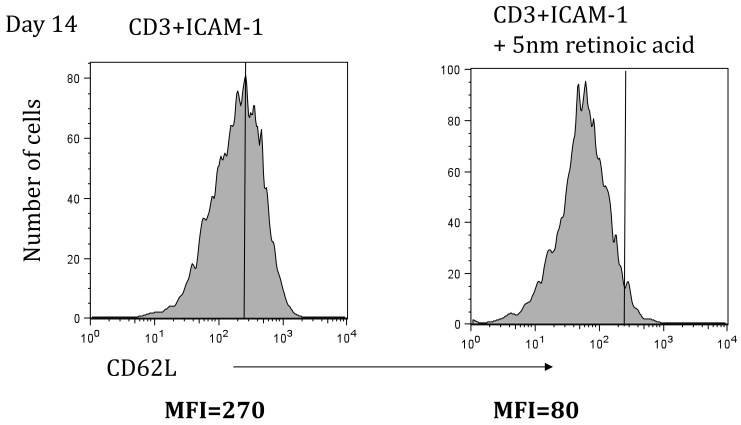

n=3

Figure 4.13-4.15. Costimulation of naïve CD4+ T cells through ICAM-1 or CD28 drastically increased expression of gut homing integrin α4β7 when co-cultured with retinoic acid. A) Percent of isolated CD4+ naïve T cells positive for α4β7 was determined by flow cytometry. Naïve cells were stimulated through CD3+ICAM-1 or CD3+CD28 for 14 days. Cells were cultured with stimulus alone, 1-5 nM retinoic acid or 1 nM flagellin. Cells were gated on CD45RO and α4β7 postitve cells were determined by flow cytometry. Representative flow plots **(4.13)** and cumulative data **(4.14)** are shown. Figure **4.15)** Naïve cells were stimulated through CD3+ICAM-1 or CD3+ICAM-1+ retinoic acid for 14 days; CD62L expression was measured by flow cytometry. Data are presented as mean ± SEM, *$p<0.05$, ***$p<0.001$ using two tailed t-Test. n=5, naïve cells; n=5, CD3+CD54; n=3, CD3+CD28; n=4, CD3+CD54+RA; n=2, CD3+CD28+RA; n=4, CD3+CD54+flagellin; n=2, CD3+CD28+flagellin.

effector and memory T cells in the gut mucosa while T cells in other lymphoid tissue remained unaltered (57). The biosynthesis of retinoic acid from vitamin A is an enzymatic process performed by retinaldehyde dehydrogenases (RALDHs). Vitamin A is produced by dendritic cells in Peyer's patches and draining mesenteric lymph nodes but not spleen or peripheral lymph nodes (57). Retinoic acid is essential for inducing gut homing properties in T cells. We wanted to determine if we could modulate gut homing properties of cells using our stimulation system in conjunction with retinoic acid. After 14 days of costimulation through ICAM-1 or CD28 in the presence of exogenous retinoic acid, the expression of $\alpha4\beta7$ sharply increased compared to costimulation alone **(Fig. 4.14, 4.15)**. Nearly all of the cells were positive for $\alpha4\beta7$ and this observation is supported by the simultaneous decrease in the PLN homing molecule, CD62L, following stimulation through CD3+ICAM-1 with retinoic acid as opposed to stimulation without retinoic acid **(Fig. 4.15)**.

Bacterial flagellin protein and its receptor, toll like receptor 5 (TLR5), have been implicated as an inducing factor of the inflammatory bowel disease, Crohn's disease (CD) (59,60). Inflammatory bowel disease (IBD) is characterized by infiltrating colitogenic effector/memory $CD4^+$ T cells into the mucosa and subsequently induced gut wall damage by inflammation (61). Activation of the TLR pathway, directed by MyD88, has been directly implicated in the maintenance of IBD through expansion of colitogenic CD4+ T cells (62). To address the question whether flagellin protein also plays a role in modulating migration of our effector/memory T cells, CD4+ naïve T cells were costimulated through ICAM-1 or CD28 in the presence of flagellin, and $\alpha4\beta7$ expression was measured after 14 days. The cells cultured with flagellin did not increase their $\alpha4\beta7$

expression compared to cells stimulated without flagellin. This indicates that triggering TLR5 on the surface of activated T cells did not play a role in modulating homing patterns of the cells in our stimulation system **(Fig. 4.14)**.

Expression of small intestine homing chemokine receptor CCR9 was not induced by costimulation of naïve CD4+ T cells through ICAM-1 or CD28 regardless of the addition of retinoic acid or bacterial flagellin protein

CCR9 is a chemokine receptor that is important in homing of effector T cells to the gut (63). The ligand for CCR9, CCL25, is expressed on endothelial cells in the small intestine and on lamina propria cells but not in epithelium from the colon (63,64). Most human naïve T cells in adults lack expression of CCR9 because it is thought that CCR9 is more important for antigen-induced migration to the gut rather than peripheral circulation (65). Approximately 28% of our freshly isolated CD4+ naïve T cells express CCR9. This level of naïve T cell expression is not unreasonable since it has been suggested that recent thymic emigrants express CCR9 (66). Following costimulation of our CD4+ naïve T cells through ICAM-1 for 14 days, the percentage of CCR9 positive cells did not change suggesting that the circulating memory population retains the ability to enter the gut similar to naïve **(Fig. 4.16, 4.17)**. Retinoic acid has been shown to enhance CCR9 mRNA levels and increase migration in response to CCL25 *in vitro* when CD4+ T cells were stimulated through CD3+CD28 with retinoic acid for 2-4 days (57). With our stimulation system in the presence of retinoic acid, the percentage of differentiated cells costimulated through ICAM-1 that expressed CCR9 dropped about 20% down to about

Figure 4.16

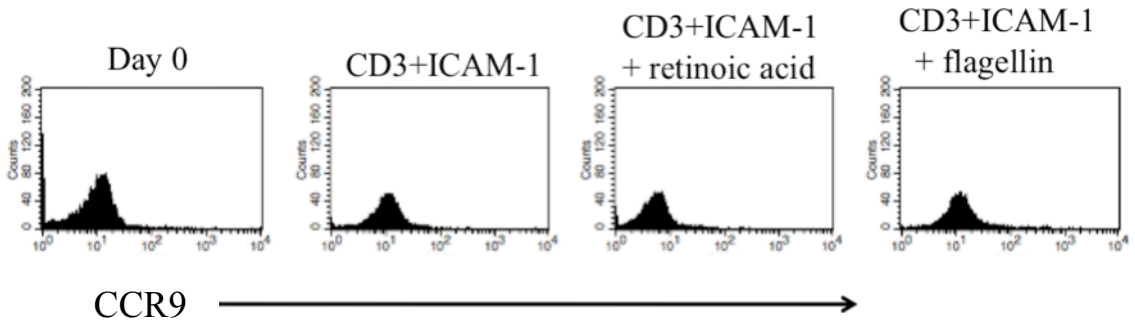

Figure 4.17

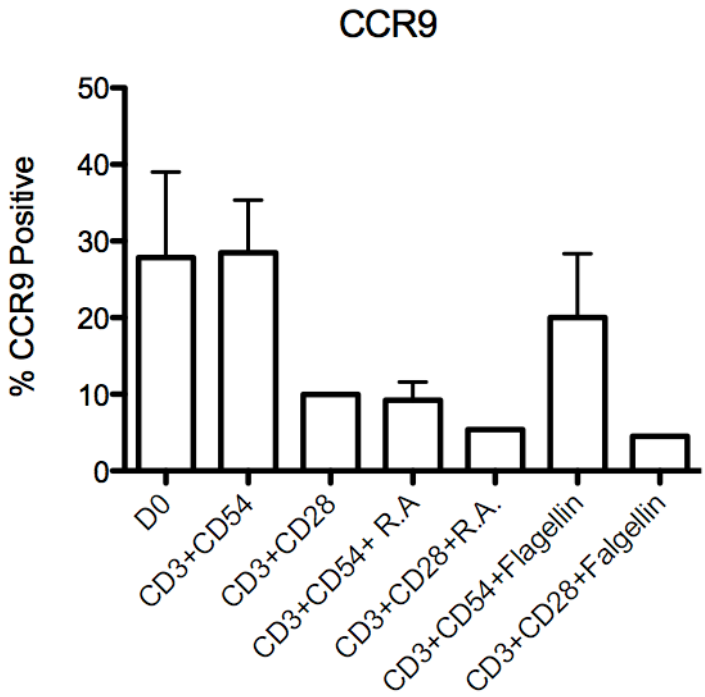

Figure 4.16, 4.17. Expression of small intestine homing chemokine receptor CCR9 is not induced by costimulation of naïve CD4+ T cells through ICAM-1 or CD28 regardless of the addition of retinoic acid or bacterial flagellin protein. Percent of isolated CD4+ naïve T cells that were positive for CCR9 was determined by flow cytometry. Naïve cells were stimulated through CD3+ICAM-1 or CD3+CD28 for 14 days. Cells were cultured with stimulus alone, 1-5 nM retinoic acid or 1 nM flagellin. Cells were gated on CD45RO and CCR9 positive cells were determined by flow cytometry. Representative flow plots **(4.16)** and cumulative data **(4.17)** are shown. Data are presented as mean ± SEM and significance was determined using two tailed t-Test. n=3, naïve cells; n=3, CD3+CD54; n=1, CD3+CD28; n=3, CD3+CD54+RA; n=1, CD3+CD28+RA; n=3, CD3+CD54+flagellin; n=1, CD3+CD28+flagellin.

10 % compared with stimulation without retinoic acid **(Fig. 4.16, 4.17)**. Therefore, stimulation of our CD4+ naïve T cells for 14 days with retinoic acid instead of total CD4+ T cells stimulated for 2-4 days with the addition of retinoic acid indicates that the increase observed in CCR9 expression by other labs may be an activation induced expression from primed cells that does not continue with an effector memory or central memory population differentiated from naïve cells. We also wanted to determine if triggering TLR5 with flagellin protein had an affect on CCR9 expression as we did in the Figure 7A where we measured $\alpha 4\beta 7$. The addition of bacterial flagellin protein to CD4+ naïve T cells stimulated through CD3+ICAM-1 for 14 days induced minimal change in the percent of CCR9 positive cells, only decreasing the percent positive about 8% from cells stimulated without flagellin **(Fig. 4.16, 4.17)**. Preliminary data of CCR9 expression with cells costimulated through CD28 indicates that the percent of differentiated cells that express CCR9 is low (about 10%) following 14 days of stimulation through CD3+CD28 alone (Fig. 8). The addition of either retinoic acid or flagellin to costimulation through CD28 did not have much impact on the percent of CCR9 positive cells, dropping it to about 5% **(Fig. 4.17)**. This suggests that costimulation of CD4+ naïve T cells through CD28 does not maintain a significant CCR9 expressing population and, as with cells costimulated through ICAM-1, the addition of retinoic acid or flagellin did not induce a CCR9 dependent gut homing population. Although CCR9 is thought to be an important component for T cell homing to the gut (especially the small intestine) supported by the fact that blocking CCL25 or a deficiency in CCR9 leads to reduced antigen specific CD8+ T cells in the small intestine (67, 68), more recent evidence suggests that a large subset of CD4+ effector T cells home to the small intestine in a CCR9 independent

manner (69). Therefore, the ability to modulate CCR9 expression may not be as important that the ability to modulate α4β7 expression when the desired outcome is to develop an effector memory or central memory T cell that has gut homing capabilities.

Discussion

Expression of chemokine receptors and other developmental or homing receptors on the surface of T cells provide homing guidance during migration and in this context, indicate differentiated subpopulations following activation. In the present study we initiated a characterization of some of these cell surface receptors as they occur when human CD4+ naïve T cells differentiate in our *in vitro* system. The goal was to identify changes in homing characteristics following stimulation, what phenotype the differentiated cells displayed and whether these parameters differed between costimulation through ICAM-1 and CD28. Overall, our data suggests that we are of creating a PLN homing memory population when we costimulate CD4+ naïve T cells through ICAM-1. We found no significant differences between costimulation through ICAM-1 or CD28 in the expression of many of the surface homing molecules studied. Slight difference in surface molecule expression were seen but were never greater than a ten percent differential. Costimulation of CD4+ naïve T cells through ICAM-1 or CD28 for 14 days led to mature CD45RO+ cells that expressed many memory-like phenotype receptors such as CCR7, CD62L, CXCR4 and to a lesser extent CD127 and CXCR5. The homing receptors CCR7 and CD62L direct T cells to the lymph node and help to define a central memory cell population (24) along with CD127, which is necessary for long-term memory cell survival (36-38). CXCR5 is often co-expressed with CCR7 in the periphery to define a subset of memory cells that are required for rapid antibody response by follicular B cells (53, 70) and CXCR4 has multiple roles in homing and function but its expression similarity to CCR7 may suggest facilitation of homing to the PLNs (49). A small percentage of the CD45RO+ cells also expressed CCR5, which is an

inflammatory homing molecule (39). CCR5 is only expressed on activated cells and given the low percentage of CCR5 expressing cells that we observed, it can be speculated that these cells are part of a late activating subset that remain in the culture as the effector cells undergo contraction. Another factor that may support our hypothesis that we are of creating a PLN homing memory population is that after costimulation through ICAM-1 or CD28 for 14 days, gut homing receptors $\alpha4\beta7$ and CCR9 generally diminished in expression (with the exception of CCR9 after ICAM-1 costimulation). This indicates to us that the differentiated population generated after costimulation through ICAM-1 or CD28 largely homes to secondary lymphoid organs, specifically PLNs, and not to effector sites. Also, these homing patterns can be modulated as shown with the increase in $\alpha4\beta7$ and decrease of CD62L upon addition of retinoic acid in culture. This suggests a plasticity reminiscent of that observed using *in vivo* studies and supports our assertion that our in vitro model replicates the *in vivo* situation in many ways.

The role that CD28 costimulation plays in cell migration has been studied in considerable detail. CD28 assists in the ability of primed T cells to leave lymphoid tissue and migrate to sites of inflammation (25, 71). Also, stimulation of total T cells through CD3+CD28 increases early CCR7 dependent migration to PLN followed by a decrease in LN homing potential a few days later (72). However, many of these studies examine chemokine receptor modulation after a few days of activation, not through long-term development to memory phenotype or with a starting naïve T cell population. In addition, the impact of costimulation of naïve T cells through ICAM-1 on chemokine receptor expression is largely unknown.

Figure 4.18 diagrams what is known about where differentiated subsets of T cells can home. It is known that CD4+ naïve T cells use CCR7, CD62L and possibly CXCR4 to enter the peripheral lymph nodes through high endothelial venules (HEVs) (16-19,25). Naïve cells also can circulate through the mesenteric lymph nodes and peyer's patches using the integrin $\alpha4\beta7$ (58). Upon activation, effector and effector memory T cells change their homing potential allow them to target sites where they are no longer just monitoring microenvironments but can carry out necessary immunological functions. CCR5 can facilitate cell migration to sites of inflammation (39) while CCR9 and $\alpha4\beta7$ help in cellular homing to the gut laminia propria (55, 56, 63). Central memory T cells display a lymph node homing, nonpolarized phenotype, much like naïve cells. Some central memory cells can also circulate to the gut via $\alpha4\beta7$ (25) and through the periphery and bone marrow based on using CXCR4 and the widespread expression of its ligand, SDF-1 (73). **Figure 4.19** illustrates that costimulation of naïve T cells through ICAM-1 generates CD45RO+ cells that resemble the population with central memory-like homing capabilities from **Figure 4.18** after 14 days of stimulation. Additionally, following the same culturing protocol with costimulation through CD28 yields similar results to ICAM-1.

Our results also support the premise that, under the right conditions, the homing outcome of stimulated cells can be changed. We observed this by using the addition of retinoic acid to cause an increase of $\alpha4\beta7$ expression. The ability to harness and/or modulate T cells' homing potential could have important implications in the development of T cell therapies or in treating autoimmune diseases. For example, during acute HIV-1 infection CD4+ T cells are rapidly depleted from the gut and remain depleted even after

Figure 4.18

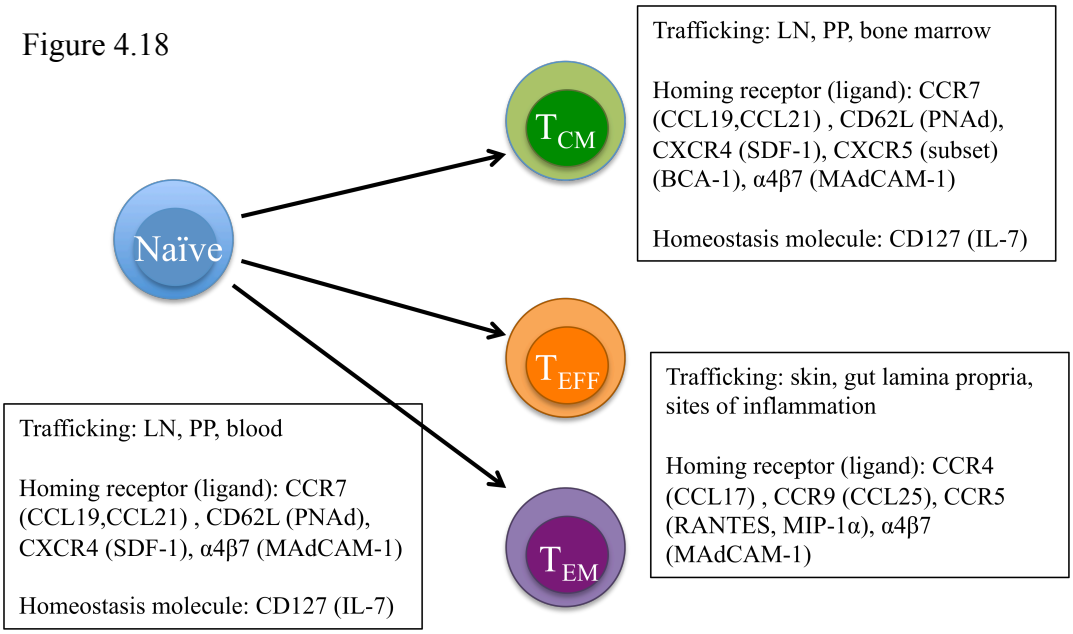

Figure 4.19

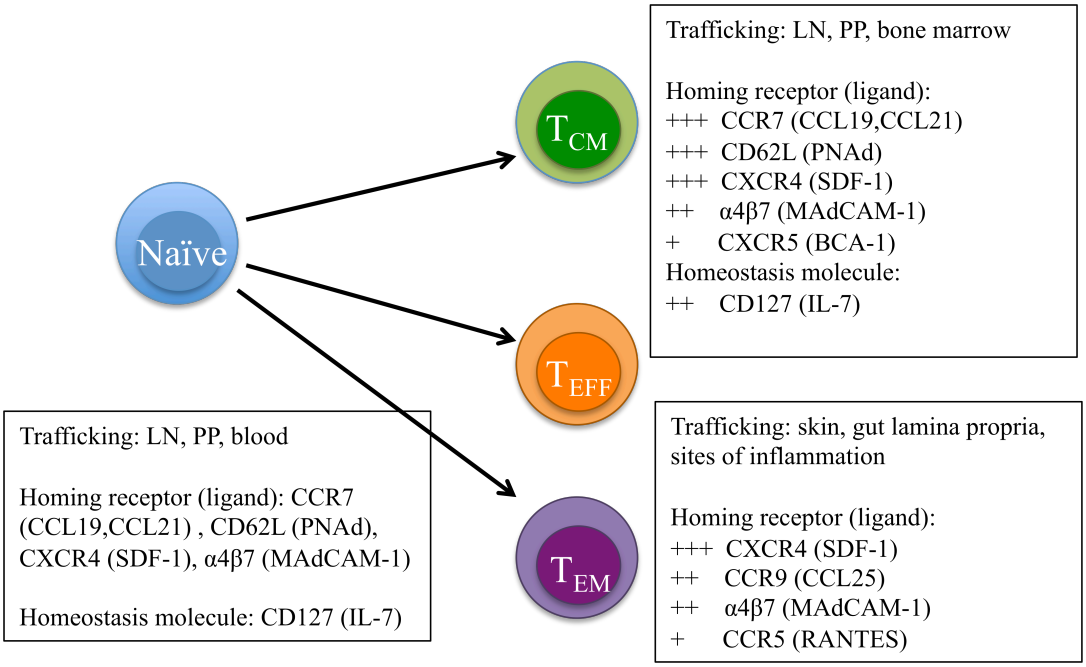

Figure 4.18) Diagram of known chemokine receptor and cell surface markers at naïve, central memory (T_{CM}), effector (T_{EFF}), and effector memory (T_{EM}) developmental stages of activation. Figure 4.19) Semi-quantification of surface molecule expression in our study after CD4+ naïve T cells were stimulated through CD3+ICAM-1 for 14 days. (+++) indicates high expression, (++) indicates medium expression and (+) indicates low expression. LN= lymph node, PP= peyer's patch. Figure adapted from FM Marelli-Berg, et al. (25).

antiviral therapy due to defective recruitment (74). The ability to upregulate the expression of α4β7 on T cells to induce gut migration could provide help in reconstituting the immune system in immunodeficient patients since the gut is an essential component in maintaining immunological competence. Similarly, induction of gut homing T cells could have a vast impact on controlling diarrheal diseases, which can be devastating and frequently fatal for children in developing countries. Hammerschmidt, et al. demonstrated some success in increasing the presence of gut homing T cells using subcutaneous injections of retinoic acid in mice, this treatment increased α4β7 expression on T cells by 30-40 percent in skin-draining lymph nodes (75). We observed a dramatic increase of α4β7 when we added retinoic acid to our cultures. The concept of specifically increasing the numbers of antigen specific T cells that home to the gut using costimulation through ICAM-1 along with retinoic acid could be a powerful and efficient tool to induce a specific immune response in the intestine.

Chemokines and their receptors are also involved in the development of cancers and are currently being investigated as targets of therapies. SDF-1 and CXCR4 have been shown to have roles in the development and progression of breast, prostate, colon, ovarian and other tumor types (76-79). In ovarian cancer, SDF-1 produced in the tumor microenvironment and CXCR7 (a second SDF-1 receptor) expressed on tumor cells are responsible for proliferation and survival of tumor cells (80). SDF-1 also is responsible for recruitment of immunosuppressive cells into the tumor to combat the anti-tumor effects of leukocytes (81). It is conceivable that using our stimulation system, which leads to a high percentage of CXCR4 T cells when costimulated through ICAM-1, we could generate tumor specific T cells *in vitro.* The tumor specific T cells would be used

for their homing capabilities to lymph nodes and tumor microenvironments to sustain long term anti-tumor activity.

In summary, we have identified a pattern of expression of chemokine receptors and other cell surface molecules on the T cells that we generated using ICAM-1 costimulation. This pattern apperars to define effector memory and central memory populations based on the homing capabilities provided by the various cell surface proteins. In addition, we have demonstrated an ability to modulate homing potential of these cells to the gut as measured increased expression of $\alpha 4\beta 7$ with the addition of retinoic acid to ICAM-1 or CD28 stimulation. The work presented here may also have important implications in the development of possible immunotherapies for infections and cancers.

References

1. Benedict SH, Cool KM, Dotson AL, Chan MA. Immunological Accessory Molecules. Encyclopedia of Life Sciences, John Wiley & Sons, Ltd. 2007; doi: 10.1002/9780470015902.a0000923.pub2
2. Rossi D, Zlotnik A. The biology of chemokines and their receptors. Annu. Rev. Immunol. 2000;18:000–00
3. Ebert LM, Schaerli P, Moser B. Chemokine-mediated control of T cell traffic in lymphoid and peripheral tissues. Molecular Immunology. 2005; 42: 799–809.
4. Loetscher, P., Moser, B. & Baggiolini, M. Chemokines and their receptors in lymphocyte traffic and HIV infection. Adv. Immunol. 2000; 74: 127–180.
5. Zlotnik, A. & Yoshie, O. Chemokines: a new classification system and their role in immunity. Immunity. 2000; 12: 121–127
6. Murphy PM, Baggiolini M, Charo IF, Hébert CA, Horuk R, Matsushima K, Miller LH, Oppenheim JJ, Power CA. International union of pharmacology. XXII. Nomenclature for chemokine receptors. Pharmacol. Rev. 2000; 52: 145–176
7. Thelen, M. Dancing to the tune of chemokines. Nat. Immunol. 2001; 2: 129–134.
8. Moser B, Willimann K. Chemokines: role in inflammation and immune surveillance. Ann Rheum Dis. 2004; 63: 84-89.
9. Sallusto, F., Mackay, C. R. & Lanzavecchia, A. The role of chemokine receptors in primary, effector, and memory immune responses. Annu. Rev. Immunol. 2000; 18: 593–620

10. Sallusto, F., Mackay, C. R. & Lanzavecchia,A.The role of chemokine receptors in primary, effector, and memory immune responses. Annu. Rev. Immunol. 2000; 18: 593–620
11. Butcher, E. C.,Williams, M.,Youngman, K., Rott, L. & Briskin, M. Lymphocyte trafficking and regional immunity. Adv. Immunol. 1999; 72: 209–253
12. Moser B, Loetscher P. Lymphocyte traffic control by chemokines. nature immunology. 2001; 2(2): 123-128
13. Rot A, von Andrian UH. Chemokines in innate and adaptive host defense: basic chemokinese grammar for immune cells. Annu Rev Immunol 2004; 22: 891–928
14. Von Andrian, U.H., Mempel, T.R. Homing and cellular traffic in lymph nodes. Nat. Rev. Immunol. 2003; 3: 867–878.
15. Sallusto, F., Lenig, D., Forster, R., Lipp, M., Lanzavecchia, A. Two subsets of memory T lymphocytes with distinct homing potentials and effector functions. Nature. 1999; 401: 708–712.
16. Gunn, M.D., Tangemann, K., Tam, C., Cyster, J.G., Rosen, S.D., Williams, L.T. A chemokine expressed in lymphoid high endothelial venules promotes the adhesion and chemotaxis of naive T lymphocytes. Proc. Natl. Acad. Sci. U.S.A. 1998; 95: 258–263.
17. Stein, J.V., Rot, A., Luo, Y., Narasimhaswamy, M., Nakano, H., Gunn, M.D., Matsuzawa, A., Quackenbush, E.J., Dorf, M.E., Von Andrian, U.H. The CC chemokine thymus-derived chemotactic agent 4 (TCA-4, secondary lymphoid tissue chemokine, 6Ckine, exodus- 2) triggers lymphocyte function-associated antigen 1-

mediated arrest of rolling T lymphocytes in peripheral lymph node high endothelial venules. J. Exp. Med. 2000; 191: 61–75.

18. Banchereau, J., Steinman, R.M. Dendritic cells and the control of immunity. Nature 1998; 392: 245–252.
19. Sprent, J., Surh, C.D. T cell memory. Annu. Rev. Immunol. 2002; 20: 551–579.
20. Gunn MD, Kyuwa S, Tam C, Kakiuchi T, Matsuzawa A, Williams LT, Nakano H. Mice lacking expression of secondary lymphoid organ chemokine have defects in lymphocyte homing and dendritic cell localization. J. Exp. Med. 1999; 189: 451–60.
21. Foerster R, Schubel A, Breitfeld D, Kremmer E, Renner-Muller I, Wolf E, Lipp M. CCR7 coordinates the primary immune response by establishing functional microenvironments in secondary lymphoid organs. Cell. 1999; 99:23–33
22. Förster R, Schubel A, Breitfeld D, Kremmer E, Renner-Müller I, Wolf E, Lipp M. CCR7 coordinates the primary immune response by establishing functional microenvironments in secondary lymphoid organs. Cell. 1999; 99: 23–33
23. Sallusto, F., Lenig, D., Förster, R., Lipp, M. & Lanzavecchia,A. Two subsets of memory T lymphocytes with distinct homing potentials and effector functions. Nature. 1999; 401: 708–712
24. Lisa M. Ebert, Patrick Schaerli, Bernhard Moser. Chemokine-mediated control of T cell traffic in lymphoid and peripheral tissues. Molecular Immunology. 2005; 42: 799–809.
25. FM Marelli-Berg, L Cannella, F Dazzi and V Mirenda. The highway code of T cell trafficking. J Pathol. 2008; 214: 179–189.

26. Guenin-Macé L, Carrette F, Asperti-Boursin F, Le Bon A, Caleechurn L, Di Bartolo V, Fontanet A, Bismuth G, Demangel C. Mycolactone impairs T cell homing by suppressing microRNA control of L-selectin expression. PNAS. 2011; 108(31): 12833–12838.

27. Mora JR, von Andrian UH. T-cell homing specificity and plasticity: new concepts and future challenges. Trends Immunol. 2006; 27(5):235-43

28. Moore TV, Clay BS, Cannon JL, Histed A, Shilling RA, Sperling AI. Inducible costimulator controls migration of T cells to the lungs via down-regulation of CCR7 and CD62L. Am J Respir Cell Mol Biol. 2011; 45(4):843-50.

29. Li, J., G. Huston, and S. L. Swain. 2003. IL-7 promotes the transition of CD4 effectors to persistent memory cells. J. Exp. Med. 198: 1807–1815.

30. Schluns, K. S., W. C. Kieper, S. C. Jameson, and L. Lefrancois. Interleukin-7 mediates the homeostasis of naive and memory CD8 T cells in vivo. Nat. Immunol. 2000; 1: 426–432.

31. Dooms, H., K. Wolslegel, P. Lin, and A. K. Abbas. Interleukin-2 enhances CD4 T cell memory by promoting the generation of IL-7R α-expressing cells. J. Exp. Med. 2007; 204: 547–557.

32. Kaech, S. M., Tan J. T., Wherry E. J., Konieczny B. T., Surh C. D., and Ahmed R. Selective expression of the interleukin-7 receptor identifies effector CD8 T cells that give rise to long-lived memory cells. Nat. Immunol. 2003; 4: 1191–1198.

33. Harrington, L. E., K. M. Janowski, J. R. Oliver, A. J. Zajac, and C. T. Weaver. Memory CD4 T cells emerge from effector T-cell progenitors. Nature 2008; 452: 356 –360

34. McKinstry, K. K., S. Golech, W. H. Lee, G. Huston, N. P. Weng, and S. L. Swain. Rapid default transition of CD4 T cell effectors to functional memory cells. J. Exp. Med. 2007; 204:2199 –2211.

35. Colpitts SL, Dalton NM and Scott P. IL-7 Receptor Expression Provides the Potential for Long-Term Survival of Both CD62L high Central Memory T Cells and Th1 Effector Cells during Leishmania major Infection. J Immunol 2009;182;5702-5711

36. Kondrack, R. M., J. Harbertson, J. T. Tan, M. E. McBreen, C. D. Surh, and L. M. Bradley. Interleukin 7 regulates the survival and generation of mem- ory CD4 cells. J. Exp. Med. 2003; 198: 1797–1806.

37. Akashi, K., M. Kondo, U. von Freeden-Jeffry, R. Murray, and I. L. Weissman. Bcl-2 rescues T lymphopoiesis in interleukin-7 receptor-deficient mice. Cell. 1997; 89: 1033–1041.

38. Wofford, J. A., H. L. Wieman, S. R. Jacobs, Y. Zhao, and J. C. Rathmell. IL-7 promotes Glut1 trafficking and glucose uptake via STAT5-mediated activa- tion of Akt to support T-cell survival. Blood. 2008; 111: 2101–2111.

39. Moser B and Loetscher P. Lymphocyte traffic control by chemokines. Nature Immunology. 2001; 2 (2). 123-128.

40. Loetscher P, Uguccioni M, Bordoli L, Baggiolini M, Moser B, Chizzolini C, et al. CCR5 is characteristic of Th1 lymphocytes. Nature 1998; 391:344–345.

41. Luther SA, Cyster JG. Chemokines as regulators of T cell differentiation. Nat Immunol 2001; 2:102–107.

42. Qin S, Rottman JB, Myers P, Kassam N, Weinblatt M, Loetscher M, Koch AE, Moser B, Mackay CR. The chemokine receptors CXCR3 and CCR5 mark subsets of

T cells associated with certain inflammatory reactions. J. Clin. Invest. 1997; 101:746–54

43. Balashov KE, Rottman JB, Weiner HL, Hancock WW. CCR5(+) and CXCR3(+) T cells are increased in mul- tiple sclerosis and their ligands MIP- 1alpha and IP-10 are expressed in demyelinating brain lesions. Proc. Natl.Acad. Sci. USA 1999; 96:6873–78
44. Chirathaworn C, Kohlmeier JE, Tibbetts SA, Rumsey LM, Chan MA, Benedict SH. Stimulation through intercellular adhesion molecule-1 provides a second signal for T cell activation. J Immunol. 2002; 168:5530–7.
45. Agace WW, Amara A, Roberts AI, Pablos JL, Thelen S, Uguccioni M, Li XY, Marsal J, Arenzana-Seisdedos F, Delaunay T, Ebert EC, Moser B, Parker CM. Constitutive expression of stromal derived factor-1 by mucosal epithelia and its role in HIV transmission and propagation. Curr. Biol. 2000; 10: 325–328
46. Pablos JL, Amara A, Bouloc A, Santiago B, Caruz A, Galindo M, Delaunay T, Virelizier JL, Arenzana-Seisdedos F. Stromal-cell derived factor is expressed by dendritic cells and endothelium in human skin. Am. J. Pathol. 1999; 155: 1577–1586
47. Nagasawa T, Hirota S, Tachibana K, Takakura N, Nishikawa S, Kitamura Y, Yoshida N, Kikutani H, Kishimoto T. Defects of B-cell lymphopoiesis and bone-marrow myelopoiesis in mice lacking the CXC chemokine PBSF/SDF-1. Nature. 1996; 382: 635–638
48. Tachibana K, Hirota S, Iizasa H, Yoshida H, Kawabata K, Kataoka Y, Kitamura Y, Matsushima K, Yoshida N, Nishikawa S, Kishimoto T, Nagasawa T. The chemokine

receptor CXCR4 is essential for vascularization of the gastrointestinal tract. Nature. 1998; 393: 591–594

49. Scimone ML, Felbinger TW, Mazo IB, Stein JV, von Andrian UH, Weninger W. CXCL12 mediates CCR7-independent homing of central memory cells, but not naive T cells, in peripheral lymph nodes. J Exp Med 2004; 199: 1113–1120.
50. Förster R, Mattis AE, Kremmer E, Wolf E, Brem G, Lipp M. A putative chemokine receptor, BLR1, directs B cell migration to defined lymphoid organs and specific anatomic compartments of the spleen. Cell. 1996; 87: 1037–1047
51. Ansel KM, Ngo VN, Hyman PL, Luther SA, Förster R, Sedgwick JD, Browning JL, Lipp M, Cyster JG. A chemokine-driven positive feedback loop organizes lymphoid follicles. Nature. 2000; 406: 309–314
52. Schaerli, P., Loetscher, P., Moser, B. Cutting edge: induction of follicular homing precedes effector Th cell development. J. Immunol. 2001; 167: 6082–6086.
53. Schaerli, P., Willimann, K., Lang, A.B., Lipp, M., Loetscher, P., Moser, B. CXC chemokine receptor 5 expression defines follicular homing T cells with B cell helper function. J. Exp. Med. 2000; 192: 1553–1562.
54. Wagner N, Löhler J, Kunkel EJ, Ley K, Leung E, Krissansen G, Rajewsky K, Müller W. Critical role for b7 integrins in formation of the gut-associated lymphoid tissue. Nature. 1996; 382: 366–370
55. Berlin C, Berg EL, Briskin MJ, Andrew DP, Kilshaw PJ, Holzmann B, Weissman IL, Hamann A, Butcher EC. a4b7 integrin mediates lymphocyte binding to the mucosal vascular addressin MAdCAM-1. Cell. 1993; 74: 185–195

56. Nakache M, Berg EL, Streeter PR, Butcher EC. The mucosal vascular addressin is a tissue-specific endothelial cell adhesion molecule for circulating lymphocytes. Nature. 1989; 337: 179–181

57. Iwata M, Hirakiyama A, Eshima Y, Kagechika H, Kato C, Song SY. Retinoic acid imprints gut-homing specificity on T cells. Immunity. 2004; 21: 527–538

58. Christopher C. DeNucci, Jason S. Mitchell, and Yoji Shimizu. Integrin function in T-cell homing to lymphoid and nonlymphoid sites: getting there and staying there.Crit Rev Immunol. 2009 ; 29(2): 87–109.

59. Targan SR, Landers CJ, Yang H, Lodes MJ, Cong Y, Papadakis KA, Vasiliauskas E, Elson CO, Hershberg RM. Antibodies to CBir1 flagellin define a unique response that is associated independently with complicated Crohn's disease. Gastroenterology. 2005; 128: 2020–2028.

60. Gewirtz AT, Vijay-Kumar M, Brant SR, Duerr RH, Nicolae DL, Cho JH. Dominant-negative TLR5 polymorphism reduces adaptive immune response to flagellin and negatively associates with Crohn's disease. Am J Physiol Gastrointest Liver Physiol. 2006; 290: G1157–1163.

61. Strober, W., I. J. Fuss, R. S. Blumberg. The immunology of mucosal models of inflammation. Annu. Rev. Immunol. 2002; 20: 495-549.

62. Tomita T, Kanai T, Fujii T, Nemoto Y, Okamoto R, Tsuchiya K, Totsuka T, Sakamoto N, Akira S, Watanabe M. MyD88-Dependent Pathway in T Cells Directly Modulates the Expansion of Colitogenic $CD4^+$ T Cells in Chronic Colitis. The Journal of Immunology. 2008; 180: 5291 -5299

63. Zabel BA, Agace WW, Campbell JJ, Heath HM, Parent D, Roberts AI, Ebert EC, Kassam N, Qin S, Zovko M, LaRosa GJ, Yang LL, Soler D, Butcher EC, Ponath PD, Parker CM, Andrew DP. Human G protein-coupled receptor GPR-9- 6/CC chemokine receptor 9 is selectively expressed on intestinal homing T lymphocytes, mucosal lymphocytes, and thymocytes and is required for thymus-expressed chemokine-mediated chemotaxis. J Exp Med. 1999;190(9):1241-56.

64. Papadakis KA, Prehn J, Nelson V, Cheng L, Binder SW, Ponath PD, Andrew DP, Targan SR. The role of thymus-expressed chemokine and its receptor CCR9 on lymphocytes in the regional specialization of the mucosal immune system. J Immunol 2000;165(9):5069–76.

65. Klonowski KD, Williams KJ, Marzo AL, Blair DA, Lingenheld EG, Lefrançois L. Dynamics of blood-borne CD8 memory T cell migration in vivo. Immunity. 2004; 20: 551–562

66. Olaussen RW, Farstad IN, Brandtzaeg P, Rugtveit J. Age-related changes in CCR9þ circulating lymphocytes: are CCR9þ naive T cells recent thymic emigrants? Scand J Immunol 2001;54:435–439.

67. Svensson M, Marsal J, Ericsson A, Carramolino L, Brodén T, Márquez G, Agace WW. CCL25 mediates the localization of recently activated CD8abC lymphocytes to the small-intestinal mucosa. J. Clin. Invest. 2002; 110: 1113–1121

68. Johansson-Lindbom B, Svensson M, Wurbel MA, Malissen B, Márquez G, Agace W. Selective generation of gut tropic T cells in gut-associated lymphoid tissue (GALT): requirement for GALT dendritic cells and adjuvant. J. Exp. Med. 2003; 198: 963–969

69. Stenstad H, Ericsson A, Johansson-Lindbom B, Svensson M, Marsal J, Mack M, Picarella D, Soler D, Marquez G, Briskin M, Agace WW. Gut-associated lymphoid tissue–primed CD4+ T cells display CCR9-dependent and -independent homing to the small intestine. Blood. 2006;107(9):3447-54.

70. MacLeod MK, David A, McKee AS, Crawford F, Kappler JW, Marrack P. Memory CD4 T cells that express CXCR5 provide accelerated help to B cells. J Immunol. 2011;186(5):2889-96.

71. Mirenda V, Jarmin SJ, David R, Dyson J, Scott D, Gu Y, Lechler RI, Okkenhaug K, Marelli-Berg FM. Physiological and aberrant regulation of memory T cell trafficking by the co-stimulatory molecule CD28. Blood. 2007;109: 2968-2977

72. Schaeuble K, Hauser MA, Singer E, Groettrup M, Legler DF. Cross-Talk Between TCR and CCR7 Signaling Sets a Temporal Threshold for Enhanced T Lymphocyte Migration. J Immunol 2011; 187; 5645-5652.

73. Mazo IB, Honczarenko M, Leung H, Cavanagh LL, Bonasio R, Weninger W, et al. Bone marrow is a major reservoir and site of recruitment for central memory CD8+ T cells. Immunity 2005; 22: 259 – 270.

74. Mavigner M, Cazabat M, Dubois M, L'Faqihi FE, Requena M, Pasquier C, Klopp P, Amar J, Alric L, Barange K, Vinel JP, Marchou B, Massip P, Izopet J, Delobel P. Altered CD4+ T cell homing to the gut impairs mucosal immune reconstitution in treated HIV-infected individuals. J Clin Invest. 2012; 122(1): 62-9.

75. Hammerschmidt SI, Friedrichsen M, Boelter J, Lyszkiewicz M, Kremmer E, Pabst O, Förster R. Retinoic acid induces homing of protective T and B cells to the gut after subcutaneous immunization in mice. J Clin Invest. 2011; 121(8): 3051–3061.

76. Müller A, Homey B, Soto H, Ge N, Catron D, Buchanan ME, McClanahan T, Murphy E, Yuan W, Wagner SN, Barrera JL, Mohar A, Verástegui E, Zlotnik A. Involvement of chemokine receptors in breast cancer metastasis. Nature. 2001; 410(6824): 50–56.

77. Zeelenberg IS, Ruuls-Van Stalle L, Roos E. The chemokine receptor CXCR4 is required for outgrowth of colon carcinoma micrometastases. Cancer Research. 2003; 63(13): 3833–3839.

78. Waugh DJJ, Wilson C, Seaton A, Maxwell PJ. Multi-faceted roles for CXC-chemokines in prostate cancer progression. Frontiers in Bioscience. 2008; 13(12): 4595–4604.

79. Scotton CJ, Wilson JL, Scott K, Stamp G, Wilbanks GD, Fricker S, Bridger G, Balkwill FR. Multiple actions of the chemokine CXCL12 on epithelial tumor cells in human ovarian cancer. Cancer Research. 2002; 62(20): 5930–5938.

80. Burns JM, Summers BC, Wang Y, Melikian A, Berahovich R, Miao Z, Penfold ME, Sunshine MJ, Littman DR, Kuo CJ, Wei K, McMaster BE, Wright K, Howard MC, Schall TJ. A novel chemokine receptor for SDF-1 and I-TAC involved in cell survival, cell adhesion, and tumor development. Journal of Experimental Medicine. 2006; 203(9): 2201–2213.

81. Ray P, Lewin SA, Mihalko LA, Schmidt BT, Luker KE, Luker GD. Noninvasive imaging reveals inhibition of ovarian cancer by targeting CXCL12-CXCR4. Neoplasia. 2011;13(12):1152-61.

Chapter 5

Costimulation of CD4+ naïve T cells through ICAM-1 generates a memory phenotype in older individuals

Introduction

With age, the immune response can lose ability to respond to disease causing organisms and to be properly regulated. Older humans produce and harbor fewer thymic derived naive T cells and this has been proposed as one of the factors involved in declining function of the immune system also known as immunosenescence (1). The capability of naive CD4+ human T cells from older individuals to activate and respond to a specific foreign disease causing organism (immunogen) is not fully characterized and description of this capability should lead to conclusions about immunosenescence.

As mentioned earlier, naïve T cells require two signals in order to become fully activated. The first is through the T cell receptor (TCR)/CD3 complex. The second signal is delivered through the costimulatory molecule and is independent of antigen specificity (2). After antigen encounter, naïve T cells undergo differentiation and clonal expansion into an effector cell population which eventually contracts leaving memory cells (3,4). Without the presence of this second signal the cell can become anergic or apoptotic (5,6). Memory T cells are longer lived in the body than effector cells, activate quicker and require less costimulation than naïve T cells (7-9).

In young, healthy individuals, naïve T cells are capable of being activated by multiple different costimulatory molecules. CD28 is a well-characterized costimulatory molecule. Costimulation through CD28 by its ligands B7-1 and B7-2 on an APC can induce cell proliferation and IL-2 secretion, generate Th1 and Th2 subsets, protect the cell from apoptosis and lead to an increase in memory T cells (10-12). Leukocyte Function-associated Antigen-1 (LFA-1) on the T cell surface also can serve a costimulatory role when interacting with ICAM-1 on APCs. Costimulation through

LFA-1 can initiate cell activation and proliferation but does not drive cells to memory and many of the cells die by apoptosis (13-15). Intercellular Adhesion Molecule-1 (ICAM-1) resident on T cells also functions as a classic second signal. Costimulation of human naïve CD4+ T cells from younger subjects through ICAM-1 induces differentiation to memory T cells, making ICAM-1 the only molecule identified thus far besides CD28 that is expressed on human naïve T cells and capable of costimulation leading to generation of memory cells (15). It has also been observed that costimulation through ICAM-1 can differentiate naïve CD4+ T cells into suppressive regulatory T cells (16).

Age associated changes in T cells are in part responsible for a decline in the immune response in the elderly. Older individuals display both a reduced diversity of T cells as well as an accumulation in T cells that are defective in activation and function. The defect in T cell proliferation, differentiation and survival can be partially attributed to an increase in T cells that lack CD28 expression (17-20). This CD28(-) T cell population is not seen in mice. However, murine CD4+ cells from older mice showed a decrease in IL-2 production after stimulation with anti-CD3 and anti-CD28 mAb when compared to younger mice illustrating a decrease in T cell CD28 response with age despite CD28 expression (21). There is also evidence that in older mice, Tregs expressing an effector/memory phenotype can induce a downregulation in expression of the CD28 counter-receptor, CD86, in dendritic cells leading to an impaired T cell response (22).

The accumulation of defects in CD4+ T cells, in addition to costimulation defects, lead to the weakened immune function observed older individuals. A reduction in TCR signaling can be attributed to inefficient immunological synapse formation and reduction

in intracellular signaling complex formation (23-25). Impaired TCR signaling likely has a role in diminished T cell expansion and IL-2 secretion observed in aging mouse models (26) DNA damage from chronic infection or defects in DNA damage repair is shown to accelerate immune aging (27). Additionally, CD4+ T cells in older individuals are impaired in their ability to effectively activate B cells following vaccine, thereby reducing antibody production (28-31).

Taken together, these data support the hypothesis that malfunctions in T cell signaling in older individuals play a role in a weakened immune response. The need to understand how T cells activate and differentiate with age is important in determining when and where T cell function is impaired. The present study examines the effects of different costimulation of CD4+ naïve T cells from older individuals on T cell activation and differentiation.

Materials and methods

Antibodies and Reagents

Hybridomas expressing anti-CD11a (HB202), and anti-CD54 (R6.5D6) were purchased from American Type Culture Collection (ATCC, Rockville, MD) and purified from serum-free culture medium with protein G-sepharose (Amersham Pharmacia, Piscataway, NJ). Anti-CD28 (clone ANC28.1) was purchased from Ancell (Minneapolis, MN) and anti-CD3 (OKT3) was purchased from eBioscience (San Diego, CA). Anti-CD11a-FITC, anti-CD3-FITC, anti-CD25-FITC, anti-CD27-PE, anti-CD134-PE, anti-CD54-PE, anti-CD28-TriColor, anti-CD45RA-TriColor and anti-CD45RO-TriColor were purchased from Caltag Laboratories (Burlingame, CA). Anti-CD25-TriColor (Caltag) and anti-CD25-PE-Cy5 (Becton Dickenson, San Jose CA) were used interchangeably with similar results. Foxp3 was detected using the Anti-Human Foxp3 Staining Set (eBioscience) in both FITC and PE, and used interchangeably with anti-Foxp3-PE (Miltenyi Biotec Inc., Auburn, CA) with similar results. Anti-CD137-PE-Cy5, anti-CD154-FITC, Annexin V-PE and 7-AAD were purchased from BD Pharmingen. CFSE (5-(and-6) carboxyfluorescein diacetate, succinimidyl ester) was purchased from Molecular Probes (Eugene, OR) and used at 2.5 μM in labeling experiments.

Cell Purification

Naïve human CD4+ T cells were isolated from peripheral blood of multiple donors by negative selection using a naïve T cell enrichment kit (Stem Cell Technologies, Vancouver, BC, Canada) as we have reported previously (15,16). All magnetically selected naïve CD4+ T cell populations were of >98% purity as assessed by flow

cytometry. In the present work, purified naïve human T cells represents cells that are CD4(+) CD45RA(+)RO(-) CD11a^{lo} CD27(+). Isolation of T cells with a differentiated phenotype was accomplished by negative selection of stimulated populations with antibodies against CD45RA and CD27 (Stem Cell Technologies), resulting in T cells with a CD4(+) CD45RA(-) CD11a^{hi} CD27(-) phenotype.

T cell Stimulation

Antibodies in PBS were attached to tissue culture-treated plates (Midwest Scientific, St. Louis, MO) by incubation at 37°C for 2 hours or overnight at 4°C, and wells were washed three times with PBS to remove unbound antibody. Naïve CD4+ T cells were added at a concentration of $1x10^6$-2×10^6 / ml, and stimulated with 1 μg/ml anti-CD3 plus 10 μg/ml anti-ICAM-1, or 5 μg/ml anti-LFA-1, or 5 μg / ml anti-CD28. Optimal antibody concentrations were determined based on the minimum dose that led to maximum T cell proliferation (not shown).

Flow Cytometry

Flow cytometry was performed using the FACScan (Becton Dickenson, San Jose CA) or the Accuri C6 Flow Cytometer System (Accuri Cytomoters, Ann Arbor MI). The FACScan was calibrated using CaliBRITE beads (Becton Dickinson), and the Accuri C6 was calibrated using Sphero APC Calibration Particles (Spherotech, Inc. Lake Forest, IL). This was supplemented by compensation using singly stained cells. Data were analyzed using Cell Quest (Becton Dickinson), FlowJo (Tree Star Inc, Ashland, OR) and CFlow (Accuri Cytometers).

Measurement of cell proliferation and apoptosis

After stimulation, naïve CD4(+) T cells were harvested on the days indicated and stained with AnnexinV-PE and 7-AAD at 2 μg/ml prior to flow cytometric analysis. Viable cell number was quantified by comparing the number of non-apoptotic or non-necrotic cells [AnnexinV(-) and 7-AAD(-)] acquired on the flow cytometer during one minute at a constant flow rate. Calibration standards of known cell concentrations were used to calculate the number of viable cells within each population. To measure the induction of apoptosis, CFSE-labeled cells were stained as indicated above and the numbers of apoptotic cells were determined [apoptotic cells are designated as AnnexinV(+) and 7-AAD(-)]. The data shown are the percentage of apoptotic cells within each cell generation.

Statistical analysis.

Statistical analysis was performed using GraphPad Prism (GraphPad Software, La Jolla, CA.) or SigmaStat (Systat Software Inc. San Jose, CA). Statistical tests and significance for individual figures are indicated in figure legends.

Results

Characterization of resting peripheral T cells and CD4+ naïve T cells in older individuals.

Healthy young individuals express CD28 on the surface of their naïve CD4+ T cells as well as low levels of ICAM-1 (32). Their naïve T cells also express the chemokine receptor CCR7 and L-selectin CD62L. Both of these promote homing into lymph nodes (33). Our data support the high expression of CCR7 and CD62L on naïve CD4+ T cells in young individuals **(Fig 5.1)**. We characterized surface molecule expression on both naïve and peripheral T cells from older individuals. T cells represented about 48% of total peripheral blood mononuclear cells (PBMC) and of those T cells, 45% were CD45RO+ non-naive, 63% were naïve-like and about 7% were a memory-like phenotype **(Fig. 5.2)**. Seventy-three percent of the T cells were CD4+, 25% were CD8+ and we observed a small population of T cells, averaging about 6%, that expressed both CD4 and CD8 **(Fig. 5.2)**. As in young subsets, resting T cells from older individuals expressed a low level (10 %) of CD54 (ICAM-1), 80% of the cells were CD28 positive and 9% of T cells were double positive for both CD54 and CD28 (Fig. 1B). Lymph node homing molecule CCR7 was expressed on about 65% of T cells from older individuals while 85% were positive for CD62L; almost all of the CCR7+ cells (60%) were also double positive for CD62L **(Fig. 5.2)**.

The purity of the apparently naïve CD4+ T cells that were used to characterize the resting naïve phenotype averaged 92% once isolated from PBMC of elderly donors using negative magnetic selection **(Fig. 5.3)**. This was consistently lower than the apparent purity observed many times with younger subjects (98%) and suggests an as yet

described basic young/old difference. CD54 expression was just slightly lower on naïve cells (8%) of older individuals than on total T cells, CD28 expression (85%) was slightly higher on naïve cells from older subjects while only 5% expressed both CD54 and CD28 **(Fig. 5.3)**. Naïve cells that expressed CCR7 were reduced to about 77% compared to CCR7 expression (98%) on CD4+ naïve T cells from younger individuals **(Fig. 5.1)** while CD62L expression remained high (91%) and almost all of the cells that were positive for CCR7 were also positive for CD62L **(Fig. 5.3)**.

Naïve T cells are thought to be largely homogeneous in phenotype and multi-potent in the ability to differentiate. It should be noted here that at low expression levels, percent positive cell populations are delimited by the gating procedures and control measures to establish non or low expressing populations. Hence cells excluded for CD54, for example, may still be positive for CD54 but simply express CD54 at a level that falls below the limit of detection with flow cytometry. These data should not be interpreted as supporting the hypothesis of naïve T cell subsets. **Figures 5.4, 5.5** shows the histogram plots that correspond with **Figures 5.2 and 5.3**. These plots illustrate the subsets present for molecules on the surface of total T cells compared to the homogeneous shift in fluorescence intensity that correlates with an increase in surface molecule expression observed in the naïve plots.

Figure 5.1

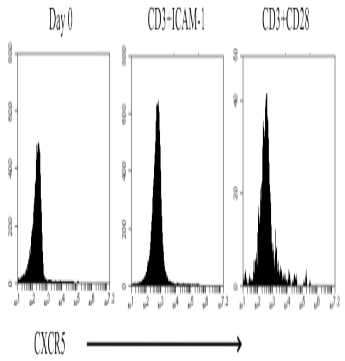

Figure 5.2

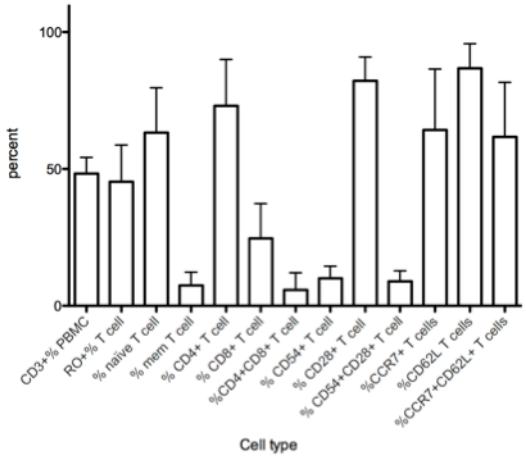

Figure 5.3

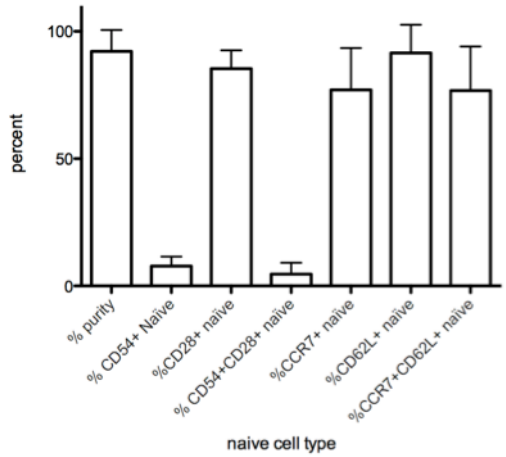

Figure 5.4

T cell surface molecule expression

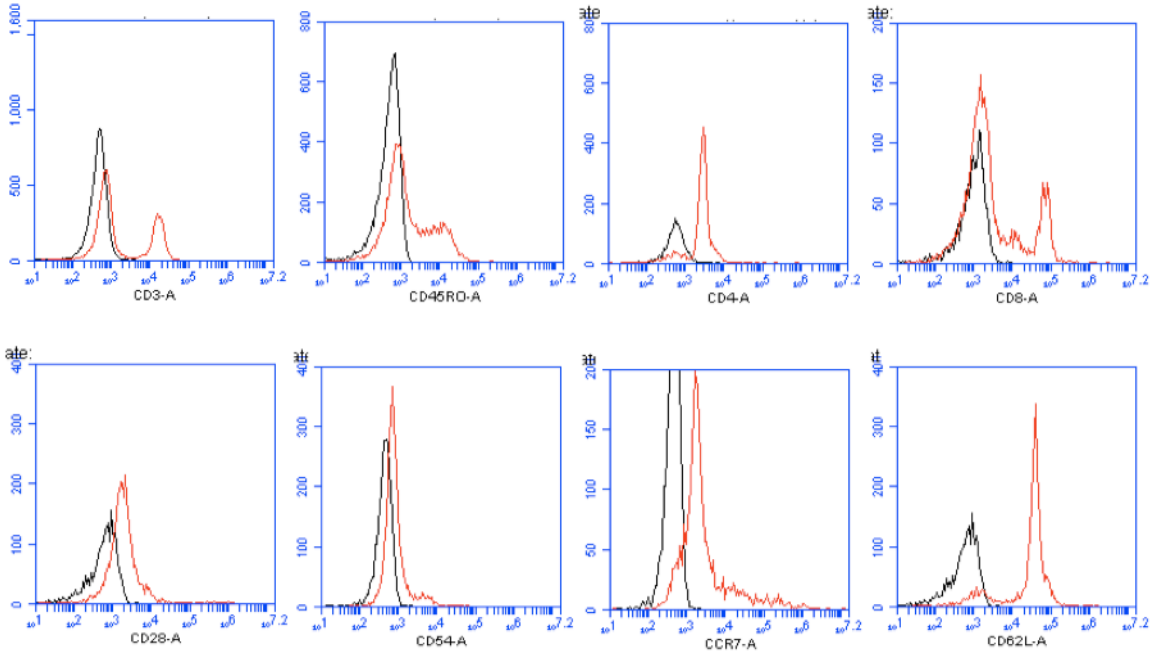

Figure 5.5

CD4+ naïve T cell surface molecule expression

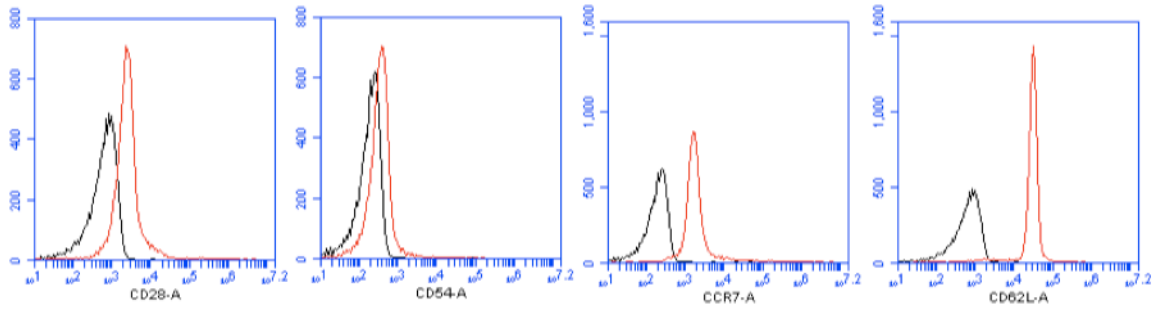

Figure 5.1-5.5. Characterization of resting peripheral T cells and CD4+ naïve T cells in older individuals. **5.1)** Percent positive CCR7 and CD62L cells in freshly isolated CD4+ naïve T cells isolated in healthy young individuals. CCR7 n=9. CD62L n=6. **5.2)** Phenotype of T cells from older individuals at day 0. PBMCs were isolated from peripheral blood and T cells were gated via CD3 expression. Naïve-like cells were CD11a(-) and CD27+, and memory-like cells were CD11a+ and CD27(-.) Other phenotypes were determined by expression of CD4, CD8, CD54, CD28, CCR7 and CD62L. n=4. **5.3)** Phenotype of CD4+ Naïve T cells from older individuals at day 0. **5.4)** Histogram plots of T cell surface molecule expression. **5.5)** Histogram plots of CD4+ naïve T cell surface molecule expression. Black like is unstained control and red line is surface fluorescence. Naïve cells were isolated using a negative selection magnetic column and purity was determined by percent expressing a naïve phenotype (CD45RO(-), CD11a(-), CD27+). Naïve cell phenotype was verified by cell surface expression of CD54, CD28, CCR7 and CD62L. n=4

Kinetic expression of tertiary costimulatory molecules following activation of CD4+ naïve T cell from older individuals is unregulated compared to that of younger individuals.

To study how activation of naïve CD4+ T cells and progression from naïve to effector and memory phenotypes might differ between younger and older individuals, we measured the expression of cell surface tertiary costimulatory molecules. Tertiary costimulatory molecules help to promote T cell differentiation, effector function and survival. CD40L, OX40 and 4-1BB are tertiary costimulatory molecules that are only expressed on activated T cells and are important in propagating T cell responses to memory. We wanted to initially characterize the kinetic expression of each tertiary costimulatory molecule on CD4+ T cells from healthy young individuals as they went from naïve to effector or memory phenotype with stimulation through different second signals. This characterization would help to define which molecules stayed on or were turned on then off as the cells progressed through activation and which molecules are able to receive third signals to direct cells to effector or memory **(Fig. 5.6)**. Naïve CD4+ T cells that were stimulated through CD3+CD28 (red diamonds) experienced intermediate expression of all three tertiary signals that peaked at around 30% to 40% positive by day 7 and began to decline to day 11. Costimulation through LFA-1 (CD11a) (green squares) induced the highest expression of all three tertiary signaling proteins and, similar to CD28 costimulation, peaked at 7 days before a slight decline in OX-40 and 4-1BB and a more drastic decline in CD40L **(Fig. 5.7)**. Unlike costimulation through CD28 or LFA-1, stimulation through CD3+ICAM-1 (blue triangles) activated the tertiary costimulatory molecules with slower responses but did not plateau during the

Figure 5.6

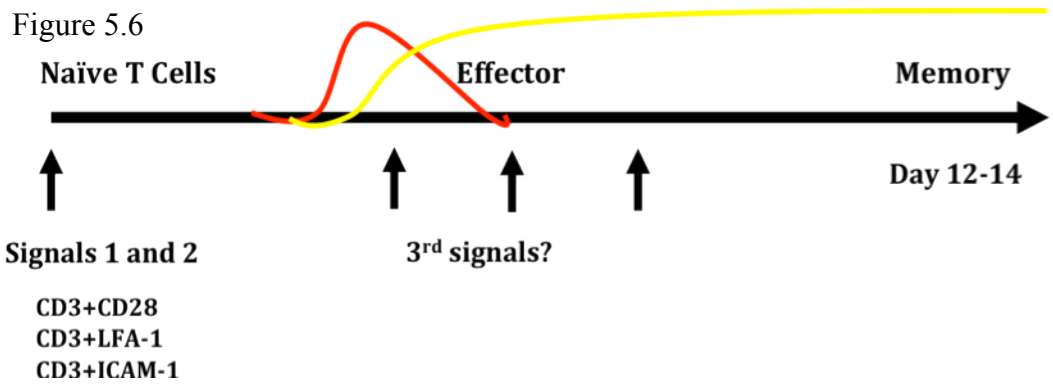

Figure 5.7

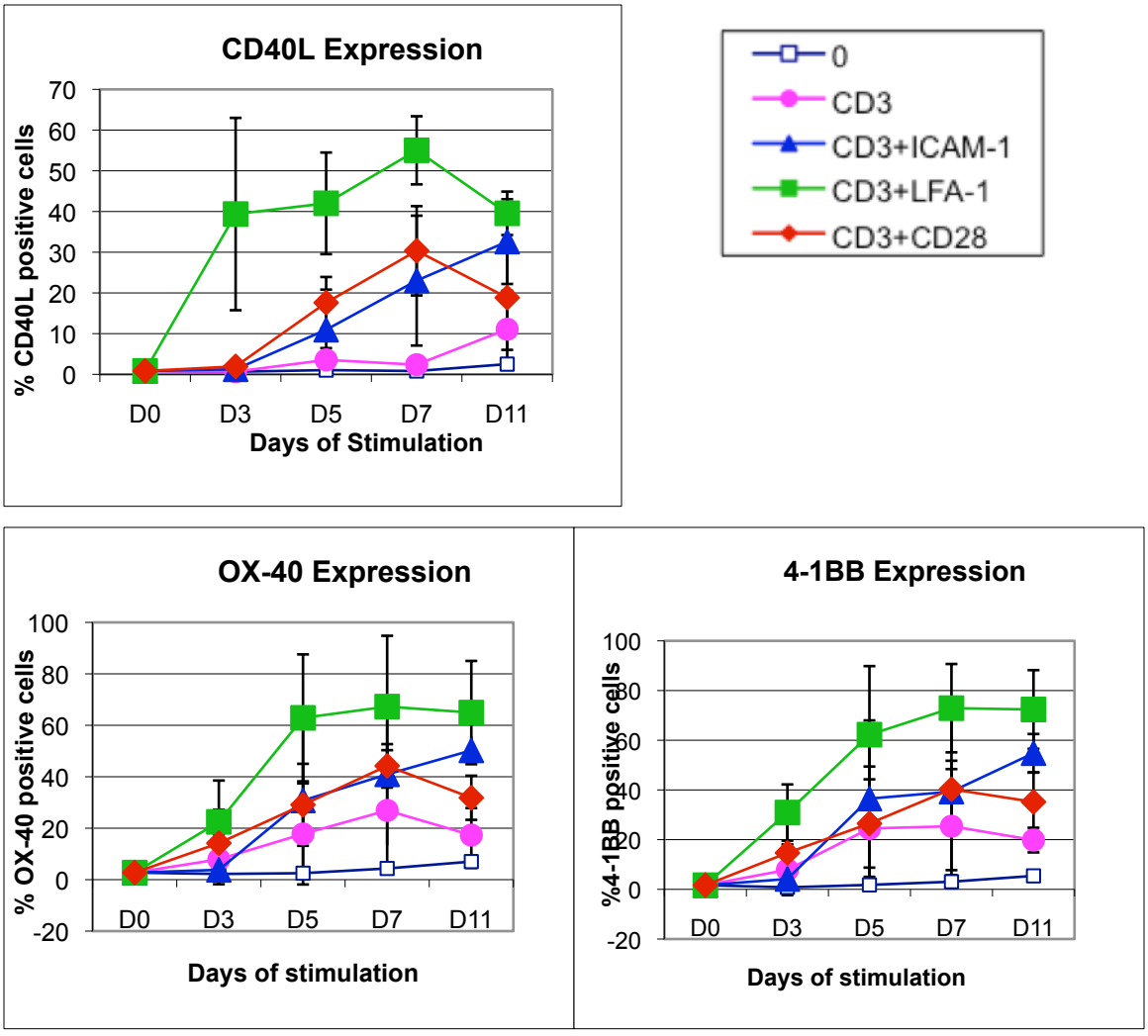

Figure 5.6, 5.7. Costimulation of naïve CD4+ T cells from younger individuals through ICAM-1 induces different kinetics of expression of tertiary stimulatory molecules compared with costimulation through CD28 or LFA-1. **5.6)** Schematic representation of possible tertiary costimulatory molecule timeline expression as a naïve cell activates and differentiates. Arrows indicate points where tertiary signals that are turned on can receive a signal to propogate differentiation to a memory phenotype. **5.7)** Cell surface expression of tertiary costimulatory molecules, CD40L, OX-40 and 4-1BB, at day 0 and 3, 5, 7, and 11 days after stimulation through either CD3, CD3+ICAM-1, CD3+LFA-1, CD3+CD28 or cells left unstimulated. Error representated at SD. n=3.

studied time interval and continued increasing through 11 days after stmulation to a higher expression than costimulation through CD28 **(Fig. 5.7)**. As expected, stimulation through the TCR (CD3) alone or cells that were left unstimulated exhibited low or no increase in CD40L, OX-40 or 4-1BB positive cells, respectively **(Fig. 5.7)**.

Kinetic expression of CD40L, OX-40 and 4-1BB on stimulated CD4+ cells differed vastly in pattern of expression between older and younger individuals as well as among different older subjects. CD4+ T cells from individual "A" showed and immediate and high expression of all tertiary costimulatory molecules by day 3 of stimulation through CD3+LFA-1 (green squares) that declined slightly to day 10 whereas costimulation through CD28 or ICAM-1 gave lower expression of tertiary costimulatory molecules that peaked at day 5 for CD28 (red diamonds) and was delayed but still increasing to day 10 with ICAM-1 (blue triangles) **(Fig. 5.8)**. Individuals "B" and "C" expressed low levels of CD40L with costimulation through CD28 or ICAM-1 that continued to rise through day 10 with CD28 stimulated cells only **(Fig. 5.8)**. OX-40 and 4-1BB positive cells were greater for individual "B" when costimulated through ICAM-1 but peaked at days 5 and 7, respectively, where cells costimulated through CD28 began to plateau in expression from days 3-10 **(Fig. 5.8)**. OX-40 and 4-1BB expression were also greater with cells costimulated through ICAM-1 for individual "C", however OX-40 expression peaked at day 5 for both CD28 and ICAM-1 cells whereas 4-1BB continued to rise in expression for both stimulations **(Fig. 5.8)**. Costimulation through CD28, LFA-1 or ICAM-1 induced a quick and high expression of all three tertiary costimulatory molecules for individual "D" that peaked at day 7 for CD28 stimulated cells and remained constant or increased for cells stimulated through LFA-1 or ICAM-1 **(Fig. 5.8)**.

Figure 5.8

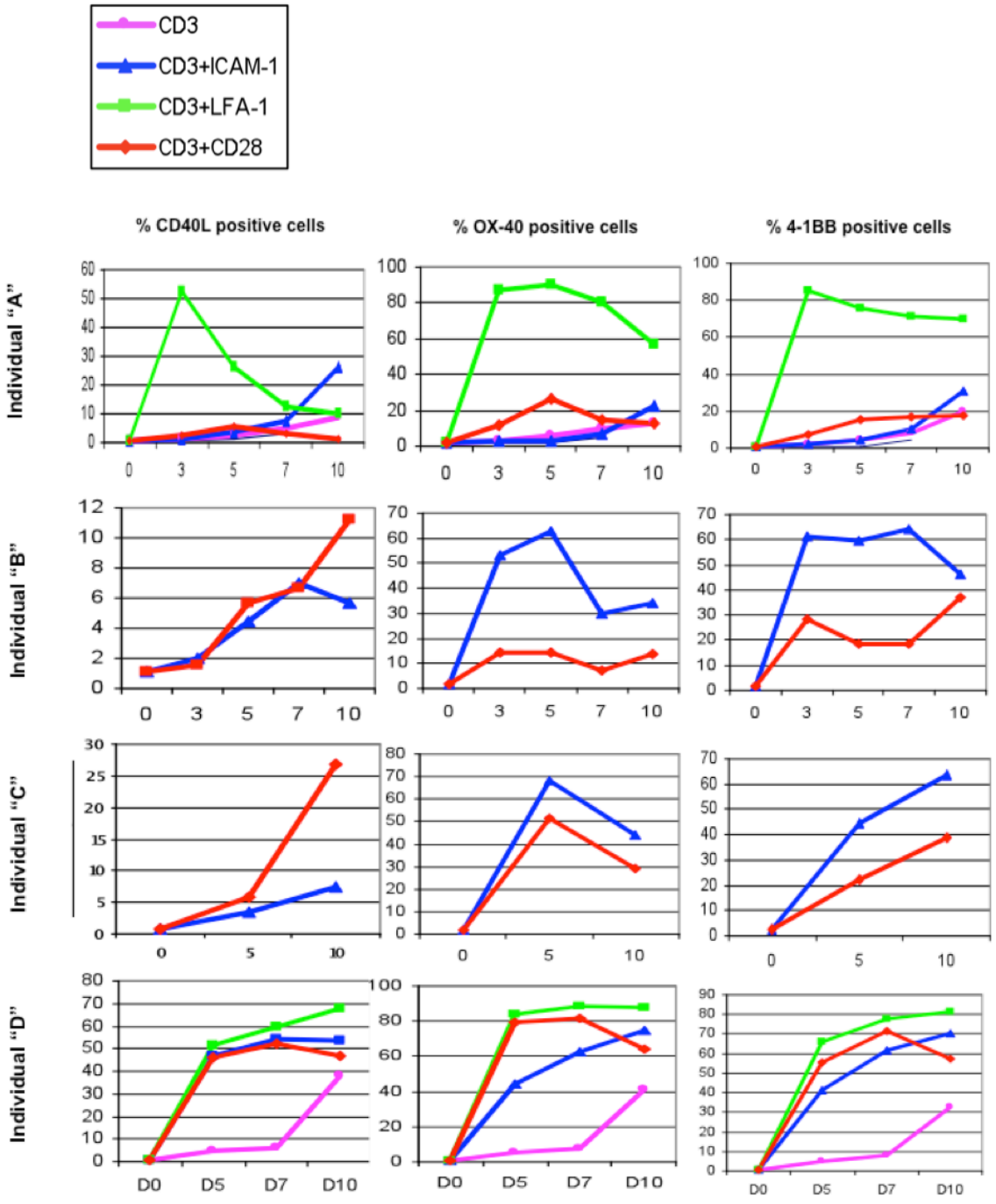
CD3
CD3+ICAM-1
CD3+LFA-1
CD3+CD28
% CD40L positive cells
% OX-40 positive cells
% 4-1BB positive cells
Individual "A"
Individual "B"
Individual "C"
Individual "D"
D0
D5
D7
D10

Figure 5.8. Costimulation of naïve CD4+ T cells from 4 older individuals through ICAM-1 generated different expression patterns for tertiary stimulatory molecules. Cell surface expression of tertiary costimulatory molecules, CD40L, OX-40 and 4-1BB, at day 0 and 3, 5, 7, and/or 10 days after stimulation through either CD3, CD3+ICAM-1, CD3+LFA-1 or CD3+CD28. Number of stimuli and frequency of days that tertiary cosimulatory molecule expression was measured was dependent on the amount of naïve cells able to be isolated.

Stimulation through the TCR (CD3) alone unexpectedly led to a slight increase in CD40L, OX-40 and 4-1BB in individual "D". Taken together, these data suggest that activation and expression of tertiary costimulatory molecules is inconsistent in stimulated T cells from older individuals as compared with our observation of relatively consistent responses in cells from younger individuals **(Fig. 5.7).**

ICAM-1 costimulation of naïve CD4+ T cells from older individuals does not confer a regulatory T cell phenotype in contrast to T cells from younger subjects.

Previous work from our lab and published by Kelli Williams, et al. demonstrates that costimulation in the absence of exogenous cytokines of CD4+ naïve T cells through ICAM-1 but not CD28 or LFA-1 can lead to a regulatory T cell phenotype capable of suppressive function *in vitro* (15). To further compare differentiation of naïve CD4+ T cells between older and younger individuals we looked for the ability of naïve CD4+ T cells from older individuals to develop into a regulatory T cell phenotype. Representative dot plots provided by Kelli Williams of Treg markers, Foxp3 and CD25, indicate that costimulation of naïve CD4+ T cells from older individuals through either CD28 or ICAM-1 did not induce differentiation to a regulatory phenotype greater than baseline (CD3 alone) **(Fig. 5.9)**. Compiled averages of percent $Foxp3^{hi}$CD25+ cells are shown in **Figure 5.10**. Costimulation of naïve CD4+ T cells through CD28 does not induce a sizable Treg population, similar to that in young individuals **(Fig. 5.10)**. However, unlike differentiation of CD4+ T cells from younger individuals, costimulation of naïve CD4+ T cells from older individuals through ICAM-1 no longer seems able to induce a significant

Figure 5.9

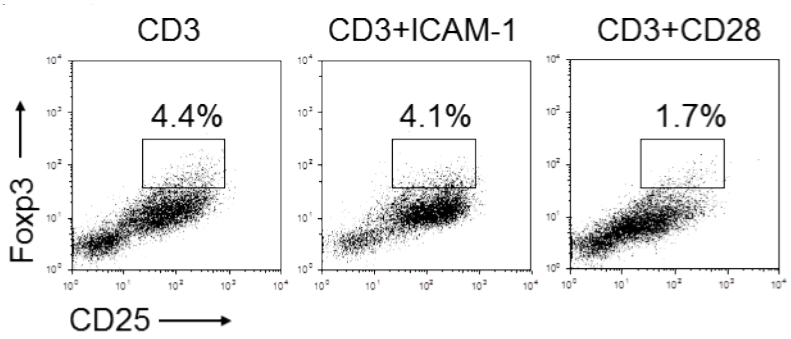

Figure 5.10

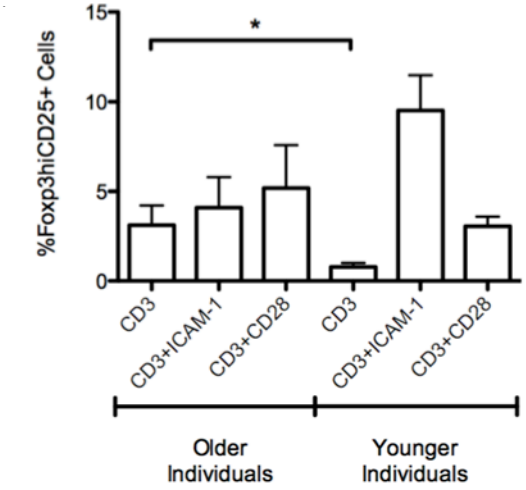

Treg population under these circumstances **(Fig. 5.10)**. This suggests that certain activation and differentiation functions differ or decline with age.

Costimulation of naïve CD4+ T cells from older individuals through CD3+ICAM-1 generated a memory phenotype in contrast to costimulation through CD3+CD28.

The differences in activation/differentiation of CD4+ naïve T cells from older individuals compared to younger may give some insight to the inability to effectively fight disease and respond to vaccine as we age. Since naïve CD4+ T cells from older individuals do not differentiate to a regulatory phenotype when costimulated through ICAM-1 in contrast to the situation with younger individuals, we wanted to investigate the possibility that those same naïve T cells would be able to differentiate into an alternate memory phenotype. In **Figure 5.11** cells that were stimulated through CD3+LFA-1 divided but did not differentiate efficiently and did not express any memory phenotype cells (lower right quadrant). The lack of memory phenotype in cells costimulated through LFA-1 mimics the outcome of costimulation through LFA-1 in cells from young individuals. However, in older individuals we observed diminished differentiation to effector as well.

Costimulation of CD4+ naïve T cells from older individuals through CD28 induced differentiation that does not follow the dogma established in young subjects and produced effector (upper right quadrant) but not memory cells by day 14 **(Fig. 5.11)**. In contrast, CD3+ICAM-1-stimulated naïve cells from older individuals proliferated and differentiated into both effector and memory phenotypes similar to the response observed in ICAM-1 costimulated naïve cells from younger individuals **(Fig. 5.11)**. When these

Figure 5.11

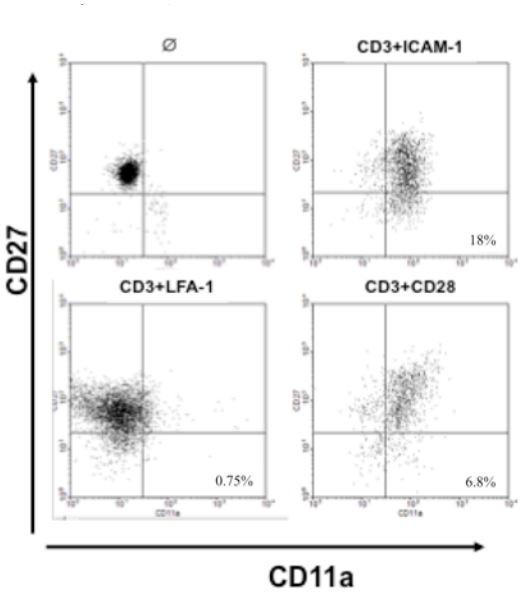

Figure 5.12

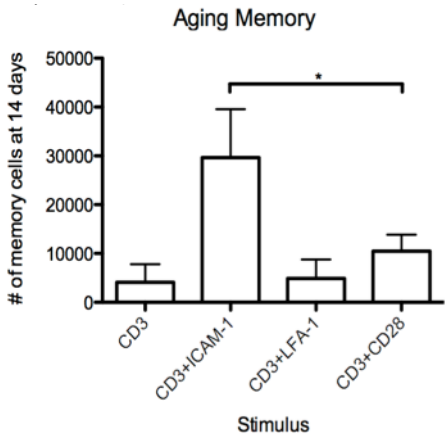

Figure 5.13

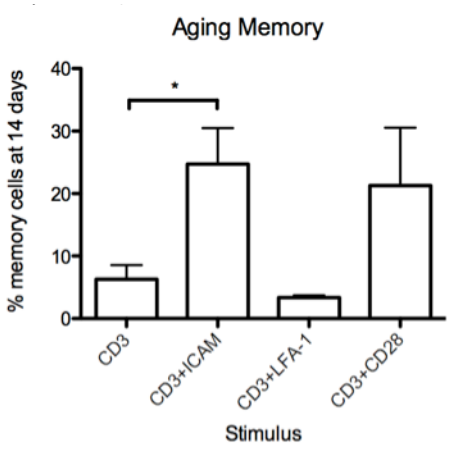

Figure 511-5.13. Costimulation of naïve CD4+ T cells from older individuals through CD3+ICAM-1 generated a memory phenotype in contrast to costimulation through CD3+CD28. **5.11)** Representative dot plot of memory cell phenotypes after 14 days. Naïve T cells from older individuals were left unstimulated or stimulated though CD3+LFA-1, CD3+ICAM-1 or CD3+CD28. Cells are gated on CD45RO+ and memory phenotype is CD11a+, CD27(-). **5.12)** Number of memory cells quantified after 14 days of stimulation. **5.13)** Percent of total cells that are memory after 14 days of stimulation. Data represented as mean ± SEM, *$p<0.05$ using two tail t-Test. n=4, CD3; n=6 CD3+ICAM-1 and CD3+CD28; n=3, CD3+LFA-1.

data are quantified, the total number of memory T cells produced from costimulation through ICAM-1 is significantly greater than those produced by CD28 **(Fig. 5.12)**. When looking at the percent of memory cells at day 14 of culture, minimal difference was observed between the cells costimulated through CD28 and ICAM-1 **(Fig 5.13)** which does not agree with the number of memory cells produced **(Fig. 5.12)**. The discrepancy is due to a lower number of total cells alive at day 14, therefore skewing the memory percentages. This will be discussed further in the next section. Cumulatively, these data suggest that although naïve CD4+ T cells from older individuals do not stimulate or differentiate in a similar manner to cells stimulated from younger individuals, only costimulation through ICAM-1 could produce a T cell phenotype capable of exhibiting memory characteristics.

Costimulation of Naïve CD4+ T cells from older individuals through ICAM-1 increases viable cell counts compared to other stimuli.

For young individuals, naïve CD4+ T cells costimulated through CD28 or ICAM-1 but not LFA-1 are protected from apoptosis (10, 14, 13). The discrepancy between percent and numbers of memory cells from **Figures 5.12 and 5.13** led us to investigate cell numbers being produced, proliferation and apoptosis of CD4+ naïve T cells from older individuals following costimulation through ICAM-1, LFA-1 and CD28. Cell counts were taken at 0, 5, 7, 10 and 14 days after stimulation and, as expected with our control, stimulation through the TCR (CD3) alone led to a consistent decline in cell number **(Fig. 5.14)**. Costimulation of naïve cells through LFA-1 maintained cell numbers, and costimulation through ICAM-1 gave the only increase in cells through 14

Figure 5.14

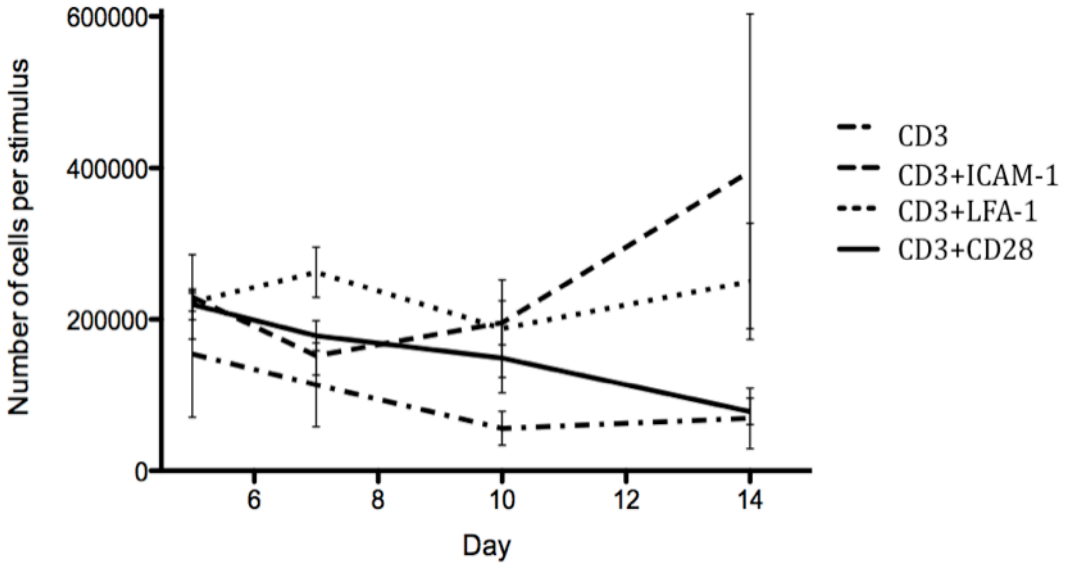
600000
400000
200000
0
Number of cells per stimulus
6
8
10
12
14
Day
CD3
CD3+ICAM-1
CD3+LFA-1
CD3+CD28

Figure 5.14. Costimulation of Naïve CD4+ T cells from older individuals through ICAM-1 increases viable cell counts compared to other stimuli. Naïve CD4+ T cells from older individuals were stimulated through CD3, CD3+ICAM-1, CD3+LFA-1 or CD3+CD28 and cell numbers were enumerated at days 0, 5, 7, 10 and 14. Cell counts were done using flow cytometry. Live cells were gated on and cell numbers were determined based on a known number of polystyrene counting beads in the sample at the time of analysis. n=5 for days 7 and 14; n=3 for days 5 and 10.

days of stimulation **(Fig. 5.14)**. Interestingly, costimulation of CD4+ naïve T cells through CD28 led to a consistent decline in cell numbers, similar to stimulation through the TCR alone **(Fig. 5.14)**. This finding contradicts what is known for cells stimulated through CD28 from young individuals and explains the low total memory cell number compared to the percent in **Figure 5.12**. Since memory cells are long lived and effector cell numbers contract following an immune response, the few memory cells produced by the CD28 costimulation skewed their percent of the total population as effector and naïve cells died.

Preliminary data: Costimulation of Naïve CD4+ T cells from older individuals through ICAM-1 leads to increased cells at 2 and 3 divisions and protection from apoptosis up to 4 divisions.

To decipher whether the lower cell counts from **Figure 5.14** were due to lack of proliferation or cell death, CFSE dilution and AnnexinV expression were characterized. Proliferating cells that have been stained with CFSE will dilute the amount of CFSE within the cell by 50% for each cell division. This allows for individual divisions to be quantified and when co-stained with AnnexinV the percent of apoptotic cells in each division can also be determined. As a control, stimulation through the TCR (CD3) alone did not induce much cell division with the majority of the cells remaining undivided **(Fig. 5.15)**; as well, the few cells that did divide were highly apoptotic, especially in divisions 1-3 **(Fig. 5.16)**. Naïve CD4+ T cells from older individuals that were stimulated through CD3+LFA-1 (hatched bars) underwent a high level of proliferation, peaking at 2 and 3 divisions **(Fig. 5.15)**, yet those cells were also highly apoptotic in undivided cells as well

Figure 5.15

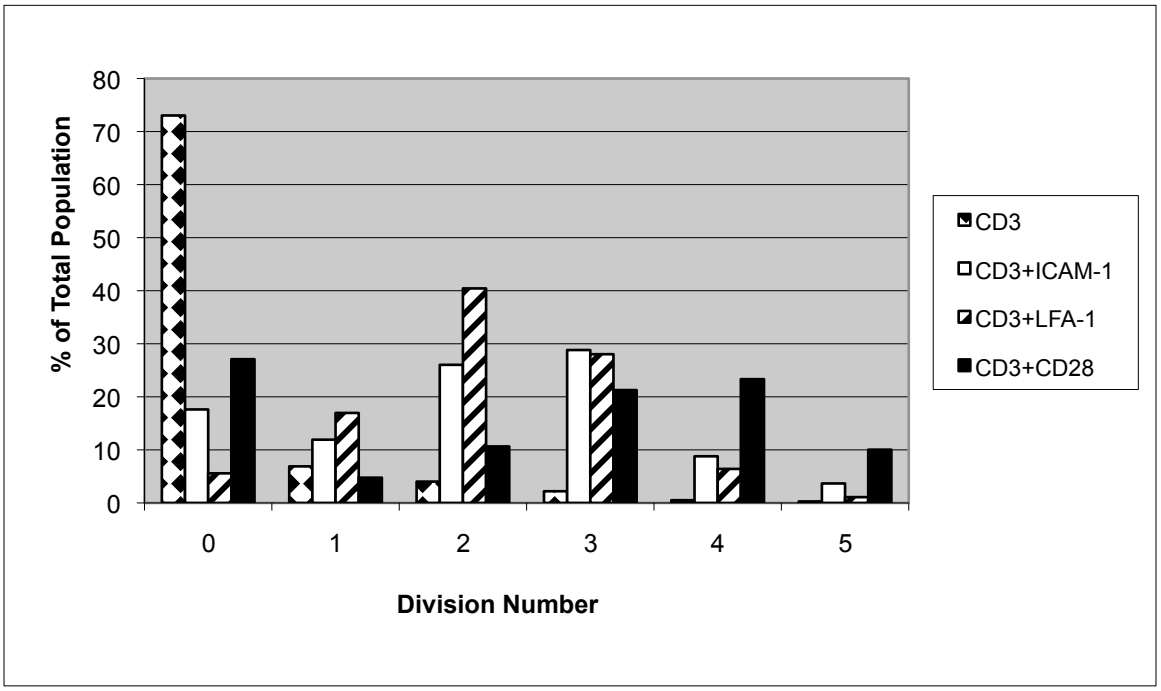

Figure 5.16

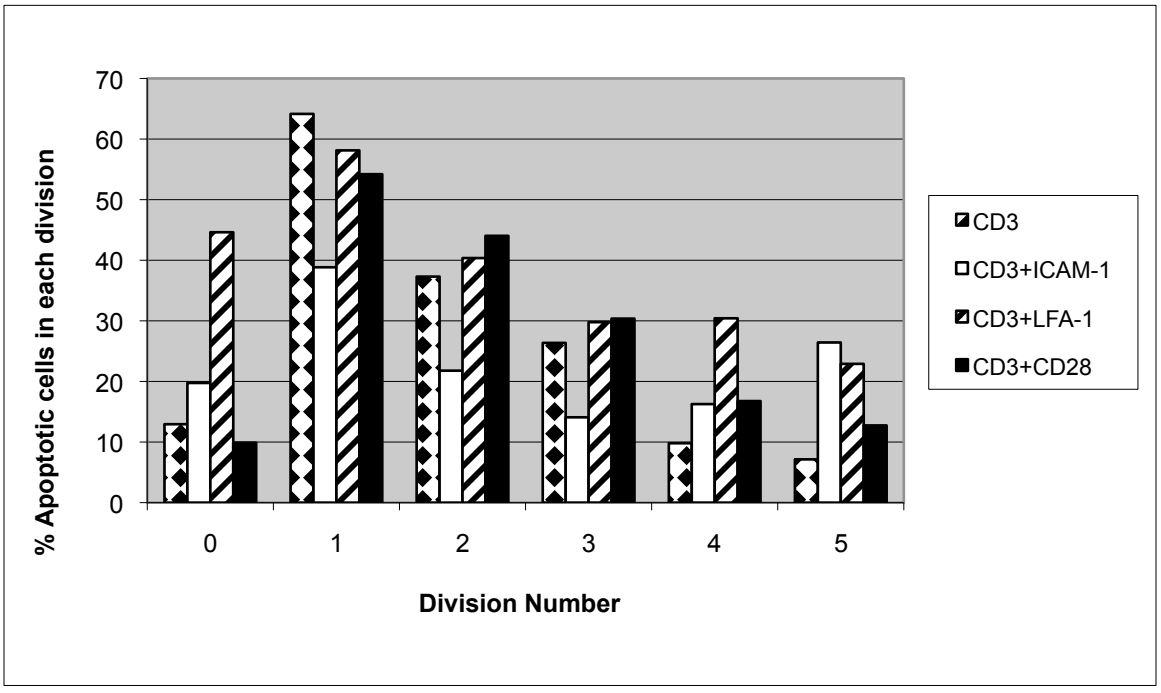

Figure 5.15, 5.16. Preliminary Data: Costimulation of Naïve CD4+ T cells from older individuals through ICAM-1 leads to increased cell numbers at 2 and 3 divisions and protection from apoptosis up to 4 divisions. Naïve CD4+ T cells from older individuals were stained with CFSE and stimulated through CD3, CD3+ICAM-1, CD3+LFA-1 or CD3+CD28. At day 7, cells were stained with AnnexinV and analyzed using flow cytometry. **5.15)** CFSE dilution was analyzed and the percent of cells in cach division was calculated based on the total population. **5.16)** AnnexinV positive cells were calculated against cell division to determine the percent of apoptotic cells in each cell division. n=1.

as all divisions examined **(Fig. 5.16)** which remains consistent with the maintained and level cell counts from **Figure 5.14**. Cells that were costimulated through CD28 (filled bars) exhibited a moderate level of cellular division that peaked at 3 and 4 divisions **(Fig. 5.15)** but displayed a high level of apoptosis, particularly for divisions 1-3 **(Fig. 5.16)**. This observation explains that the low cell count from **Figures 5.12 and 5.14** was not due to lack of proliferation but rather the inability to protect the activated cells from apoptosis. Costimulation of naïve CD4 T cells from older individuals through ICAM-1 (open bars) led to a substantial level of proliferation **(Fig. 5.15)**, peaking at 2 and 3 divisions, that were also protected from apoptosis in a manner greater than cells costimulated through either LFA-1 or CD28 for the vast majority of cell divisions (1-4) **(Fig. 5.16)**. Taken together, these preliminary data suggest that costimulation of naïve CD4+ T cells from older individuals through ICAM-1 leads to proliferation and protection from cell death that contributes to a collective increase in cell number over time and that ICAM-1 might function better as a costimulator during immunosenescence than do either CD28 or LFA-1.

Discussion

Age related decline of the immune system can be attributed to numerous factors including but not limited to changes in T cell subsets, impaired function of those subsets, decreased thymic output and a T cell compartment that harbors quiescent or semi-quiescent cells (34-36). In the current study, we aimed (i) to define and compare the total T cell and naïve T cell subsets in older individuals and (ii) characterize their activation and differentiation from naïve T cells using a system of stimulation that we have defined extensively in young subsets (15,16). Our overall goal was to investigate and design new strategies to promote an effective and functional T cell compartment in the elderly.

The primary decrease in expression of the naïve marker CD45RA within the total T cell population occurs before the age of 30 (especially in CD4+ cells); and between the ages of 30 to 65, CD45RA expression only decreases slightly (37). Our observations support the presence of a sizable naïve population in older people as seen in **figure 1**. The majority of naïve phenotype cells in the elderly, however, are not thymus derived. The naïve cell numbers are maintained by antigen-independent proliferation without differentiation leaving the majority of the naïve population (over 95%) being proliferation derived (1). Naïve cells from healthy young individuals circulate between the periphery and lymph nodes using cell surface molecules CCR7 and CD62L (33). Our data show a decrease in CCR7 expression on CD4+ naïve T cells. This decrease has also been observed in aging mice and leads to an age related decrease in lymphocyte migration to secondary lymphoid organs (38-40). Our data also show that as is the case in young subjects, naïve T cells from older individuals express a low level of ICAM-1 on

their surface and as previously documented CD28 is slightly downregulated. However, the expression of CD28 was lower on the total T cells that we examined compared to the CD4+ naïve T cells. This observation is consistent with the fact that loss of CD28 is more prominent in CD8+ T cells than CD4+ cells (41). Loss of CD28 on CD4+ T cells has been correlated with a decreased autocrine proliferative capacity as well as altered cytokine secretion (42,43)

Due to the dramatic decrease of recent thymic emigrants in older individuals it is important to characterize the ability of these cells to activate and differentiate. Measurement of tertiary costimulatory molecule expression facilitates in the assessment of how cells are progressing toward differentiation with respect to function. CD40L increases T cell proliferation and cytokine secretion (44), OX-40 serves to prolong T cell division increase cell survival and increase memory cell development (45,46) and 4-1BB can induce IL-2 production and sustain cell activation (47,48). The irregularly regulated patterns of expression of CD40L, OX-40 and 4-1BB that we observed in older individuals suggest that not only do naïve T cells from older individuals activate differently than in young but differentiation may be impaired or skewed as a result.

In our stimulation system we observe a dramatic difference in differentiation of naïve cells from younger to older individuals. Unlike young subjects, stimulation of naïve T cells from older individuals through CD3+ICAM-1 did not induce differentiation to a regulatory phenotype. This is of interest because it has been reported that regulatory T cells accumulate in the elderly and impair effective immune responses to infection and disease (49).

Naïve CD4+ T cells from older individuals also differentiate to a memory phenotype unlike of the case with younger individuals because only costimulation through ICAM-1 will generate memory cells in high numbers. This suggests that even though CD28 is present on most of the CD4+ naïve T cells from older individuals, costimulation through CD28 is not capable of initiating efficient differentiation to either a regulatory or memory phenotype.

In addition to impairment of differentiation, costimuation of CD4+ naïve T cells from older individuals through LFA-1 or CD28 was not able to maintain a healthy, viable cell population. Costimulation through ICAM-1 was able to increase total cell numbers, drive cells to proliferation and largely protect them from apoptosis. In contrast, costimulation through LFA-1 or CD28 could induce proliferation but not protect the cells from apoptosis, thus not maintaining cell numbers as effectively as ICAM-1. Without effective expansion of the differentiated T cell population, naïve T cells from older individuals cannot carryout specific immune functions.

In summary, we have shown that CD4+ Naïve T cells from older individuals have a slightly different phenotype from naïve cells in younger individuals. Naïve cells from older individuals activate and differentiate into specific T cell subpopulations differently than similar cells in young individuals and the activation process is not regulated in the same manner as it is in young. Costimulation of CD4+ naïve T cells from older individuals through LFA-1 induces activation that does not lead to differentiation or protection from apoptosis. Similarly, costimulation of the same naïve T cells through CD28 does not always give efficient activation as determined by expression of tertiary costimulatory molecules and does not lead to cell differentiation or survival. However,

CD4+ naïve T cells from older individuals can proliferate, differentiate to a memory phenotype and are more protected from apoptosis when costimulated through ICAM-1. Taken together, these data suggest that costimulation through ICAM-1 can provide signals to aging naïve T cells that might be more functional or effective than signals through other signaling molecules. Due to the senescence of the immune system and increased incidence of disease as we age, it is imperative to investigate alternative strategies for reinstituting T cell immune responses to new antigens. ICAM-1 as a T cell costimulatory molecule may provide new methods and understanding of our ability to maintain an effective immune system as we get older, and may suggest new targets for interuption in immune suppression.

References

1. Murray JM, Kaufmann GR, Hodgkin PD, Lewin SR, Kelleher AD, Davenport MP, Zaunders JJ. Naive T cells are maintained by thymic output in early ages but by proliferation without phenotypic change after age twenty. Immunology and Cell Biology. 2003; 81, 487–495
2. Mueller DL, Jenkins MK, Schwartz RH. Clonal expansion versus functional clonal inactivation: A costimulatory signalling pathway determines the outcome of T cell antigen receptor occupancy. Annu Rev Immunol. 1989; 7:445–480.
3. Dutton RW, Bradley LM, Swain SL T cell memory. Annu Rev Immunol. 1998; 16:201–223.
4. Ahmed R, Gray D. Immunological memory and protective immunity: Understanding their relation. Science. 1996; 272:54–60
5. Harding FA, McArthur JG, Gross JA, Raulet DH, Allison JP. CD28-mediated signalling co-stimulates murine T cells and prevents induction of anergy in T-cell clones. Nature. 1992; 356:607–9.
6. Powell JD, Ragheb JA, Kitagawa-Sakakida S, Schwartz RH. Molecular regulation of interleukin-2 expression by CD28 co- stimulation and anergy. Immunol Rev. 1998; 165:287–300
7. Kedl RM, Mescher MF. Qualitative differences between naive and memory T cells make a major contribution to the more rapid and efficient memory CD8+ T cell response. J Immunol. 1998; 161:674–683.

8. Veiga-Fernandes H, Walter U, Bourgeois C, McLean A, Rocha B. Response of naïve and memory CD8+ T cells to antigen stimulation in vivo. Nat Immunol. 2000; 1:47–53.
9. Croft M, Bradley LM, Swain SL. Naive versus memory CD4 T cell response to antigen. Memory cells are less dependent on accessory cell costimulation and can respond to many antigen-presenting cell types including resting B cells. J Immunol. 1994;152:2675–2685.
10. Fraser JD, Irving BA, Crabtree GR, Weiss A. Regulation of interleukin-2 gene enhancer activity by the T cell accessory molecule CD28. Science. 1991; 251:313–16
11. Boise LH, Minn AJ, Noel PJ, June CH, Accavitti MA, Lindsten T, Thompson CB. CD28 costimulation can promote T cell survival by enhancing the expression of Bcl-x. Immunity. 1995; 3:87–98.
12. Lenschow DJ, Walunas TL, Bluestone JA. CD28/B7 system of T cell costimulation. Annu Rev Immunol. 1996; 14:233–58.
13. Shibuya K, Shirakawa J, Kameyama T, et al. CD226 (DNAM-1) is involved in lymphocyte function-associated antigen 1 costimulatory signal for naive T cell differentiation and proliferation. J Exp Med. 2003; 198:1829–39.
14. Damle N, Klussman K, Leytze G, Aruffo A, Linsley P, Ledbetter J. Costimulation with integrin ligands intercellular adhesion molecule-1 or vascular cell adhesion molecule-1 augments activation-induced death of antigen-specific CD4+ T lymphocytes. J Immunol. 1993; 151:2368–79.

15. Kohlmeier JE, Chan MA, Benedict SH. Costimulation of naïve human CD4+ T cells through intercellular adhesion molecule-1 promotes differentiation to a memory phenotype that is not strictly the result of multiple rounds of cell division. Immunology. 2006; 118(4): 549-58.
16. Williams KM, Dotson AL, Otto AR, Kohlmeier JE, Benedict SH. Choice of resident costimulatory molecule can influence cell fate in human naïve CD4+ T cell differentiation. Cell Immunol. 2011; 271(2):418-27.
17. Effros RB, N Boucher, V Porter, XM Zhu, C Spaulding, RL Walford, M Kronenberg, D Cohen, and F Schachter. Decline in CD28+ T cells in centenarians and in log-term T cell cultures: a possible cause for both in vivo and in vitro immunosenescence. Exp. Gerontol. 1994; 29:601-609.
18. Weyand CM, JC Brandes, D Schmidt, JW Fullbright, JJ Gorozny. Functional properties of CD4+ CD28- T cells in the ageing immune system. Mech. Ageing Dev. 1998; 102:131-147. 61.
19. Bukczynski J, T Wen, and TH Watts. Costimulation of human CD28- T cells by 4-1BB ligand. Eur. J. Immunol. 2003; 33:446-454.
20. Nan-ping Weng1, Arne N. Akbar2 and Jorg Goronzy3. CD28- T cells: their role in the age- associated decline of immune function. Trends in Immunology. 2009; 30(7): 306-312.
21. Dobber, R., Tielemans, M., Deweerd, H., Nagelkerken, L. Mel14(+) CD4(+) T cells from aged mice display functional and phenotypic characteristics of memory cells. Int. Immunol. 1994; 6: 1227–1234.
22. Chiu BC, Stolberg VR, Zhang H, Chensue SW. Increased Foxp3(+) Treg cell

activity reduces dendritic cell co-stimulatory molecule expression in aged mice. Mech Ageing Dev 2007; 128:618–27.

23. Maue AC, Yager EJ, Swain SL, Woodland DL, Blackman MA, Haynes L. T-cell immunosenescence: lessons learned from mouse models of aging. Trends Immunol. 2009;30(7):301-5
24. Tamir A, Eisenbraun MD, Garcia GG, Miller RA. Age-dependent alterations in the assembly of signal transduction complexes at the site of T cell/APC interaction. J. Immunol. 2000;165, 1243–1251
25. Garcia, G.G. and Miller, R.A. Single-cell analyses reveal two defects in peptide-specific activation of naive T cells from aged mice. J. Immunol. 2001; 166, 3151–3157
26. Haynes L, Lefebvre JS. Age-related Deficiencies in Antigen-Specific CD4 T cell Responses: Lessons from Mouse Models. Aging Dis. 2011;2(5):374-81
27. Le Saux S, Weyand CM, Goronzy JJ. Mechanisms of immunosenescence: lessons from models of accelerated immune aging. Ann N Y Acad Sci. 2012; 1247:69-82
28. Haynes, L. and Eaton, S.M. The effect of age on the cognate function of CD4+ T cells. Immunol. Rev. 2005; 205, 220–228
29. Linton PJ, Li SP, Zhang Y, Bautista B, Huynh Q, Trinh T. Intrinsic versus environmental influences on T-cell responses in aging. Immunol. Rev. 2005; 205, 207–219
30. Haynes, L. and Swain, S.L. Why aging T cells fail: implications for vaccination. Immunity. 2006; 24, 663–666
31. Eaton SM, Burns EM, Kusser K, Randall TD, Haynes L. Age-related defects in

CD4 T cell cognate helper function lead to reductions in humoral responses. J Exp Med. 2004;200:1613–1622.

32. Roebuck K, Finnegan A. Regulation of intercellular adhesion molecule-1 (CD54) gene expression. J Leukoc Biol 1999; 66: 876–88.
33. Mackay,C. R. Homing of naive, memory and effector lymphocytes. Curr. Opin. Immunol. 1993; 5: 423–427.
34. Pawelec G, Hirokawa K, Fulo T. Altered T cell signalling in ageing. Mechanisms of Ageing and Development. 2001; 122: 1613–1637
35. Chakravarti B and GN Abraham. Aging and T cell mediated immunity. Mech. Ageing Dev. 1999; 108:183-206.
36. Pawlec G, Y Barnett, R Forsey, D Frasca, A Globerson, J McLeod, C Caruso, C Franceschi, T Fulop,S Gupta, E Mariani, E Mocchegiani, and R Solana. T cells and aging, January 2002 update. Front. Biosci. 2002; 7:1056-1183.
37. Cossarizza A, Ortolani C, Paganelli R, Barbieri D, Monti D, Sansoni P, Fagiolo U, Castellani G, Bersani F, Londei M, Franceschi C. CD45 isoforms expression on CD4+ and CD8+ T cells throughout life, from newborns to centenarians: implications for T cell memory. Mech Ageing Dev. 1996; 86(3):173-95.
38. Mo R, Chen J, Han Y, Bueno-Cannizares C, Misek DE, Lescure PA, Hanash S, Yung RL. T Cell Chemokine Receptor Expression in Aging. The Journal of Immunology. 2003; 170: 895–904.
39. Anokhin, I., A. A. Iarilin, and T. A. Norets. Age-related changes in splenic lymphocyte migration in mice. Ontogenez. 1980; 11:511.
40. Zatz, M. M., A. L. Golstein, and A. White. Lymphocyte populations of AKR-J

mice. I. Effect of aging on migration patterns, response to PHA and expression of antigen. J. Immunol. 1973; 111:1514.

41. Vallejo, A.N., Nestel, A.R., Schirmer, M., Weyand, C.M., Goronzy, J.J. Aging-related deficiency of CD28 expression in CD4+ T cells is associated with the loss of gene-specific nuclear factor binding activity. J. Biol. Chem. 1998; 273: 8119–8129.
42. Adibzadeh, M., Pohla, H., Rehbein, A., Pawelec, G. Long-term culture of monoclonal human T lymphocytes: models for immunosenescence. Mech. Ageing Dev. 1995; 83: 171–183.
43. Pawelec, G., Rehbein, A., Haehnel, K., Merl, A., Adibzadeh, M. Human T cell clones as a model for immunosenescence. Immunol. Rev. 1997; 160: 31–43.
44. Howland KC, Ausubel LJ, London CA, Abbas AK. The roles of CD28 and CD40 ligand in T cell activation and tolerance. J Immunol. 2000; 164(9): 4465-70.
45. Gramaglia I., Weinberg A.D., Lemon M. and Croft M. OX40 ligand: a potent costimulatory molecule for sustaining primary CD4+ T cell responses. J. Immunol. 1998; 161: 6510-6517.
46. Gramaglia I., Jember A., Pippig S.D., Weinberg A.D., Killeen N., and Croft M. The OX40 costimulatory receptor determines the development of CD4 memory by regulating primary clonal expansion. J. Immunol. 1999; 165: 3043-3050.
47. Vinay D.S. and Kwon B.S. Role of 4-1BB in immune responses. Semin. Immunol. 1998; 10: 481-489
48. DeBenedette M.A., Shahinian A., Mak T.W., and Watts T.H. Costimulation

of CD28- lymphocytes by 4-1BB ligand. J. Immunol. 1997; 158: 551-559.

49. Lages CS, Suffia I, Velilla PA, Huang B, Warshaw G, Hildeman DA, Belkaid Y, Chougnet C. Functional Regulatory T Cells Accumulate in Aged Hosts and Promote Chronic Infectious Disease Reactivation. The Journal of Immunology, 2008; 181: 1835 -1848

Chapter 6

Stimulation methods to generate murine memory T cells using ICAM-1

Introduction

As with CD4+ naïve T cells from humans, mouse cells also require two signals to become fully activated and differentiate. Costimulation of murine naïve T cells through CD28 has been widely studied, and many of the differentiation to memory studies have been done in mice. CD28 expression, function, sequence and gene expression are closely related between human and mice (1, 2). Studies of CD28 costimulation in mice demonstrate that the costimulatory molecule plays roles in differentation to a memory and regulatory T cell population (3, 4).

The role of ICAM-1 as a costimulatory molecule of CD4+ T cells or CD4+ naïve T cells has not yet been defined in mice. The ICAM-1 molecule is not completely conserved among species and although our lab has previously defined ICAM-1 as a costimulatory molecule on human CD4+ naïve T cells its function may differ in mice. The sequence of ICAM-1 is not highly conserved between human and mice, exhibiting only 50% protein and 65% DNA homology (5). Additionally, genomic blots of human DNA exhibited no hybridization when probed with murine ICAM-1 cDNA and ICAM-1:LFA-1 interactions do not occur between species indicating that the ICAM-1 gene is poorly conserved throughout evolution (5, 6). The cytoplasmic tail of human ICAM-1 contains a Src-homology (SH3) binding domain that is not conserved in mice, therefore the intracellular signaling may occur differently in mice than human and have different outcomes.

In this chapter, we aim to employ the same *in vitro* ICAM-1 costimulation system that we have characterized with CD4+ T cells and CD4+ naïve T cells in human with mouse cells to determine, despite ICAM-1 differences, if they can differentiate in a

similar manner with similar resulting phenotypes. Our goal is to describe the different methods that we use to costimulate mouse T cells through ICAM-1 and the outcomes that are observed. The ability to differentiate T cells from mice with ICAM-1 could provide useful tools in mouse disease models and development possible immunotherapies. The data presented here represent half of a manuscript written in conjunction with Kelli Williams of the Benedict lab.

Methods and materials

Mice

Male Balb/c mice (Jackson Laboratories, Bar Harbor,ME) were obtained at 6 weeks of age. Animal experiments were performed with approval from the University of Kansas Animal Care and Use Committee.

Antibodies and Reagents

Anti-CD44-PECy5, anti-CD127-PE and anti-CD69-FITC were all purchased from Becton Dickenson (San Jose, CA). Anti-CD62L-FITC and anti-CD69-PE were purchased from Caltag Laboratories (Burlingame, CA). Anti-CD3 clones 145-2C11, 500A2; anti-ICAM-1 clone 3E2; and anti-CD28 clone 37.51 were purchased from Becton Dickenson. Anti-CD3 clone C363.29B was purchased from Southern Biotech (Birmingham, Alabama). Anti-ICAM clones YN1 (YN1/1.7.4) and KAT-1 were purchased from eBioscience (San Diego, CA). Anti-ICAM-1 clone R6.5D6 (R6.5) was purchased from BioXCell (West Lebanon, NH). Mouse recombinant IL-2 and anti-ICAM-1 clone 166623 were purchased from R&D Systems (Minneapolis, MN). Anti-CD3 clone KT3 and anti-ICAM-1 clone 3E2B were purchased from Chemicon International (Temecula, CA). Anti-ICAM-1 clone BE29G1 was purchased from Biodesign International (Saco, ME).

Description of stimulating antibodies

145-2C11: Hamster anti-mouse monoclonal CD3 antibody that binds to the epsilon chain and shares properties with OKT3 (the CD3 antibody used in our human

stimulations *in vitro*) (7). KT3: Rat anti-mouse monoclonal CD3 antibody that binds to the epsilon chain (8). 500A2: Hamster anti-mouse monoclonal CD3 antibody that binds to the epsilon chain (9). C363.29B: Rat anti-mouse monoclonal CD3 antibody that binds to the epsilon chain. 3E2B: Hamster anti-mouse monoclonal ICAM-1 antibody (10). BE29G1: Rat anti-mouse monoclonal ICAM-1 antibody (11). 3E2: Hamster anti-mouse monoclonal ICAM-1 antibody (12). 166623: Rat anti-mouse monoclonal ICAM-1 antibody (13). YN1: Rat anti-mouse monoclonal ICAM-1 antibody (14). R6.5D6 (R6.5): mouse anti-human monoclonal ICAM-1 antibody was tested for possible cross reactivity with mouse ICAM-1 (15). KAT-1: Rat anti-mouse monoclonal ICAM-1 antibody (16)

Cell Purification

Spleens were harvested from Balb/c mice between 8 and 12 weeks of age, minced and repeatedly pressed with a 1cc syringe plunger through a sterile 70 μm nylon mesh cell strainer. Erythrocytes were cleared by a five-minute incubation of the cell suspension in ACK lysis buffer (0.15M NH_4Cl, 10mM $KHCO_3$, 0.1mM Na_2EDTA, pH 7.2) at 37^oC. CD4+ T splenocytes were isolated from spleens of Balb/c mice by negative selection using a CD4+ T cell enrichment kit (Stem Cell Technologies, Vancouver, BC, Canada). Naïve CD4+CD62L+ T cells were further purified by a positive selection using CD62L microbeads (Miltenyi Biotec, Auburn, CA). CD5+ T cells were separated from total splenocytes using CD5 positive selection microbeads also from Miltenyi Biotec.

Cell Stimulation

Antibodies in PBS were attached to 96 well tissue culture plates (Midwest Scientific, St. Louis, MO) by incubation at 37^{o}C for two hours and plates were washed three times with PBS before the addition of splenocytes. Stimulatory antibody clones and concentrations are indicated in figures and text. All cells were stimulated at a concentration of $2x10^{6}$ cells/ml.

Flow Cytometry

Flow cytometry was performed using the FACScan (Becton Dickenson, San Jose CA) and was calibrated using CaliBRITE beads (Becton Dickinson). This was supplemented by compensation using singly stained cells. Data were analyzed using Cell Quest (Becton Dickenson).

Results

Titration of stimulating antibodies on Balb/c CD4+ T splenocytes to induce optimal CD69 expression

The initial goal of finding the appropriate concentration of stimulating antibodies was to verify that we were inducing CD4+ T cell activation by the induction of CD69 expression. CD69 is a well studied early activation marker that is expressed within hours of stimulation (17). We titrated anti-CD3 alone, anti-CD3 with 2.5ug/mL of anti-CD28, and CD3 with anti-ICAM-1. Our goal was to find a concentration of anti-CD3 that would initiate expression of CD69 but would induce full CD69 expression when anti-CD3 was used in conjunction with anti-ICAM-1. That would verify that any differentiation was due to the effect of ICAM-1 costimulation and not just because of a TCR trigger. Four clones of anti-CD3 were tested at 4, 5 or 6 concentrations. Anti-CD3 clones 145-2C11 and 500A2 behaved similarly in terms of their ability to induce CD69 expression because 0.01 ug/mL-0.1 ug/mL gave increasing CD69 positivity and 0.5 ug/mL, 1 ug/mL (and 2 ug/mL with 500A2) gave similar and close to maximum CD69 expression **(Fig. 6.1)**. Anti-CD3 clones KT3 and C363.29B yielded a lower activation response compared to 145-2C11 and 500A2 and both generated under 70% CD69 positive cells with an anti-CD3 concentration of 2 ug/mL **(Fig. 6.1)**. In general, the MFI of the CD69 positive population mimicked the percent expression patterns. Stimulation with anti-CD3 clones 145-2C11 and 500A2 exhibited an increasing CD69 expression with increasing anti-CD3 concentrations, peaking at an MFI of 200 with 1 ug/mL each **(Fig. 6.2)**. As with percent expression, CD69 MFI was slightly lower with KT3 and

Figure 6.1

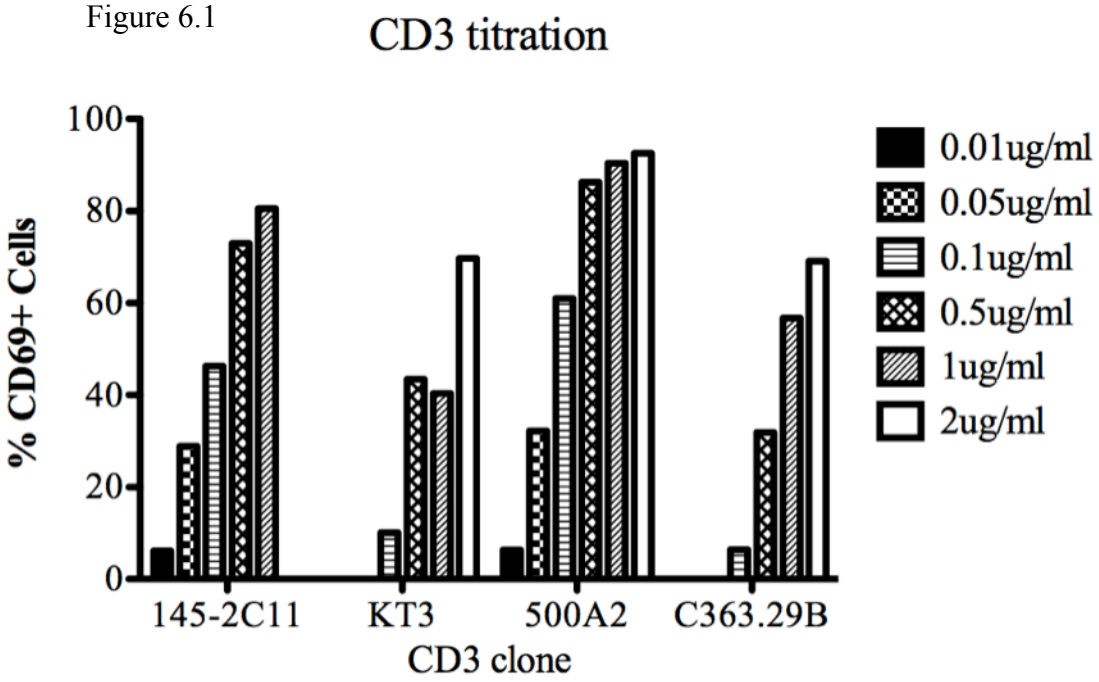

Figure 6.2

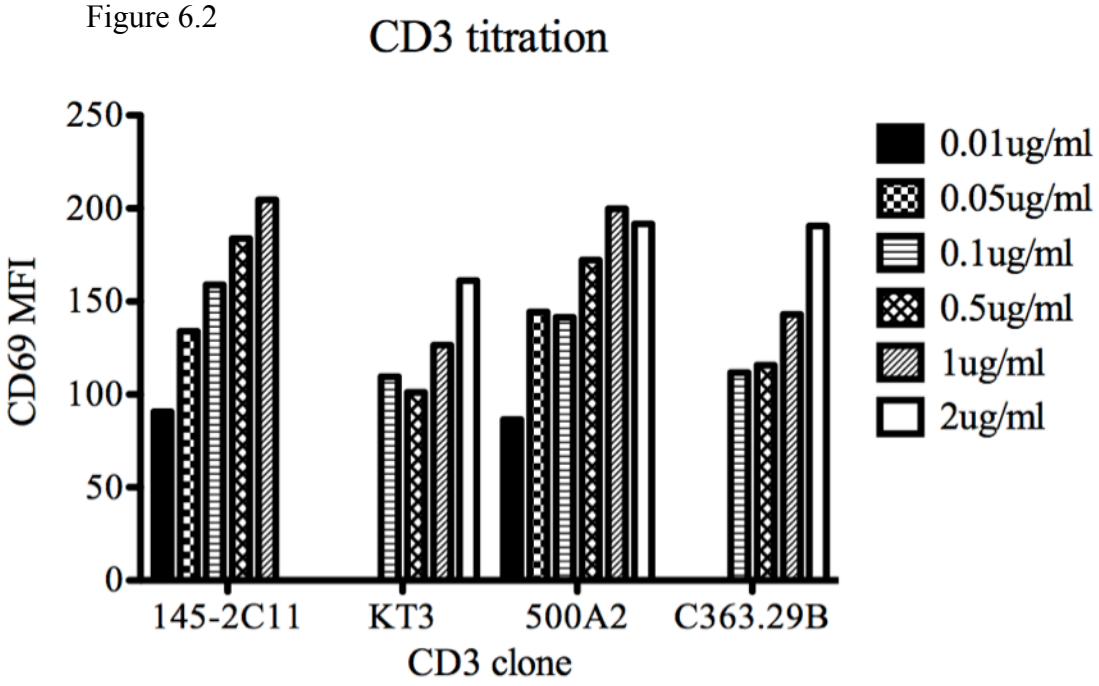

Figure 6.1-6.2. Titration of stimulating CD3 antibodies on Balb/c CD4+ T splenocytes to induce optimal CD69 expression. CD4+ T splenoctyes were stimulated for 12 hours using CD3 antibody clones and the concentrations indicated. Percent CD69 positive and **(6.1)** CD69 MFI **(6.2)** were determined using flow cytometry.

C363.29B at each anti-CD3 concentration than 145-2C11 and 500A2. Level of CD69 expression increased with concentration of anti-CD3 but had not reached an MFI of 200 with the highest concentration, 2 ug/mL, of clones KT3 or C363.29B **(Fig. 6.2)**.

When we added costimulation through CD28 (2.5 ug/mL) we observe that the percent CD69 expressing cells closely resembled that of stimulation with anti-CD3 alone **(Fig. 6.1, 6.3)**, however, the level of CD69 expression was increased with the addition of anti-CD28 **(Fig. 6.4)**. 0.5 ug/mL of anti-CD3 clones 145-2C11 or 500A2 yielded an MFI of over 200 when costimulation through CD28 was added but 1 ug/mL was needed to achieve a similar MFI when using anti-CD3 alone **(Fig. 6.2, 6.4)**. Similar effects were also observed with clones KT3 and C363.29B **(Fig. 6.2, 6.4)**. The concentration of anti-CD3 that was chosen for each clone depended on the lowest concentration to induce CD69 expression along with proliferation data that was performed by Kelli Williams (data not shown). Upcoming experiments used 0.01 ug/mL of 145-2C11, 0.5 ug/mL of KT3, 0.05 ug/mL of 500A2 and 1ug/mL of C363.29B.

Five different clones of anti-ICAM-1 mouse antibodies (3E2B, BE29G1, 3E2, 166623 and YN1) and one anti-ICAM-1 human antibody clone (R6.5) were tested for their ability to activate CD4+ T splenocytes from Balb/c by inducing expression of CD69. All anti-ICAM-1 clones were tested at 1 ug/mL and 10 ug/mL. Anti-CD3 clone 145-2C11 did not induce CD69 expression when used in combination with any of the anti-ICAM-1 clones **(Fig. 6.5)**. Anti-CD3 clone KT3 activated a higher percent of CD4+ T cells with anti-ICAM-1 clones 3E2B, 3E2, YN1 and R6.5 **(Fig. 6.5)** but the level of CD69 expression of the positive population as measured by MFI was highest with 3E2, 166623, YN1 and R6.5 **(Fig. 6.6)**. CD3 antibody clone 500A2 induced a similar level of

Figure 6.3

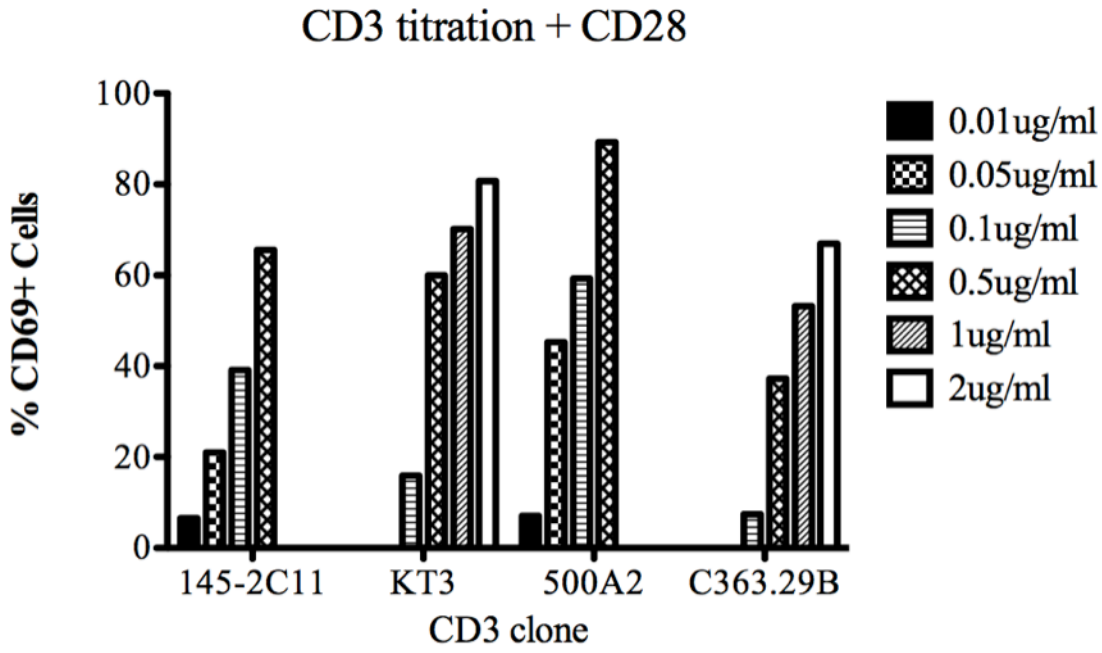

Figure 6.4

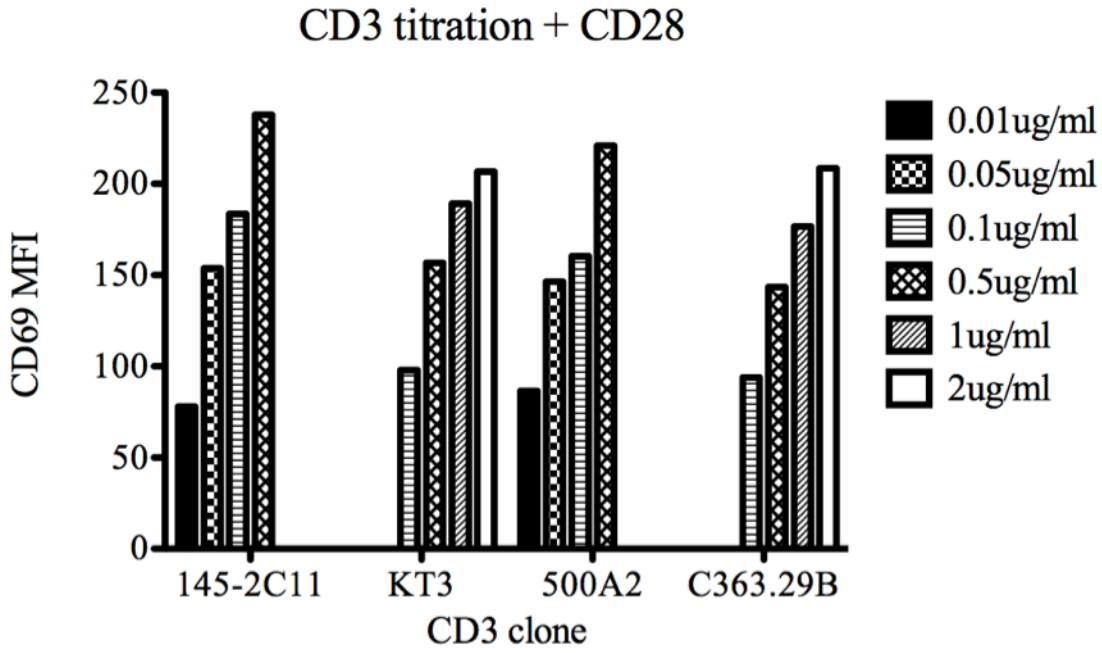

Figure 6.3-6.4. Titration of stimulating CD3 antibodies with costimulation through CD28 on Balb/c CD4+ T splenocytes to induce optimal CD69 expression. CD4+ T splenoctyes were stimulated for 12 hours using anti-CD3 clones and concentrations indicated in combination with costimulation through CD28 at 2.5 ug/mL. Percent CD69 positive and **(6.3)** CD69 MFI **(6.4)** was determined using flow cytometry.

CD69 positive cells (between 60% and 80%) as well as CD69 MFI (between 175 and 225) with all anti-ICAM-1 clones **(Fig 6.5, 6.6)**. Anti-CD3 clone C363.29B activated the most T cells with ICAM-1 antibody clones 3E2B and 3E2 by measure of CD69 positive cells **(Fig. 6.5)**, yet induced a higher CD69 MFI with 3E2 and 166623 **(Fig. 6.6)**. The two concentrations of anti-ICAM-1 antibodies induced very similar percent CD69 positive and MFI of the CD69 positive population with all of the CD3+ICAM-1 combinations with the exception of C363.29B+BE29G1 where the 10 ug/mL concentration of BE29G1 actually decreased CD69 positivity and level of expression **(Fig 6.5, 6.6)**. The ability of CD3 antibody clone 500A2 to activate all of the anti-ICAM-1 clones with similar results, in addition to the proliferation results done by Kelli Williams (not shown), led us to select it as the CD3 stimulating antibody for differentiation experiments. Since all of the ICAM-1 antibody clones activated CD4+ T cells to a similar degree with anti-CD3 500A2, we relied on the proliferation data (not shown) to select BE29G1 (10 ug/mL), 166623 (1 ug/mL) and R6.5 (10 ug/mL) for differentiation studies.

Costimulation of CD4+ and CD4+CD62L+ splenocytes through ICAM-1 induces a memory phenotype.

With optimal anti-CD3 and anti-ICAM-1 concentrations determined, we wanted to establish whether costimulation of mouse CD4+ T cells and naïve (CD4+CD62L+) T cells through ICAM-1 could not only activate cells but also differentiate them to a memory phenotype. Mouse central memory T cells are defined as $CD44^{hi}$, CD127+, CD62L+. CD4+ T cells purified from the spleens of Balb/c mice were stimulated

Figure 6.5

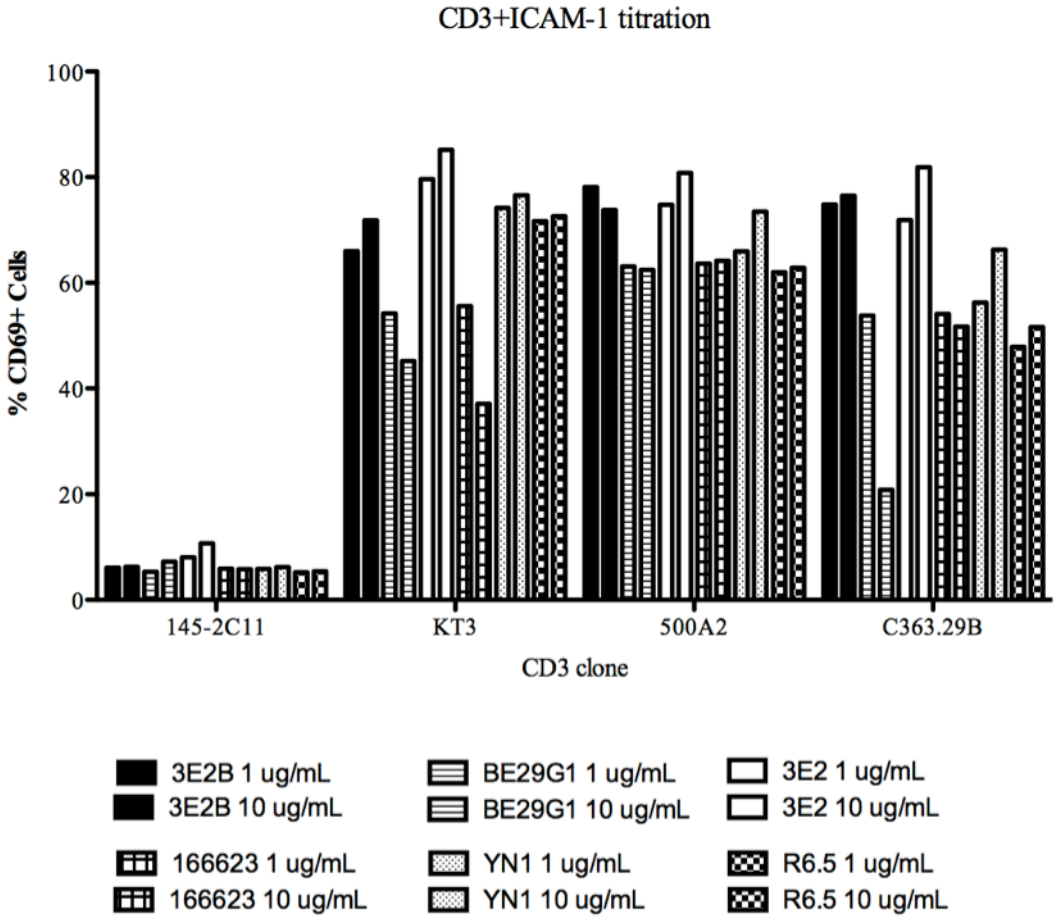
CD3+ICAM-1 titration
% CD69+ Cells
100
80
60
40
20
0
145-2C11
KT3
500A2
C363.29B
CD3 clone
3E2B 1 ug/mL
3E2B 10 ug/mL
BE29G1 1 ug/mL
BE29G1 10 ug/mL
3E2 1 ug/mL
3E2 10 ug/mL
166623 1 ug/mL
166623 10 ug/mL
YN1 1 ug/mL
YN1 10 ug/mL
R6.5 1 ug/mL
R6.5 10 ug/mL

Figure 6.6

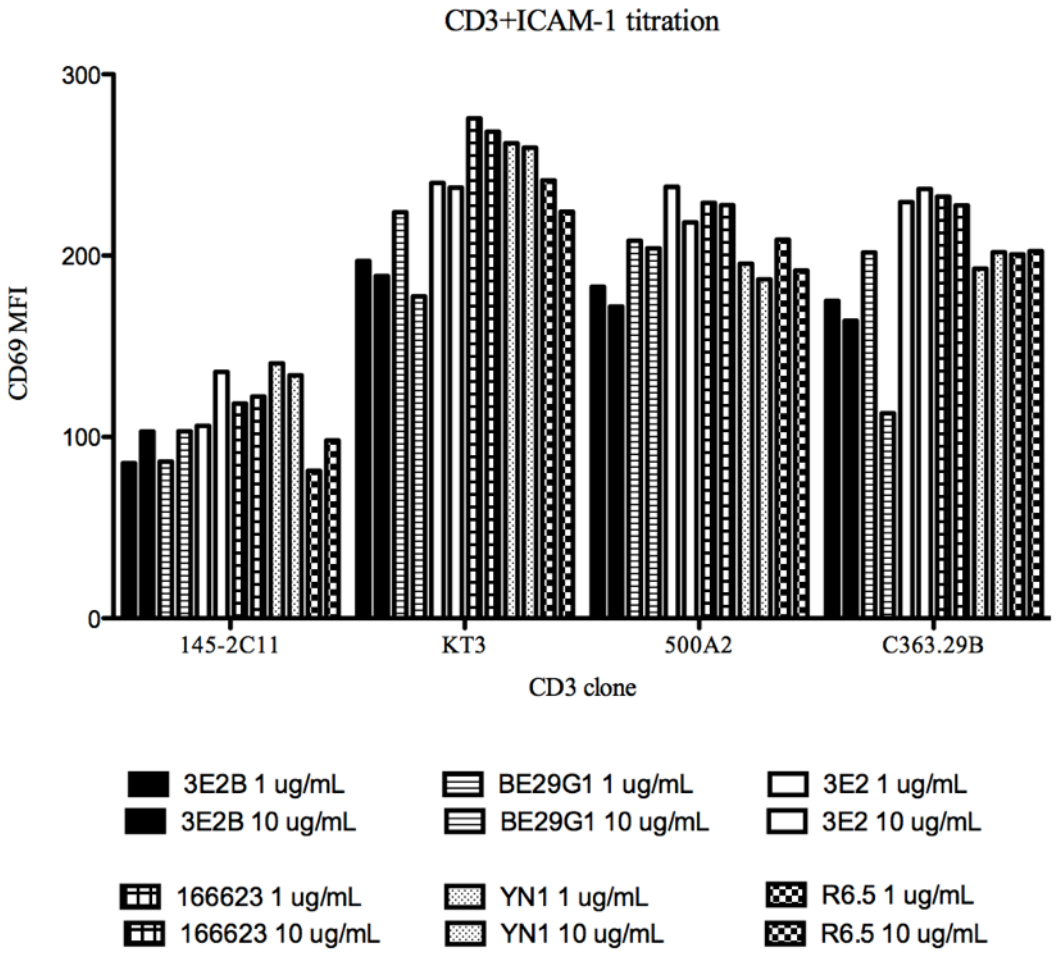
CD3+ICAM-1 titration
CD69 MFI
300
200
100
0
145-2C11
KT3
500A2
C363.29B
CD3 clone
3E2B 1 ug/mL
3E2B 10 ug/mL
BE29G1 1 ug/mL
BE29G1 10 ug/mL
3E2 1 ug/mL
3E2 10 ug/mL
166623 1 ug/mL
166623 10 ug/mL
YN1 1 ug/mL
YN1 10 ug/mL
R6.5 1 ug/mL
R6.5 10 ug/mL

Figure 6.5-6.6. Titration of stimulating ICAM-1 antibodies on Balb/c CD4+ T splenocytes to induce optimal CD69 expression. CD4+ T splenoctyes were stimulated for 12 hours through CD3 (145-2C11 at 0.1 ug/mL, KT3 at 0.5 ug/mL, 500A2 at 0.05 ug/mL and C363.29B at 1 ug/mL) and costimulated through ICAM-1 clones and concentrations as indicated. The first bar of each ICAM-1 clone represents the 1ug/mL concentration and the second bar is the 10ug/mL concentration. Percent CD69 positive and **(6.5)** CD69 MFI **(6.6)** were determined using flow cytometry.

through CD3 (clone 500A2) plus various clones of ICAM-1 or CD28 for seven days and memory phenotype was determined. **Figure 6.7** illustrates the memory phenotype generated when CD4 T cells were costimulated through ICAM-1 (166623) or CD28 but not CD3 alone. To quantify the percent of memory cells produced, cells were gated on the $CD44^{hi}$ population and the percent CD127+CD62L+ was determined. Stimulation through CD3 alone yielded a baseline of about 7 percent memory phenotype while costimulation through ICAM-1 generated between 14 and 27 percent memory cells, depending on the costimulatory antibody clone, which closely resembled the 18 percent of memory seen after CD28 costimuation **(Fig. 6.8)**. Costimulation of naïve T cells through ICAM-1 generated 30 to 56 percent memory phenotype, depending on the antibody clone, whereas costimulation through CD28 gave only 14 percent memory phenotype and was very similar to the 12 percent generated by stimulation through CD3 alone **(Fig. 6.9)**. Together, these data indicate that costimulation of murine CD4+ and naïve T cells through ICAM-1 can give rise to a memory cell phenotype that is similar or better than costimulation through CD28.

Titration of CD3 (500A2) and ICAM-1 (purified and functional grade, KAT) stimulating antibodies and mouse IL-2 on CD5+ Balb/c splenocytes.

Since we were able to produce memory T cells with costimulation through ICAM-1 of CD4+ and CD4+ naïve T cells, we decided to see if we could reproduce those data with a starting CD5+ total T cell population and using the KAT-1 ICAM-1 clone. CD5 is a T cell marker that is highly expressed on mature T cells and is also found on a small subset of B cells (18). The KAT-1 anti-mouse ICAM-1 clone has been used as a

Figure 6.7

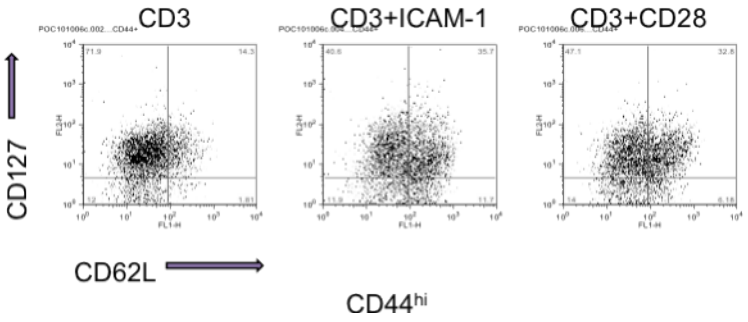

Figure 6.8

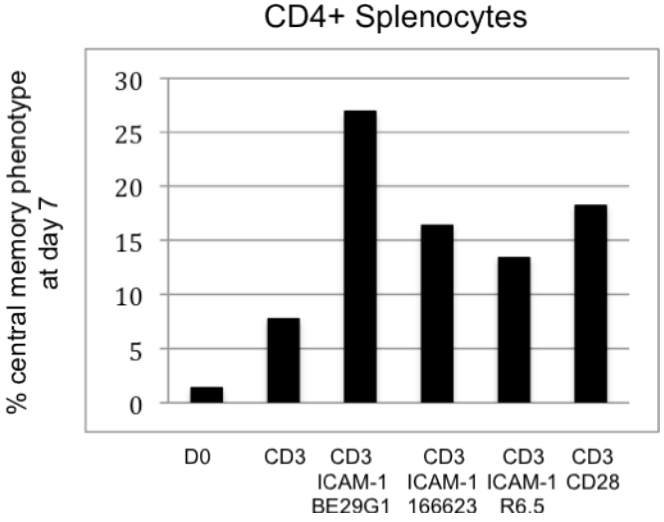

Figure 6.9

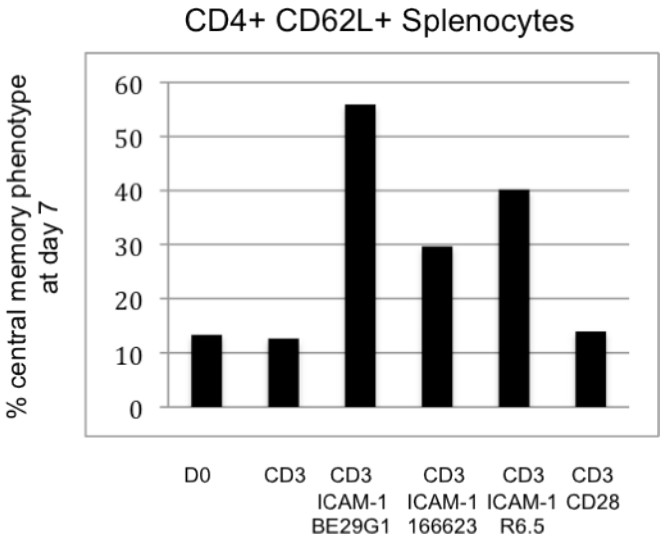

Figure 6.7-6.9. Costimulation of CD4+ and CD4+CD62L+ splenocytes through ICAM-1 induces a memory phenotype. Stimulation through CD3 was done using 0.05 ug/mL of clone 500A2. Costimulation through ICAM-1 was done using clone BE29G1 at 10 ug/mL, 166623 at 1 ug/mL or R6.5 at 10 ug/mL or through CD28 clone 37.51 at 2.5 ug/mL. **6.7)** Representative dot plots of memory phenotypes generated after CD4+ T splenocytes were stimulated for 7 days through CD3, CD3+ICAM-1 (166623) or CD3+ CD28. **6.8-6.9)** Percent of memory cells generated after CD4+ T splenocytes **(6.8)** or CD4+CD62L+ naïve T splenocytes **(6.9)** were stimulated for 7 days through antibody combinations indicated.

blocking antibody in solution and is known to bind to a different ICAM-1 epitope than the previously tested YN1 clone (16). For this experiment we examined combinations of three different concentrations of anti-CD3 clone 500A2 (0.05 ug/mL, 0.1 ug/mL, 0.25 ug/mL) and three concentrations of anti-ICAM-1 (5 ug/mL, 10 ug/mL, 20 ug/mL) with and without the presence of recombinant mouse IL-2. We also wanted to determine if there is a difference between costimulation with purified or functional grade KAT-1 clone. Functional grade KAT-1 antibody contains no sodium azide or carrier proteins/stabilizers and has an extremely low endotoxin level less than 0.001 ng/ug of antibody.

In general, we found that stimulating CD5+ T cells through CD3+ICAM-1, purified KAT-1 clone, yielded a greater percentage memory phenotype than CD3 alone or CD3+CD28. Lower concentrations of stimulating CD3 in conjunction with ICAM-1 produced the most memory cells which then dropped as anti-CD3 increased and the inverse was seen with a step-wise increase with increasing anti-ICAM-1 concentrations, therefore, the best memory T cell generating combination was 0.05 ug/mL of anti-CD3 and 10-20 ug/mL of anti-ICAM-1 **(Fig. 6.10)**. The addition of recombinant mouse IL-2 actually reduced the memory cell production with each stimulation combination **(Fig.6.10)**. Also, increasing the concentration of stimulating anti-CD3 alone, with or without exogenous IL-2, did not seem to modulate the memory cell percent **(Fig. 6.10)**. The trend seen with stimulating through purified KAT-1 ICAM-1 was largely repeated with functional grade KAT-1 and the percent of memory cells generated with each concentration was similar to purified KAT-1, indicating little difference in the stimulation between the two forms of the antibody **(Fig. 6.11)**. With most KAT-1 clone

concentrations, the 10 ug/mL concentration either yielded a very similar or better memory production to 20 ug/mL. Given the lower amount of stimulating antibody needed, 10 ug/mL would be the more economical choice for the optimal anti-ICAM-1 concentration. As expected, the addition of recombinant human IL-2 instead of mouse IL-2 decreased the percent of memory cells that were produced (data not shown).

Figure 6.10

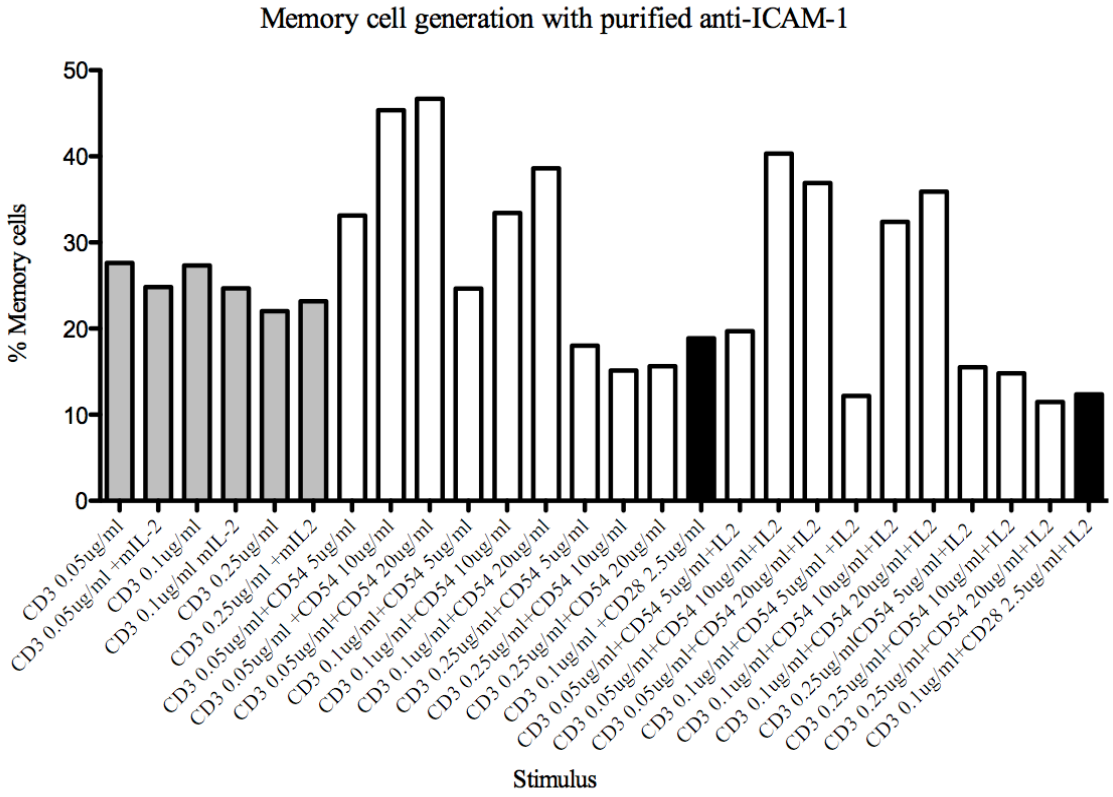
Memory cell generation with purified anti-ICAM-1
% Memory cells
50
40
30
20
10
0
CD3 0.05ug/ml
CD3 0.05ug/ml +mIL-2
CD3 0.1ug/ml
CD3 0.1ug/ml mIL-2
CD3 0.25ug/ml
CD3 0.25ug/ml +mIL2
CD3 0.05ug/ml+CD54 5ug/ml
CD3 0.05ug/ml +CD54 10ug/ml
CD3 0.05ug/ml+CD54 20ug/ml
CD3 0.1ug/ml+CD54 5ug/ml
CD3 0.1ug/ml+CD54 10ug/ml
CD3 0.1ug/ml+CD54 20ug/ml
CD3 0.25ug/ml+CD54 5ug/ml
CD3 0.25ug/ml+CD54 10ug/ml
CD3 0.25ug/ml+CD54 20ug/ml
CD3 0.1ug/ml +CD28 2.5ug/ml
CD3 0.05ug/ml+CD54 5ug/ml+IL2
CD3 0.05ug/ml+CD54 10ug/ml+IL2
CD3 0.05ug/ml+CD54 20ug/ml+IL2
CD3 0.1ug/ml+CD54 5ug/ml +IL2
CD3 0.1ug/ml+CD54 10ug/ml+IL2
CD3 0.1ug/ml+CD54 20ug/ml+IL2
CD3 0.25ug/mlCD54 5ug/ml+IL2
CD3 0.25ug/ml+CD54 10ug/ml+IL2
CD3 0.25ug/ml+CD54 20ug/ml+IL2
CD3 0.1ug/ml+CD28 2.5ug/ml+IL2
Stimulus

Figure 6.11

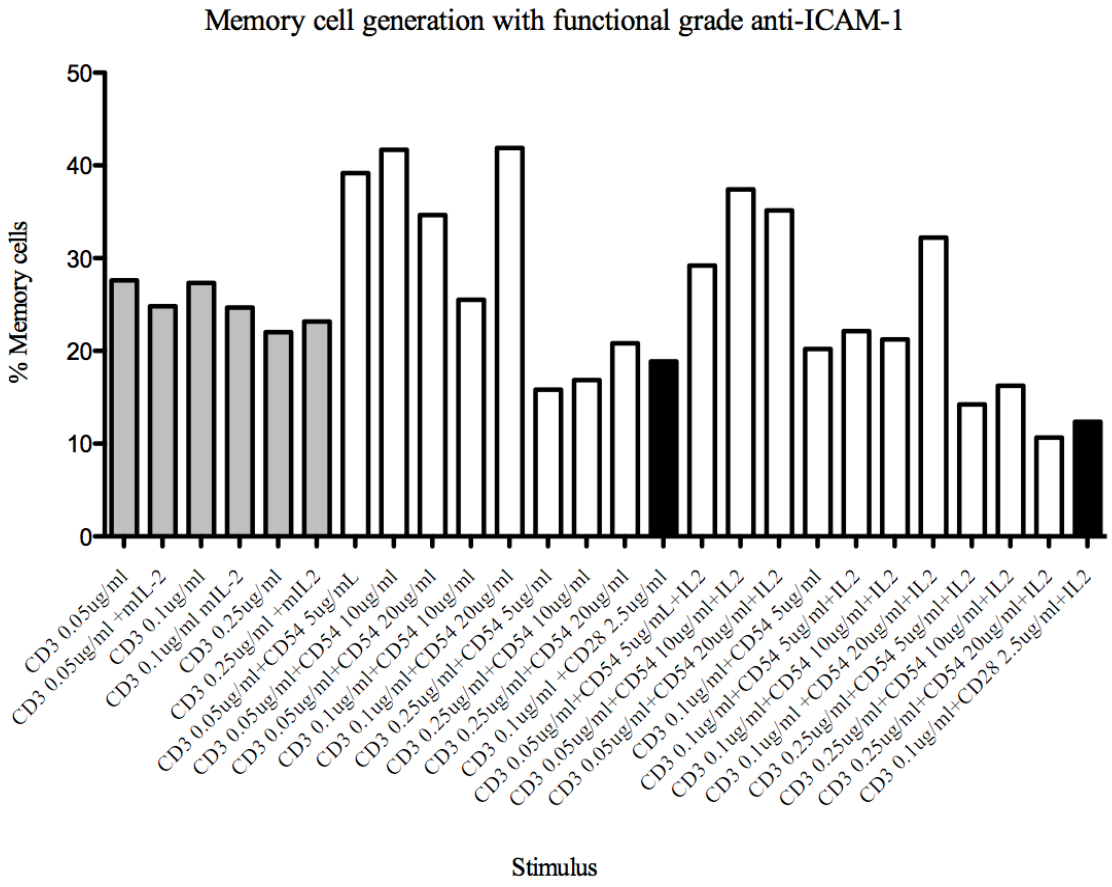
Memory cell generation with functional grade anti-ICAM-1
% Memory cells
50
40
30
20
10
0
CD3 0.05ug/ml
CD3 0.05ug/ml +mIL-2
CD3 0.1ug/ml
CD3 0.1ug/ml mIL-2
CD3 0.25ug/ml
CD3 0.25ug/ml +mIL2
CD3 0.05ug/ml+CD54 5ug/mL
CD3 0.05ug/ml+CD54 10ug/ml
CD3 0.05ug/ml+CD54 20ug/ml
CD3 0.1ug/ml+CD54 5ug/ml
CD3 0.1ug/ml+CD54 10ug/ml
CD3 0.1ug/ml+CD54 20ug/ml
CD3 0.25ug/ml+CD54 5ug/ml
CD3 0.25ug/ml+CD54 10ug/ml
CD3 0.25ug/ml+CD54 20ug/ml
CD3 0.1ug/ml +CD28 2.5ug/ml
CD3 0.05ug/ml+CD54 5ug/mL+IL2
CD3 0.05ug/ml+CD54 10ug/ml+IL2
CD3 0.05ug/ml+CD54 20ug/ml+IL2
CD3 0.1ug/ml+CD54 5ug/ml
CD3 0.1ug/ml+CD54 5ug/ml+IL2
CD3 0.1ug/ml+CD54 10ug/ml+IL2
CD3 0.1ug/ml+CD54 20ug/ml+IL2
CD3 0.25ug/ml+CD54 5ug/ml+IL2
CD3 0.25ug/ml+CD54 10ug/ml+IL2
CD3 0.25ug/ml+CD54 20ug/ml+IL2
CD3 0.1ug/ml+CD28 2.5ug/ml+IL2
Stimulus

Figure 6.10-6.11. Titration of CD3 (500A2) and ICAM-1 (purified and functional grade, KAT) stimulating antibodies and mouse IL-2 on CD5+ Balb/c splenocytes. Stimulation of CD5+ T cells through CD3 was performed using clone 500A2 and through ICAM-1 using clone KAT-1 at concentrations indicated. **Figure 6.10** uses purified KAT-1 antibody and **6.11** uses functional grade KAT-1 antibody. Mouse recombinant IL-2 was used at a concentration of 20 ng/mL. Percent of memory cells generated after CD5+ T splenocytes were stimulated for 7 days through antibody combinations indicated.

Discussion

The goal of this chapter was to determine the optimal protocol for stimulating mouse T cells through ICAM-1 to induce them to differentiate to a memory phenotype. We observed that various concentrations and stimulating antibody clones were able to induce T cell activation. Based on CD69 expression, proliferation experiments performed by Kelli Williams and cell differentiation presented here we conclude that 0.05 ug/mL of 500A2 is the best stimulating CD3 antibody. ICAM-1 clones and concentrations that worked the best based on the same parameters were 10 ug/mL of BE29G1, 1 ug/mL of 166623, 10 ug/mL of R6.5 or 10 ug/mL KAT-1.

It is noteworthy that a part of this study was to look for the ability of either mouse CD4+ T cells or CD4+CD62L+ T cells to differentiate to a regulatory phenotype using the same parameters. This was another portion of the work that was performed by Kelli Williams. Kelli found that, unlike with human T cells (19), costimulation through ICAM-1 of mouse T cells did not induce a regulatory phenotype. This discrepancy illustrates how ICAM-1 signals differently between species and the importance of seeking out various anti-ICAM-1 clones for the most efficient stimulation since different antibody clones may bind to different epitopes on the costimulatory molecule, thus altering signal sent into the cell.

The ability to stimulate murine T cells *in vitro* through ICAM-1 to induce differentiation to a memory phenotype has many possibilities in helping to understand the immune response better or for the development of therapies that can be used in mouse disease models. Adoptive transfer of memory T cells generated with ICAM-1 costimulation *in vitro* could be utilized to determine homing patterns of memory cells *in*

vivo and possibly support our chemokine receptor observations in humans. Along the same lines, we could track T cells activated through ICAM-1 as they fight infection much like Ciabattini, et al. who tracked T cells primed *in vitro* following immunization *in vivo* (20). Memory T cells generated through ICAM-1 could also be used in studies for development of immunotherapy for cancers. For example, tumor specific T cells could be selected *in vitro* using ICAM-1 costimulation and activation in the presence of tumor antigen and then applied *in vivo* as a T cell therapy to a mouse model such as the 4T1 breast cancer model in Balb/c mice (21). In summary, defining the parameters for ICAM-1 costimulation and differentiation to a memory cell phenotype is an important first step in our ability to understand the adaptive immune response, how it is affected by costimulation and study disease with the use of mouse models.

References

1. Gross JA, Callas E, Allison JP. Identification and distribution of the costimulatory receptor CD28 in the mouse. J Immunol. 1992; 149(2): 380-8.
2. Harper K, Balzano C, Rouvier E, Mattéi MG, Luciani MF, Golstein P. CTLA-4 and CD28 activated lymphocyte molecules are closely related in both mouse and human as to sequence, message expression, gene structure, and chromosomal location. J Immunol. 1991; 147(3): 1037-44.
3. Fuse S, Tsai C, Rommereim L, Zhang W, Usherwood E. Differential requirements for CD80/86-CD28 costimulation in primary and memory CD4 T cell responses to vaccinia virus. Cell Immunol. 2011; 266(2): 130–134.
4. Wang S, Chen L. T Lymphocyte Co-Signaling Pathways of the B7-CD28 Family. Cellular & Molecular Immunology. 2004; 1(1): 37-42.
5. Siu G, Hedrick SM, Brian AA. Isolation of the murine intercellular adhesion molecule 1 (ICAM-1) gene. ICAM-1 enhances antigen-specific T cell activation. J Immunol. 1989; 143(11): 3813-20.
6. Johnston SC, Dustin ML, Hibbs ML, Springer TA. On the species specificity of the interaction of LFA-1 with intercellular adhesion molecules. J Immunol. 1990; 145(4): 1181-7.
7. Alegre ML, Vandenabeele P, Depierreux M, Florquin S, Deschodt-Lanckman M, Flamand V, Moser M, Leo O, Urbain J, Fiers W, et al. Cytokine release syndrome induced by the 145-2C11 anti-CD3 monoclonal antibody in mice: prevention by high doses of methylprednisolone. J Immunol. 1991; 146(4): 1184-91.

8. Portoles P, Rojo J, Golby A, Bonneville M, Gromkowski S, Greenbaum L, Janeway CA Jr, Murphy DB, Bottomly K. Monoclonal antibodies to murine CD3 epsilon define distinct epitopes, one of which may interact with CD4 during T cell activation. J Immunol. 1989; 142(12): 4169-75.
9. Reid IM, Lundy JK, Donohue JH. The bispecific antibody 500A2 x 96.5 targets T-lymphocytes activated in vivo with staphylococcal enterotoxin B (SEB) against CL62 melanoma cells in vitro. Surg Oncol. 1994; 3(5): 279-85.
10. Andrew H. Lundberg, Kazuhiko Fukatsu, Lillian Gaber, Scott Callicutt, Malak Kotb, Henry Wilcox, Kenneth Kudsk, and A. Osama Gaber. Blocking Pulmonary ICAM-1 Expression Ameliorates Lung Injury in Established Diet-Induced Pancreatitis. Ann Surg. 2001; 233(2): 213–220.
11. Kommajosyula S, Reddy S, Nitschke K, Kanwar JR, Karanam M, Krissansen GW. Leukocytes infiltrating the pancreatic islets of nonobese diabetic mice are transformed into inactive exiles by combinational anti-cell adhesion therapy. Journal of Leukocyte Biology. 2001; 70(4):
12. T Kumasaka, W M Quinlan, N A Doyle, T P Condon, J Sligh, F Takei, A l Beaudet, C F Bennett, C M Doerschuk. Role of the intercellular adhesion molecule-1(ICAM-1) in endotoxin-induced pneumonia evaluated using ICAM-1 antisense oligonucleotides, anti-ICAM-1 monoclonal antibodies, and ICAM-1 mutant mice. J Clin Invest. 1996; 97(10):2362–2369
13. Nowak-Sliwinska P, van Beijnum JR, van Berkel M, van den Bergh H, Griffioen AW. Vascular regrowth following photodynamic therapy in the chicken embryo chorioallantoic membrane. Angiogenesis. 2010; 13(4): 281–292.

14. Kevil CG, Patel RP, Bullard DC. Essential role of ICAM-1 in mediating monocyte adhesion to aortic endothelial cells. Am J Physiol Cell Physiol. 2001; 281 (5): C1442-C1447

15. Jedrzejas MJ, Miglietta J, Griffin JA, Luo M. Structure of a monoclonal anti-ICAM-1 antibody R6.5 Fab fragment at 2.8 Å resolution. Acta Cryst. 1995; D51: 380-385

16. Lehmann JC, Jablonski-Westrich D, Haubold U, Gutierrez-Ramos JC, Springer T, Hamann A. Overlapping and selective roles of endothelial intercellular adhesion molecule-1 (ICAM-1) and ICAM-2 in lymphocyte trafficking. J Immunol. 2003; 171(5):2588-93.

17. Ziegler SF, Ramsdell F, Hjerrild KA, *et al.* Molecular characterization of the early activation antigen CD69: a type II membrane glycoprotein related to a family of natural killer cell activation antigens. Eur. J. Immunol. 1993; **23** (7): 1643–8.

18. Luo W, van de Velde H, von Hoegen I, Parnes JR, Thielemans K. Ly-1 (CD5), A Membrane Glycoprotein of Mouse T Lymphocytes and a Subset of B Cells, Is a Natural Ligand of the B Cell Surface Protein Lyb-2 (CD72). J. Immunol. 1992; 148: 1630-1634

19. Williams KM, Dotson AL, Otto AR, Kohlmeier JE, Benedict SH. Choice of resident costimulatory molecule can influence cell fate in human naïve CD4+ T cell differentiation. Cell Immunol. 2011;271(2):418-27

20. Ciabattini A, Pettini E, Fiorino F, Prota G, Pozzi G, Medaglini D. Distribution of primed T cells and antigen-loaded antigen presenting cells following intranasal immunization in mice. PLoS One. 2011;6(4):19346

21. Tao K, Alroy J, Sahagian GG. Imagable 4T1 model for the study of late stage breast cancer. BMC Cancer 2008; 8:228

Summary

The work in this dissertation illustrates an important role for ICAM-1 as a costimulatory molecule in T cell activation. We demonstrated that blocking the ICAM-1:LFA-1 interaction rendered T cells unresponsive in a NOD mouse model *in vivo* and *in vitro* and with human cells stimulated *in vitro*. The blocking peptides also inhibited or stopped T cell infiltration into the islets of the treated mice. Also, T splenocytes from peptide treated NOD mice did not initiate T1D when adoptively transferred into T cell deficient NOD-SCID mice compared to T splenocytes from saline control mice.

Costimulation through ICAM-1 of human CD4+ naïve T cells initiated differentiation to a memory phenotype days after stimulation but required constant, long-term stimulation to generate larger numbers of memory cells. This suggests different pathways for differerntiation to a memory phenotype. Even though costimulation through CD28 generated memory cell numbers statistically similar to long-term stimulation a few days before ICAM-1, the total number of memory cells with CD28 was lower than that from ICAM-1 after 14 days of continual stimulaton. Costimulation through ICAM-1 gave rise to a memory population that exhibited lymph node homing potential indicating that ICAM-1 differentiates naive T cells to a central memory phenotype.

ICAM-1 costimulation induces differentiation of naïve T cells from older individuals to a memory phenotype better than CD28. According to preliminary data, these cells are protected from apoptosis and proliferate better than differentiating cells costimulated through LFA-1 or CD28 therefore leading to a larger population of viable cells. These data have promising implications in understanding how the immune system

ages and how to develop new stratagies to fight infection, cancer and boost vaccine response as we age.